UNIVERSITY OF CALIFORNIA, SAN DIEGO

# The link between neuronal activity and activation of the cAMP/PKA cascade in developing retinal ganglion cells

A Dissertation submitted in partial satisfaction of the requirements for the degree Doctor of Philosophy

in

Biology

by

Timothy Alan Dunn

Committee in charge

Professor Nick Spitzer, Chair
Professor Marla Feller, Co-Chair
Professor Anirvan Ghosh
Professor William Loomis
Professor Roger Tsien

2008

The Dissertation of Timothy Alan Dunn is approved, and it is acceptable in quality and form for publication on microfilm

Co-Chair

Chair

University of California, San Diego

2008

TABLE OF CONTENTS

LIST OF FIGURES

ACKNOWLEDGEMENTS

I would like to thank my advisor, Marla Feller for being an excellent mentor. I would also like to thank the members of my thesis committee, Nick Spitzer, Anirvan Ghosh, William Loomis, and Roger Tsien, for their thoughtful comments on this project. Furthermore, the greater UCSD neurobiology community has provided a superb atmosphere for collaboration and engaging in scientific endeavors. Finally, I recognize the work and generosity of Roger Tsien, Jin Zhang, and Manuela Zaccolo in designing and providing the fluorescent indicators that I have based much of my dissertation work on.

I would like to thank the members of the Feller lab, current and past, for contributing to a great atmosphere in lab: Chih-Tien Wang, Aaron Blankenship, Justin Elstrott, Kevin Ford, Anastasia Anishchenko, Will Barkis, Ethan Hua, Paley Han, Jenel Bosze, Michael Colicos, Sally Firth, Jennifer Goldstein, Christine Torborg, and Kristi Hansen.

I would like to thank my family and friends for support during the last several years, particularly my parents, Kathe and Steve.

Chapter 1, in full, is a reprint of the material as it appears in Dunn TA, Feller MB. 2008. Imaging second messenger dynamics in developing neural circuits. Developmental Neurobiology 68:835-844.

Chapter 2, in full, is a reprint of the material as it appears in Dunn TA, Wang CT, Colicos MA, Zaccolo M, DiPilato LM, Zhang J, Tsien RY, Feller MB. 2006. Imaging of cAMP levels and protein kinase A activity reveals that retinal waves drive oscillations in second-messenger cascades. Journal Of Neuroscience 26:12807-12815.

Chapter 3, in part, is a draft of work to be submitted for publication

## VITA

| | |
|---|---|
| 2002 | Bachelor of Science, University of California, Santa Barbara |
| 2003-2005 | Teaching Assistant, Department of Biological Sciences, University of California, San Diego |
| 2008 | Doctor of Philosophy, University of California, San Diego |

## PUBLICATIONS

Dunn TA*, Wang CT*, Colicos MA, Zaccolo M, DiPilato LM, Zhang J, Tsien RY, Feller MB. 2006. Imaging of cAMP levels and protein kinase A activity reveals that retinal waves drive oscillations in second-messenger cascades. Journal Of Neuroscience 26:12807-12815.

Dunn TA, Feller MB. 2008. Imaging second messenger dynamics in developing neural circuits. Developmental Neurobiology 68:835-844

## FIELDS OF STUDY

Major Field: Neurobiology

Studies in Retinal Development
Professor Marla Feller

ABSTRACT OF THE DISSERTATION

The link between neuronal activity and activation of the cAMP/PKA cascade in developing retinal ganglion cells

by

Timothy Alan Dunn

Doctor of Philosophy in Biology

University of California, San Diego, 2008

Professor Nick Spitzer, Chair
Professor Marla Feller, Co-Chair

## ABSTRACT

A characteristic feature of developing neural circuits is that they exhibit spontaneous, patterned activity. The effects of this activity have been well characterized in the developing visual system, where the spontaneous activity, called retinal waves, is known to be important in the establishment of retinotopic and eye-specific maps. However, there has been little focus on the issue of cell autonomous effects of spontaneous activity. Retinal waves, like other forms of

spontaneous activity in the spinal cord and hippocampus, are characterized at the single neuron level by periodic increases in intracellular calcium concentration with a periodicity on the order of a minute. One likely mechanism by which neurons can "decode" these slow oscillations is through activation of second messenger cascades that either influence transcriptional activity or drive post-translational modifications. Recently, genetically encoded, fluorescent reporters have been developed that allow imaging of second messenger pathways other than calcium, such as the cAMP/PKA pathway.

This dissertation focuses on the use of these FRET-based, reporters of the cAMP/PKA pathway to study the activity of second messenger cascades during retinal waves. In chapter 1, recent advances in efficacy and utility of genetically encoded, fluorescent indicators of the cAMP/PKA pathway are described. In chapter 2, we report the spontaneous activation of the cAMP/PKA pathway in retinal ganglion cells (RGCs). Spontaneous activation of the cAMP/PKA pathway is dependent on, and maintains a temporally consistent relationship with retinal waves and is dependent on calcium influx. Chapter 3 describes the mechanism by which calcium influx leads to an increase in PKA activity, specifically focusing on the role of calcium activated adenylate cyclases and phosphodiesterases. We present evidence that multiple adenylate cyclases underlie the calcium-induced PKA activation in RGCs. Chapter 4 concludes with a model of the cAMP/PKA pathway in retinal ganglion cells and discussion of the possible function of periodic PKA transients in the development of visual circuits.

Chapter 1
From: Developmental Neurobiology
Special Issue: Dynamic Imaging of the developing nervous system

# Imaging second messenger dynamics in developing neural circuits

Timothy A. Dunn and Marla B. Feller

Neurobiology Section, Division of Biological Sciences, UCSD, La Jolla, CA, USA.

## ABSTRACT

A characteristic feature of developing neural circuits is that they are spontaneously active. There are several examples, including the retina, spinal cord, and hippocampus, where spontaneous activity is highly correlated among neighboring cells, with large depolarizing events occurring with a periodicity on the order of minutes. One likely mechanism by which neurons can "decode" these slow oscillations is through activation of second messenger cascades that either influence transcriptional activity or drive posttranslational modifications. Here, we describe recent experiments where imaging has been used to characterize slow oscillations in the cAMP/PKA second messenger cascade in retinal neurons. We review the latest techniques in imaging this specific second messenger cascade, its intimate relationship with changes in intracellular calcium concentration, and several hypotheses regarding its role in neurodevelopment.

## INTRODUCTION

Spontaneous neuronal activity is a common feature in the developing central nervous system, occurring in many regions including the retina (Wong et al., 1993; Feller et al., 1996), spinal cord (Gorbunova and Spitzer, 2002; Hanson and Landmesser, 2003), hippocampus (Ben-Ari et al., 1989; Garaschuk et al., 1998; Colin-Le Brun et al., 2004; Khalilov et al., 2005), neocortex (Schwartz et al., 1998; Aguilo et al., 1999; Adelsberger et al., 2005), and hindbrain (Gust et al., 2003). Although spontaneous activity is generated by circuits with vastly different synaptic connectivity, each circuit exhibits episodic events that are correlated across large populations of cells with a periodicity on the order of minutes (Feller, 1999; O'Donovan, 1999). These events are for the most part generated by depolarizations of neurons, and cause significant increases in intracellular calcium concentration.

The developing visual system serves as a model for understanding how periodic activity translates into long-term changes in neural circuits. Spontaneous activity in the retina is critical for the retinotopic and eye-specific refinement of retinal projections to the thalamus and superior colliculus prior to vision (for review, see Wong, 1999; Torborg and Feller, 2005). Retinal waves are spatially correlated bursts of activity that propagate laterally across the retina prior to the development of light responses. This activity is also periodic, occurring in a given retinal ganglion cell approximately once per minute. Most hypotheses regarding how retinal waves drive the refinement of retinal projections have been based on the assumption that spontaneous activity drives

synaptic competition that in turn leads to axonal refinement (Katz and Shatz, 1996; Huberman, 2006; Butts et al., 2007). There is also some indication that cell autonomous processes are dependent on patterned activity (Ruthazer and Cline, 2004). For example, rhythmic activity in retinal ganglion cells significantly enhances the rate of axonal outgrowth (Goldberg et al., 2002; Rodger et al., 2005). In addition, neuronal activity determines the polarity of responsiveness to chemorepulsive or chemoattractive signals (Wang and Zheng, 1998; Ming et al., 2001; Nicol et al., 2007).

Little is known about the specific mechanisms by which patterned activity is read out by the cell to produce changes in protein expression or regulation of existing proteins. Although it is likely that increases in intracellular calcium concentration and downstream calmodulin-dependent kinases are responsible for some of the resulting developmental changes, other second messenger cascades, such as the cAMP pathway, may be involved. Calcium and cAMP pathways are known to be closely interrelated. Calcium activates some adenylyl cyclases (ACs), the enzymes that convert ATP to cAMP to directly increase cAMP concentration (Xia and Storm, 1997). Indeed, mutant mice lacking calcium activated AC1 show defects in projections to both the superior colliculus and lateral geniculate nucleus, implying that calcium dependent cAMP concentration is important for map refinement (Ravary et al., 2003; Plas et al., 2004). In some cells, increases in calcium concentration lead to decreases in cAMP levels either by inhibiting some classes of ACs (Wayman et al., 1995; Wang and Storm, 2003), or by activating a distinct class of phosphodiesterases that are

responsible for the breakdown of cAMP (Sonnenburg et al., 1998). Cyclic AMP is a ubiquitous second messenger that is involved in myriad cellular processes. Downstream targets of cyclic AMP include cAMP dependent protein kinase (PKA), a guanine nucleotide exchange factor called exchange protein activated by cAMP (Epac) and cyclic nucleotide gated ion channels. PKA in turn phosphorylates a wide variety of targets, including many receptors and ion channels that govern the excitability of neurons. In addition, cAMP also influences actin dynamics (Meberg et al., 1998) and is critical for growth cone motility (Lohof et al., 1992; Kim and Wu, 1996; Song and Poo, 1999; Munck et al., 2004).

To determine the various roles of second messenger cascades in development, it is critical to characterize the effects of neural activity on second messenger dynamics. However, tools for assaying activity of second messenger pathways other than calcium have been sparse until recently. Particularly, the cAMP/PKA pathway has seen the advent of several indicators suitable for use in both mammalian systems and model organisms. Here, we review advances in the field of fluorescence-based assays of the cAMP/PKA pathway and the application of these techniques to study developing neurons.

**Indicators for dynamic imaging of cAMP/PKA cascade**

Although biochemical techniques to quantify cAMP concentration and PKA activity have existed for many years, these techniques are not appropriate for live imaging since they require the lysing of cells to obtain the measurements. The

first assay with the spatiotemporal sensitivity to do dynamic imaging was the protein FlCRhR, a tetrameric holoenzyme consisting of the catalytic and regulatory subunits of PKA fused to fluorescein and rhodamine, respectively (Adams et al., 1991). FlCRhR was used to measure evoked changes of cAMP levels by forskolin or GPCR agonists in invertebrate neurons (Bacskai et al., 1993; Hempel et al., 1996) and mammalian hippocampal neurons, (Vincent and Brusciano, 2001; Goaillard and Vincent, 2002), as well as to image spontaneous cAMP transients in spinal cord neurons (Gorbunova and Spitzer, 2002). However, the use of chemically modified recombinant proteins implies it needs to be microinjected into cells, which has more limited use in mammalian neurons where whole cell recordings dialyze the intracellular contents that may modulate second messenger signaling.

A solution to this problem is to use genetically encoded indicators. One approach is to express genetically encoded cAMP-gated cation channels (Rich et al., 2001). Though this works well in kidney cells, the introduction of novel calcium conductances may alter the excitability of neurons. The first genetically encoded indicator of cAMP was based on FlCRhR, replacing fluorescein and rhodamine with GFP and BFP (Zaccolo et al., 2000). This indicator was soon updated to use CFP/YFP fluorophores, which are more suitable for FRET (Zaccolo and Pozzan, 2002) and the linker range was modified to optimize FRET efficiency (Lissandron et al., 2005) (Figure 1.1A). The PKA-based cAMP sensor has four binding sites for cAMP – two on each regulatory subunit – each with different affinities for cAMP due to cooperative binding. The PKA-based cAMP

sensor relies on the dissociation of the regulatory and catalytic subunits to decrease FRET efficiency. The indicator is expressed throughout the cell, but since it utilizes the RII regulatory subunit of PKA, it can also localize to A-kinase anchoring proteins (AKAPs). AKAPs are thought to be involved in organizing microdomains (for review, Beene and Scott, 2007), and therefore this indicator is likely to be useful in studying very localized changes in cAMP concentration. Indeed, the PKA-based cAMP sensor has been used to detect microdomains of cAMP signaling in cardiac myocytes (Zaccolo and Pozzan, 2002; Lissandron and Zaccolo, 2006). A similar indicator has been recently developed that uses a truncated form of the CFP-RII subunit targeted to the membrane. Evanescent wave microscopy is then used to detect the translocation of the YFP-catalytic subunit away from the membrane when cAMP levels increase (Dyachok et al., 2006)

Recently, novel indicators of cAMP have been developed using proteins that have a single cAMP binding site. In particular, three groups independently developed FRET sensors based on the Exchange protein activated by cAMP (Epac) (DiPilato et al., 2004; Nikolaev et al., 2004; Ponsioen et al., 2004) (Figure 1.1B). Epac is a guanine nucleotide exchange factor with a single cAMP binding site, whose activity links cAMP to the Ras-ERK pathway (for review Holz et al., 2006). Upon binding of cAMP to the indicators, there is a decrease in FRET efficiency. There has yet to be a rigorous comparison of the various Epac indicators, which are truncated differently but appear to have similar dynamic ranges of FRET ratios. Indicators with a single cAMP binding site provide an

advantage over those that rely upon cooperative binding of cAMP in that their response times are more likely to directly reflect changes in changes in cAMP levels. FRET-based indicators have also been developed from the cAMP binding sites of the PKA regulatory subunit (Nikolaev et al., 2004) and the cAMP gated channel HCN2 (Nikolaev et al., 2006).

A third type of indicator was developed to report on PKA activity. This indicator was designed as an archetype for reporting kinase activity via FRET. AKARs consist of a fusion of CFP, a PKA target substrate, a phosphobinding region, and the YFP variant citrine (Zhang et al., 2001) (Figure 1.1C). Efforts to further improve AKAR have focused on increasing the off-kinetics (Zhang et al., 2005) and the dynamic range of the indicator by optimizing the orientation of YFP with respect to CFP using circular permutations of the YFP variant, Venus (Nagai et al., 2004; Allen and Zhang, 2006). The AKAR FRET paradigm has also been used to study the activity of other kinases, including PKB/Akt (Aktus, Sasaki et al., 2003), PKC (CKAR, Violin et al., 2003), PKD (DKAR, Kunkel et al., 2007), and tyrosine kinases (Ting et al., 2001).

One advantage of genetically encoded indicators is that they can be localized to specific populations of cells using cell specific promoters. In addition, they can be mutated to allow targeting to different subcellular compartments. For example, short peptide tags have been used to localize the indicators to nuclear, mitochondrial, cytosolic, and membrane regions in hippocampal neurons (DiPilato et al., 2004; Allen and Zhang, 2006; Gervasi et al., 2007). This ability to

obtain subcellular localization is likely to be critical for distinguishing among the variety of targets of the cAMP/PKA pathways in neurons.

**Spontaneous cAMP/PKA transients in retinal ganglion cells**

We recently used two FRET indicators, ICUE2 and AKAR2.2 to assay the spontaneous activation of the cAMP/PKA pathway in retinal ganglion cells during retinal waves (Dunn, Wang, et al. 2006). Calcium influx due to retinal waves occurs approximately once per minute, and calcium dependent adenylyl cyclases are present in retinal ganglion cells suggesting cAMP/PKA might be activated by calcium influx. However, it was unknown whether this pattern of calcium transients would cause transient or sustained activation of the cAMP/PKA pathway. Briefly, retinal explants were isolated from P0-P4 rats, electroporated with either ICUE2 or AKAR2.2, and cultured overnight to allow expression of the indicator. We found that some retinal ganglion cells exhibit spontaneous transient increases in PKA activity and cAMP concentration across the cell soma (Figure 1.2). Blockade of retinal waves eliminated the PKA transients. We also found that PKA activity increased within 5 seconds following a retinal wave. This is consistent with the hypothesis that retinal waves drive activation of the cAMP/PKA pathway through a calcium mediated mechanism. The implications for a role of these second messenger transients in neurodevelopment are explored below. Here we use these data as an example for illustrating various properties of cAMP and PKA indicators.

While these indicators provide significant opportunities to advance our

understanding about the dynamics of the cAMP/PKA pathway, the results must be interpreted with caution. First, there may be a limitation to the sensitivity of the reporters. For example, during waves cAMP and PKA activity transients were observed in only a small subset of RGCs although all RGCs have spontaneous depolarizations. We found that depolarizations lasting less than one second did not reliably induce a detectable change in the FRET ratio of AKAR2.2 while depolarizations greater than two seconds did. We cannot determine from these experiments whether depolarizations less than one second induced changes in PKA activity that were below the sensitivity of our imaging system or whether activation of the cAMP/PKA pathway requires a threshold influx of calcium.

Second, the timecourse of the response is a convolution of the kinetics of the indicators and the second messenger cascade. For example, we found that the PKA-based cAMP sensor had a slower rise time to bath application of forskolin and IBMX than ICUE2. This may be due to the fact that a change in FRET ratio for the PKA-based cAMP sensor requires the binding of four cAMP molecules and dissociation of PKA, while ICUE2 requires the binding of a single cAMP molecule. Other indicators featuring a single cAMP binding site had comparable kinetics to ICUE2 (Nikolaev et al., 2004; Nikolaev et al., 2006).

The timecourse of the AKAR response is determined by three components: cAMP accumulation, PKA phosphorylation rate, and the intrinsic kinetics of the indicator. Uncaging cAMP in cardiac myocytes and hippocampal neurons led to an immediate increase in FRET ratio change of AKAR2, suggesting that the delay due to phosphorylation and the intrinsic kinetics of the

indicator is less than five seconds (Saucerman et al., 2006; Gervasi et al., 2007). Therefore, the predominant component of the time course of AKAR is cAMP accumulation. However, since AKAR reports PKA activity, and a single PKA catalytic subunit can phosphorylate many target substrates, AKAR may have faster response kinetics than the indicators relying on cAMP binding sites. Since AKAR rapidly responds to changes in cAMP concentration, the time to peak has been used as measure of the timecourse of the propagation of cAMP/PKA signals across the cytosol. In response to bath application of forskolin, the AKAR2.2 FRET ratio in the soma of hippocampal neurons increases immediately upon application of the drug, and reaches to 90% of its maximum in 2.5-minutes (Gervasi et al., 2007). In response to short depolarizations and short applications of forskolin the AKAR2.2 FRET ratio in the soma of retinal ganglion cells reaches to its maximum in 20 seconds. This difference with hippocampal neurons is likely due to the shorter stimulus time, as cAMP will continue to accumulate during constant exposure to forskolin. It is important to note that the temporal response of AKAR to phosphorylation by PKA, whether it is the onset of the response, the rate at which the ratio change increases and decreases, or the maximum FRET ratio change, may be different than the endogenous targets of PKA.

Third, overexpression of the various FRET indicators may disrupt the cAMP/PKA pathway in neurons through a variety of ways. (1) Indicators that contain high affinity binding sites for cAMP may buffer cAMP and therefore interfere with the endogenous signaling and feedback on the pathway. (2)

Indicators, particularly the PKA-based and full-length Epac-based indicators, may provide diffusion barriers that spatially sequester the cAMP more than usual. It has been suggested that the limited diffusibility of PKA allows it to serve as a barrier to cAMP diffusion in the same way that some calcium binding proteins limit the diffusion of calcium, thereby overemphasizing the presence of microdomains (Saucerman et al., 2006). (3) Catalytically active enzymes may alter PKA signaling in basal conditions, as was reported for FlCRhR (Goaillard et al., 2001). However, in hippocampal neurons, AKAR overexpression did not block PKA-dependent phosphorylation of an endogenous ion channel indicating endogenous PKA substrates were not affected (Gervasi et al., 2007).

Fourth, it has been reported that FRET ratios decrease in response to nonspecific biochemical interactions with ATP (Willemse et al., 2007). Hence, it is critical to determine whether changes in FRET ratio are a result of activation of cAMP as opposed to a result of changes in ATP. For this reason, it is advantageous to use pairs of indicators that have opposite FRET ratio changes in response to increases in the cAMP/PKA pathway, for example AKARs increase FRET ratio with increased PKA activity, while PKA- and Epac-based FRET sensors decrease FRET ratio with increased cAMP concentration.

**Imaging the interplay of intracellular cAMP and calcium concentrations**

The close interplay of cAMP and calcium pathways and the importance for both in guiding cellular responses to various inputs make combined imaging of the two an enticing prospect (DeBernardi and Brooker, 1996). For example in

developing spinal cord neurons, certain patterns of calcium influx lead to transient increases in cAMP, and, reciprocally, cAMP levels regulated the frequency of calcium transients (Gorbunova and Spitzer, 2002) (see Figure 1.3). This has led to the idea that the frequency of calcium transients is tuned to drive cAMP transients (Zaccolo and Pozzan, 2003; Borodinsky and Spitzer, 2006; Willoughby and Cooper, 2006). Simultaneous imaging of Epac based FRET reporters and the calcium indicator, fura-2, have led to detailed description of the interactions between calcium and cAMP oscillations in various non-neuronal cell types (Landa et al., 2005; Harbeck et al., 2006; Willoughby and Cooper, 2006). Applying these quantitative methods to spontaneously active neurons will yield tremendous insight into the function of periodic calcium and cAMP transients.

**Hypotheses regarding the role of periodic activation of second messengers in neurodevelopment**

There are several examples throughout the nervous system that indicate that infrequent activation of neurons is critical for driving specific developmental programs. These examples can be broken into two categories – regulation of transcription and post-translational modification. Using transcriptional assays, several groups have found that certain transcription factors are preferentially activated by rhythmic stimuli, not continuous stimuli (Itoh et al., 1995; Fields et al., 1997; Itoh et al., 1997; Dolmetsch et al., 1998; Li et al., 1998). In addition, altering the pattern of rhythmic activity in immature spinal cord neurons alters

neurotransmitter expression, likely through transcriptional regulation (Borodinsky et al., 2004). Similarly, Hanson and Landmesser found that the frequency of rhythmic bursting in spinal motoneurons was necessary for expression of ephrinA4 (Hanson and Landmesser, 2004).

There is also evidence that periodic activation of networks alters post-translational modifications of existing proteins. Post-translation modifications such as phosphorylation are typically thought of as rapid onset, transient alterations of proteins. The repetitive nature of spontaneous activity offers a mechanism by which post-translational modifications might be maintained over long periods (Wu et al., 2001). For example, decreasing the frequency of periodic bursting in spinal cord neurons leads to a lack of polysialic acid on NCAM in spinal motoneurons which leads to axon pathfinding errors, probably by way of failed defasiculation (Hanson and Landmesser, 2004). Whether this represents a general function of spontaneous activity in developing neurons remains to be determined.

**Implications for activity-dependent developmental processes in visual system**

Do slow oscillations in cAMP levels play a role in refinement of retinal ganglion cell projections? The cAMP/PKA pathway has been implicated by findings that show mice that lack adenylyl cyclase 1 (AC1) have both reduced eye-specific segregation of retinogeniculate axons within the dLGN (Ravary et al., 2003) and reduced retinotopic refinement in the SC (Ravary et al., 2003; Plas

et al., 2004). AC1 is found in the retina, dLGN, and SC (Ravary et al., 2003; Plas et al., 2004; Nicol et al., 2005). Recently, Nicol et al. (Nicol et al., 2006) used a co-culture system to demonstrate that retinal explants from WT mice refine normally in the presence of explants from an AC1-/- superior colliculus, while retinal explants from AC1-/- mice failed to refine in the presence of SC explants from WT mice. Based on these studies, it was proposed that the failure in segregation is due to a defect of AC1 in the retina.

How does AC1 in the retina regulate activity-dependent refinement? First, it may be functioning cell autonomously in retinal ganglion cells. Recently, it has been reported that AC1 is necessary in retinal ganglion cells for repulsive responses to exogenous ephrin (Nicol et al., 2006). In addition, it was demonstrated spontaneous retinal activity is necessary for repulsive responses to ephrin (Nicol et al., 2007). This lack of responsiveness is rescued by uncaging cAMP in a periodic manner. These results lead to the intriguing hypothesis that retinal waves drive periodic activation of the cAMP/PKA pathway that is required for ephrin mediated repulsion. Second, AC1 modulates synaptic transmission (Lu et al., 2006), and therefore may be that the level of reading out the activity-dependent competition that leads to refinement (Katz and Shatz, 1996; Crair, 1999; Butts, 2002; Butts et al., 2007). Third, mice lacking normal level of phosphorylated CREB, a target of PKA activity have reduced map refinement, indicating a role of postsynaptic cAMP/PKA signaling in LGN neurons (Pham et al., 2001). By using imaging to determine the spatial and temporal properties of cAMP/PKA signaling, we will be able to gain insights in the specific

developmental mechanisms by which activity influences several aspects of neural development.

**ACKNOWLEDGEMENTS**

Chapter 1, in full, is a reprint of the material as it appears in Dunn TA, Feller MB. 2008. Imaging second messenger dynamics in developing neural circuits. Developmental Neurobiology 68:835-844.

**REFERENCES**

Adams SR, Harootunian AT, Buechler YJ, Taylor SS, Tsien RY. 1991. Fluorescence ratio imaging of cyclic AMP in single cells. Nature 349:694-697.

Adelsberger H, Garaschuk O, Konnerth A. 2005. Cortical calcium waves in resting newborn mice. Nat Neurosci 8:988-990. Epub 2005 Jul 2010.

Aguilo A, Schwartz TH, Kumar VS, Peterlin ZA, Tsiola A, Soriano E, Yuste R. 1999. Involvement of cajal-retzius neurons in spontaneous correlated activity of embryonic and postnatal layer 1 from wild-type and reeler mice. J Neurosci 19:10856-10868.

Allen MD, Zhang J. 2006. Subcellular dynamics of protein kinase A activity visualized by FRET-based reporters. Biochemical And Biophysical Research Communications 348:716-721.

Bacskai BJ, Hochner B, Mahaut-Smith M, Adams SR, Kaang BK, Kandel ER, Tsien RY. 1993. Spatially resolved dynamics of cAMP and protein kinase A subunits in Aplysia sensory neurons. Science 260:222-226.

Beene DL, Scott JD. 2007. A-kinase anchoring proteins take shape. Curr Opin Cell Biol 19:192-198. Epub 2007 Feb 2020.

Ben-Ari Y, Cherubini E, Corradetti R, Gaiarsa JL. 1989. Giant synaptic potentials in immature rat CA3 hippocampal neurones. J Physiol 416:303-325.

Borodinsky LN, Root CM, Cronin JA, Sann SB, Gu X, Spitzer NC. 2004. Activity-dependent homeostatic specification of transmitter expression in embryonic neurons. Nature 429:523-530.

Borodinsky LN, Spitzer NC. 2006. Second messenger pas de deux: the coordinated dance between calcium and cAMP. Sci STKE 2006:pe22.

Butts DA. 2002. Retinal waves: implications for synaptic learning rules during development. Neuroscientist 8:243-253.

Butts DA, Kanold PO, Shatz CJ. 2007. A Burst-Based "Hebbian" Learning Rule at Retinogeniculate Synapses Links Retinal Waves to Activity-Dependent Refinement. PLoS Biol 5:e61.

Colin-Le Brun I, Ferrand N, Caillard O, Tosetti P, Ben-Ari Y, Gaiarsa JL. 2004. Spontaneous synaptic activity is required for the formation of functional GABAergic synapses in the developing rat hippocampus. J Physiol 559:129-139.

Crair MC. 1999. Neuronal activity during development: permissive or instructive? Curr Opin Neurobiol 9:88-93.

DeBernardi MA, Brooker G. 1996. Single cell Ca2+/cAMP cross-talk monitored by simultaneous Ca2+/cAMP fluorescence ratio imaging. Proc Natl Acad Sci U S A 93:4577-4582.

DiPilato LM, Cheng X, Zhang J. 2004. Fluorescent indicators of cAMP and Epac activation reveal differential dynamics of cAMP signaling within discrete subcellular compartments. Proc Natl Acad Sci U S A 101:16513-16518. Epub 12004 Nov 16515.

Dolmetsch RE, Xu K, Lewis RS. 1998. Calcium oscillations increase the efficiency and specificity of gene expression [see comments]. Nature 392:933-936.

Dunn TA, Wang CT, Colicos MA, Zaccolo M, DiPilato LM, Zhang J, Tsien RY, Feller MB. 2006. Imaging of cAMP levels and protein kinase a activity reveals that retinal waves drive oscillations in second-messenger cascades. Journal Of Neuroscience 26:12807-12815.

Dyachok O, Isakov Y, Sagetorp J, Tengholm A. 2006. Oscillations of cyclic AMP in hormone-stimulated insulin-secreting beta-cells. Nature. 439:349-352.

Feller MB. 1999. Spontaneous correlated activity in developing neural circuits. Neuron 22:653-656.

Feller MB, Wellis DP, Stellwagen D, Werblin FS, Shatz CJ. 1996. Requirement for cholinergic synaptic transmission in the propagation of spontaneous retinal waves. Science 272:1182-1187.

Fields RD, Eshete F, Stevens B, Itoh K. 1997. Action potential-dependent regulation of gene expression: temporal specificity in ca2+, cAMP-responsive element binding proteins, and mitogen-activated protein kinase signaling. J Neurosci 17:7252-7266.

Garaschuk O, Hanse E, Konnerth A. 1998. Developmental profile and synaptic origin of early network oscillations in the CA1 region of rat neonatal hippocampus. J Physiol 507 (Pt 1):219-236.

Gervasi N, Hepp R, Tricoire L, Zhang J, Lambolez B, Paupardin-Tritsch D, Vincent P. 2007. Dynamics of protein kinase A signaling at the membrane, in the cytosol, and in the nucleus of neurons in mouse brain slices. J Neurosci 27:2744-2750.

Goaillard JM, Vincent P. 2002. Serotonin suppresses the slow afterhyperpolarization in rat intralaminar and midline thalamic neurones by activating 5-HT(7) receptors. J Physiol 541:453-465.

Goaillard JM, Vincent PV, Fischmeister R. 2001. Simultaneous measurements of intracellular cAMP and L-type Ca2+ current in single frog ventricular myocytes. J Physiol 530:79-91.

Goldberg JL, Espinosa JS, Xu Y, Davidson N, Kovacs GT, Barres BA. 2002. Retinal ganglion cells do not extend axons by default: promotion by neurotrophic signaling and electrical activity. Neuron. 33:689-702.

Gorbunova YV, Spitzer NC. 2002. Dynamic interactions of cyclic AMP transients and spontaneous Ca(2+) spikes. Nature 418:93-96.

Gust J, Wright JJ, Pratt EB, Bosma MM. 2003. Development of synchronized activity of cranial motor neurons in the segmented embryonic mouse hindbrain. J Physiol 550:123-133.

Hanson MG, Landmesser LT. 2003. Characterization of the circuits that generate spontaneous episodes of activity in the early embryonic mouse spinal cord. Journal Of Neuroscience 23:587-600.

Hanson MG, Landmesser LT. 2004. Normal patterns of spontaneous activity are required for correct motor axon guidance and the expression of specific guidance molecules. Neuron 43:687-701.

Harbeck MC, Chepurny O, Nikolaev VO, Lohse MJ, Holz GG, Roe MW. 2006. Simultaneous optical measurements of cytosolic Ca2+ and cAMP in single cells. Sci STKE 2006:pl6.

Hempel CM, Vincent P, Adams SR, Tsien RY, Selverston AI. 1996. Spatio-temporal dynamics of cyclic AMP signals in an intact neural circuitm. Nature 384:166-169.

Holz GG, Kang G, Harbeck M, Roe MW, Chepurny OG. 2006. Cell physiology of cAMP sensor Epac. J Physiol 577:5-15.

Huberman AD. 2006. Nob mice wave goodbye to eye-specific segregation. Neuron 50:175-177.

Itoh K, Ozaki M, Stevens B, Fields RD. 1997. Activity-dependent regulation of N-cadherin in DRG neurons: differential regulation of N-cadherin, NCAM, and L1 by distinct patterns of action potentials. J Neurobiol 33:735-748.

Itoh K, Stevens B, Schachner M, Fields RD. 1995. Regulated expression of the neural cell adhesion molecule L1 by specific patterns of neural impulses. Science 270:1369-1372.

Katz LC, Shatz CJ. 1996. Synaptic activity and the construction of cortical circuits. Science 274:1133-1138.

Khalilov I, Le Van Quyen M, Gozlan H, Ben-Ari Y. 2005. Epileptogenic actions of GABA and fast oscillations in the developing hippocampus. Neuron 48:787-796.

Kim YT, Wu CF. 1996. Reduced growth cone motility in cultured neurons from Drosophila memory mutants with a defective cAMP cascade. J Neurosci 16:5593-5602.

Kunkel MT, Toker A, Tsien RY, Newton AC. 2007. Calcium-dependent regulation of protein kinase D revealed by a genetically encoded kinase activity reporter. J Biol Chem 282:6733-6742.

Landa LR, Jr., Harbeck M, Kaihara K, Chepurny O, Kitiphongspattana K, Graf O, Nikolaev VO, Lohse MJ, Holz GG, Roe MW. 2005. Interplay of Ca2+ and cAMP signaling in the insulin-secreting MIN6 beta-cell line. J Biol Chem 280:31294-31302. Epub 32005 Jun 31229.

Li W, Llopis J, Whitney M, Zlokarnik G, Tsien RY. 1998. Cell-permeant caged InsP3 ester shows that Ca2+ spike frequency can optimize gene expression. Nature 392:936-941.

Lissandron V, Terrin A, Collini M, D'Alfonso L, Chirico G, Pantano S, Zaccolo M. 2005. Improvement of a FRET-based indicator for cAMP by linker design and stabilization of donor-acceptor interaction. Journal Of Molecular Biology 354:546-555.

Lissandron V, Zaccolo M. 2006. Compartmentalized cAMP/PKA signalling regulates cardiac excitation-contraction coupling. Journal Of Muscle Research And Cell Motility 27:399-403.

Lohof AM, Quillan M, Dan Y, Poo MM. 1992. Asymmetric modulation of cytosolic cAMP activity induces growth cone turning. J Neurosci. 12:1253-1261.

Meberg PJ, Ono S, Minamide LS, Takahashi M, Bamburg JR. 1998. Actin depolymerizing factor and cofilin phosphorylation dynamics: response to signals that regulate neurite extension. Cell Motil Cytoskeleton 39:172-190.

Ming G, Henley J, Tessier-Lavigne M, Song H, Poo M. 2001. Electrical activity modulates growth cone guidance by diffusible factors. Neuron 29:441-452.

Munck S, Bedner P, Bottaro T, Harz H. 2004. Spatiotemporal properties of cytoplasmic cyclic AMP gradients can alter the turning behaviour of neuronal growth cones. Eur J Neurosci. 19:791-797.

Nagai T, Yamada S, Tominaga T, Ichikawa M, Miyawaki A. 2004. Expanded dynamic range of fluorescent indicators for Ca(2+) by circularly permuted yellow fluorescent proteins. Proc Natl Acad Sci U S A 101:10554-10559.

Nicol X, Muzerelle A, Bachy I, Ravary A, Gaspar P. 2005. Spatiotemporal localization of the calcium-stimulated adenylate cyclases, AC1 and AC8, during mouse brain development. J Comp Neurol. 486:281-294.

Nicol X, Muzerelle A, Rio JP, Metin C, Gaspar P. 2006. Requirement of adenylate cyclase 1 for the ephrin-A5-dependent retraction of exuberant retinal axons. J Neurosci. 26:862-872.

Nicol X, Voyatzis S, Muzerelle A, Narboux-Neme N, Sudhof TC, Miles R, Gaspar P. 2007. cAMP oscillations and retinal activity are permissive for ephrin signaling during the establishment of the retinotopic map. Nat Neurosci 10:340-347.

Nikolaev VO, Bunemann M, Hein L, Hannawacker A, Lohse MJ. 2004. Novel single chain cAMP sensors for receptor-induced signal propagation. J Biol Chem 279:37215-37218. Epub 32004 Jul 37211.

Nikolaev VO, Bunemann M, Schmitteckert E, Lohse MJ, Engelhardt S. 2006. Cyclic AMP imaging in adult cardiac myocytes reveals far-reaching beta1-adrenergic but locally confined beta2-adrenergic receptor-mediated signaling. Circ Res 99:1084-1091. Epub 2006 Oct 1012.

O'Donovan MJ. 1999. The origin of spontaneous activity in developing networks of the vertebrate nervous system. Curr Opin Neurobiol 9:94-104.

Pham TA, Rubenstein JL, Silva AJ, Storm DR, Stryker MP. 2001. The cre/creb pathway is transiently expressed in thalamic circuit development and contributes to refinement of retinogeniculate axons. Neuron 31:409-420.

Plas DT, Visel A, Gonzalez E, She WC, Crair MC. 2004. Adenylate Cyclase 1 dependent refinement of retinotopic maps in the mouse. Vision Res 44:3357-3364.

Ponsioen B, Zhao J, Riedl J, Zwartkruis F, van der Krogt G, Zaccolo M, Moolenaar WH, Bos JL, Jalink K. 2004. Detecting cAMP-induced Epac activation by fluorescence resonance energy transfer: Epac as a novel cAMP indicator. Embo Reports 5:1176-1180.

Ravary A, Muzerelle A, Herve D, Pascoli V, Ba-Charvet KN, Girault JA, Welker E, Gaspar P. 2003. Adenylate cyclase 1 as a key actor in the refinement of retinal projection maps. J Neurosci 23:2228-2238.

Rich TC, Fagan KA, Tse TE, Schaack J, Cooper DM, Karpen JW. 2001. A uniform extracellular stimulus triggers distinct cAMP signals in different compartments of a simple cell. Proc Natl Acad Sci U S A 98:13049-13054. Epub 12001 Oct 13016.

Rodger J, Goto H, Cui Q, Chen PB, Harvey AR. 2005. cAMP regulates axon outgrowth and guidance during optic nerve regeneration in goldfish. Mol Cell Neurosci. 30:452-464.

Ruthazer ES, Cline HT. 2004. Insights into activity-dependent map formation from the retinotectal system: a middle-of-the-brain perspective. J Neurobiol 59:134-146.

Sasaki K, Sato M, Umezawa Y. 2003. Fluorescent indicators for Akt/protein kinase B and dynamics of Akt activity visualized in living cells. J Biol Chem 278:30945-30951.

Saucerman JJ, Zhang J, Martin JC, Peng LX, Stenbit AE, Tsien RY, McCulloch AD. 2006. Systems analysis of PKA-mediated phosphorylation gradients in live cardiac myocytes. Proc Natl Acad Sci U S A 103:12923-12928.

Schwartz TH, Rabinowitz D, Unni V, Kumar VS, Smetters DK, Tsiola A, Yuste R. 1998. Networks of coactive neurons in developing layer 1. Neuron 20:541-552.

Shah RD, Chandrasekaran AR, Anishchenko A, Dunn TA, Elstrott J, Wang C-T, Feller MB, Crair MC. 2007. Personal coummunication. In.

Song HJ, Poo MM. 1999. Signal transduction underlying growth cone guidance by diffusible factors. Curr Opin Neurobiol 9:355-363.

Sonnenburg WK, Rybalkin SD, Bornfeldt KE, Kwak KS, Rybalkina IG, Beavo JA. 1998. Identification, quantitation, and cellular localization of PDE1 calmodulin-stimulated cyclic nucleotide phosphodiesterases. Methods 14:3-19.

Ting AY, Kain KH, Klemke RL, Tsien RY. 2001. Genetically encoded fluorescent reporters of protein tyrosine kinase activities in living cells. Proc Natl Acad Sci U S A 98:15003-15008.

Torborg CL, Feller MB. 2005. Spontaneous patterned retinal activity and the refinement of retinal projections. Progress In Neurobiology 76:213-235.

Vincent P, Brusciano D. 2001. Cyclic AMP imaging in neurones in brain slice preparations. J Neurosci Methods 108:189-198.

Violin JD, Zhang J, Tsien RY, Newton AC. 2003. A genetically encoded fluorescent reporter reveals oscillatory phosphorylation by protein kinase C. J Cell Biol 161:899-909.

Wang H, Storm DR. 2003. Calmodulin-regulated adenylyl cyclases: cross-talk and plasticity in the central nervous system. Mol Pharmacol 63:463-468.

Wang Q, Zheng JQ. 1998. cAMP-mediated regulation of neurotrophin-induced collapse of nerve growth cones. J Neurosci 18:4973-4984.

Wayman GA, Impey S, Storm DR. 1995. Ca2+ inhibition of type III adenylyl cyclase in vivo. J Biol Chem 270:21480-21486.

Willemse M, Janssen E, de Lange F, Wieringa B, Fransen J. 2007. ATP and FRET--a cautionary note. Nat Biotechnol 25:170-172.

Willoughby D, Cooper DM. 2006. Ca2+ stimulation of adenylyl cyclase generates dynamic oscillations in cyclic AMP. J Cell Sci 119:828-836.

Wong RO, Meister M, Shatz CJ. 1993. Transient period of correlated bursting activity during development of the mammalian retina. Neuron 11:923-938.

Wong ROL. 1999. Role of retinal waves in visual system development. Annual Review of Neuroscience 22.

Wu GY, Deisseroth K, Tsien RW. 2001. Spaced stimuli stabilize MAPK pathway activation and its effects on dendritic morphology. Nat Neurosci 4:151-158.

Xia Z, Storm DR. 1997. Calmodulin-regulated adenylyl cyclases and neuromodulation. Curr Opin Neurobiol 7:391-396.

Zaccolo M, De Giorgi F, Cho CY, Feng LX, Knapp T, Negulescu PA, Taylor SS, Tsien RY, Pozzan T. 2000. A genetically encoded, fluorescent indicator for cyclic AMP in living cells. Nature Cell Biology 2:25-29.

Zaccolo M, Pozzan T. 2002. Discrete microdomains with high concentration of cAMP in stimulated rat neonatal cardiac myocytes. Science 295:1711-1715.

Zaccolo M, Pozzan T. 2003. CAMP and Ca2+ interplay: a matter of oscillation patterns. Trends Neurosci 26:53-55.

Zhang J, Hupfeld CJ, Taylor SS, Olefsky JM, Tsien RY. 2005. Insulin disrupts beta-adrenergic signalling to protein kinase A in adipocytes. Nature 437:569-573.

Zhang J, Ma Y, Taylor SS, Tsien RY. 2001. Genetically encoded reporters of protein kinase A activity reveal impact of substrate tethering. Proc Natl Acad Sci U S A 98:14997-15002.

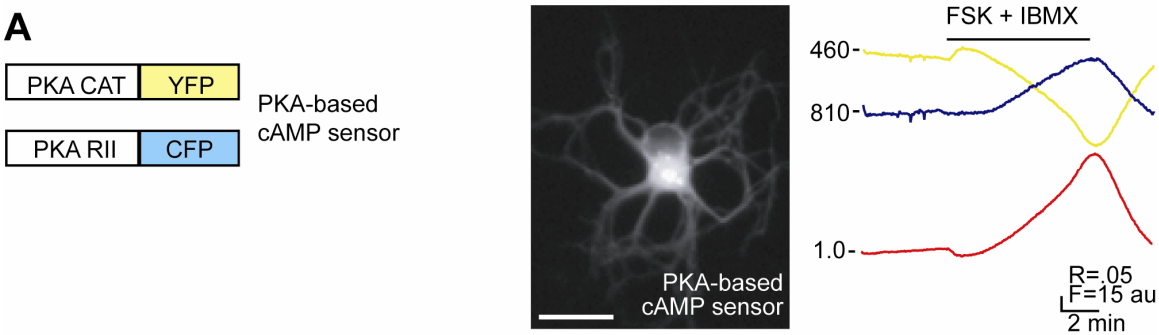


**Figure 1.1 Schematics of genetically encoded, FRET based cAMP level and PKA activity sensors**.

A. LEFT: Schematic of the PKA-based cAMP sensors. CFP and YFP are C-terminal fusions to the regulatory and catalytic subunits of PKA (Lissandron, 2005). MIDDLE: Fluorescence image of a dissociated retinal neuron expressing PKA based cAMP sensor. RIGHT: Time course of $F_{CFP}$ (blue), $F_{YFP}$ (yellow), and the FRET ratio (red) of $F_{YFP}/F_{CFP}$ for the PKA-based cAMP sensor during application of both the adenylyl cyclase activator forskolin (10µM) and phosphodiesterase inhibitor IBMX (100µM). Bar represents time of drug applications. All ratios are corrected for CFP bleedthrough into YFP channel and differential bleaching of the two fluorophores. Elevation of cAMP leads to decreases in FRET ratio. Ratio trace is inverted to show increases in cAMP as upward deflections.

MIDDLE and RIGHT, Modified from Dunn, Wang et al. 2006

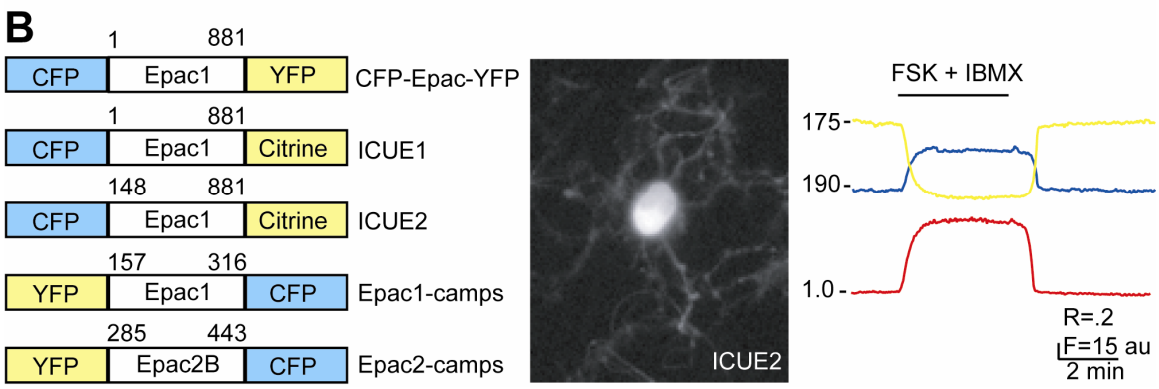


**Figure 1.1 (continued)**
B. LEFT: Schematics of EPAC-based sensors: Different truncations of the exchange protein activated by CAMP (Epac) are sandwiched between a CFP/YFP FRET pair. The different variations have different binding affinities for cAMP (Ponsioen, 2004). MIDDLE: Fluorescence image of a dissociated retinal neuron expressing ICUE2. RIGHT: Time course of $F_{CFP}$ (blue), $F_{YFP}$ (yellow), and the FRET ratio (red) of $F_{YFP}/F_{CFP}$ for ICUE2 where elevation of cAMP leads to decreases in FRET ratio. Ratio trace is inverted to show increases in cAMP as upward deflections.
MIDDLE and RIGHT, Modified from Dunn, Wang et al. 2006

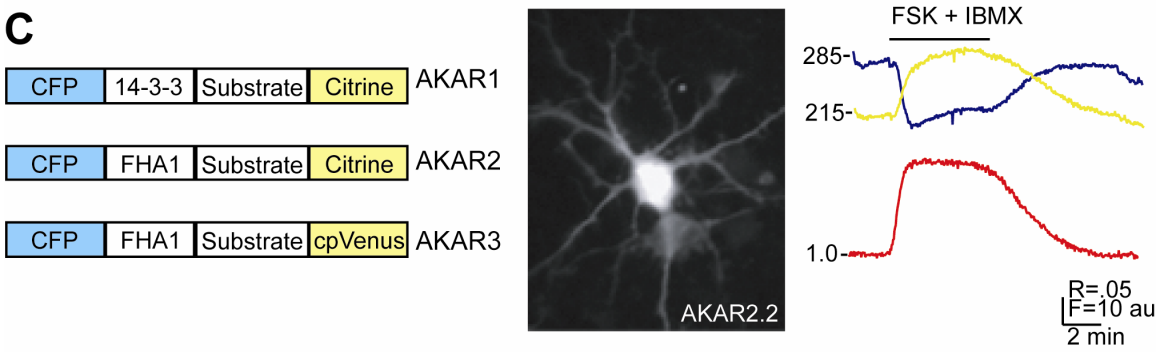


**Figure 1.1 (continued)**
C. LEFT: Schematic of the PKA activity reporters. Modified from Zhang, 2001. A-kinase activity reporters (AKARs) consist of a fusion of CFP and YFP to either a FHA1 or 14-3-3 phosphobinding region and PKA target substrate. Different variations have varying dynamic range and dephosphorylation rates. MIDDLE: Fluorescence image of a dissociated retinal neuron expressing AKAR2.2. RIGHT: Time course of $F_{CFP}$ (blue), $F_{YFP}$ (yellow), and the FRET ratio (red) of $F_{YFP}/F_{CFP}$ for the AKAR2.2 where elevation of PKA activity leads to increases in FRET ratio.
MIDDLE and RIGHT, Modified from Dunn, Wang et al. 2006

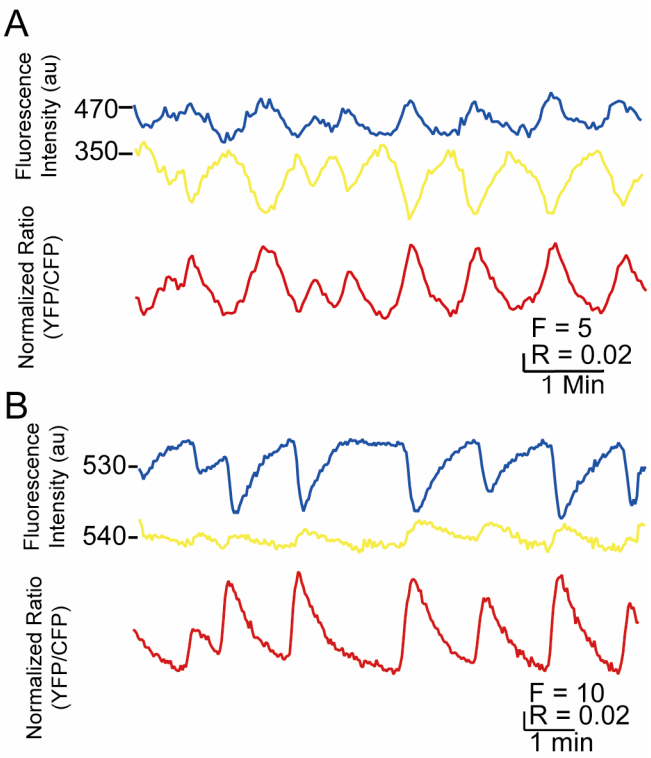


**Figure 1.2 Spontaneous changes in cAMP levels and PKA activity in retinal ganglion cells during retinal waves.**

A. Time course of $F_{CFP}$ (blue), $F_{YFP}$ (yellow) recorded simultaneously and averaged over the cell body of a RGC expressing ICUE2. The ICUE2 FRET ratio is computed as $F_{YFP}/F_{CFP}$, inverted to show cAMP increases as upward deflections, corrected for CFP bleedthrough into YFP channel, and corrected for differential bleaching of CFP and YFP.

B. Time course of $F_{CFP}$ (blue), $F_{YFP}$ (yellow) recorded simultaneously and averaged over the cell body of a RGC expressing AKAR2.2. The ratio is computed as $F_{YFP}/F_{CFP}$, corrected for CFP bleedthrough into YFP channel and corrected for differential bleaching. From Dunn, Wang et al., 2006.

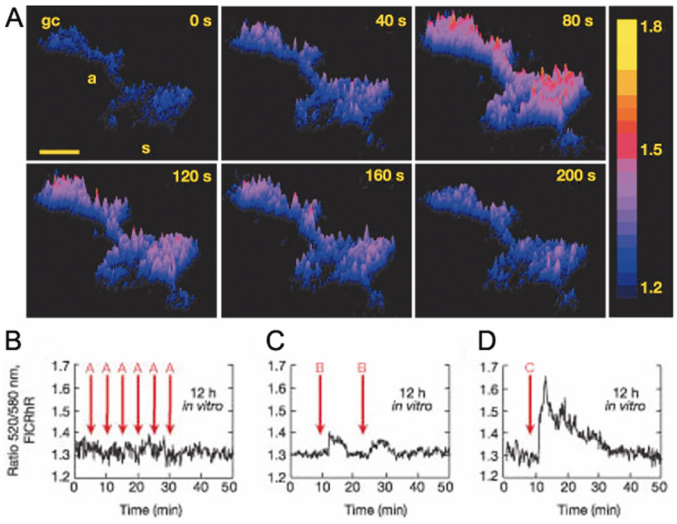


**Figure 1.3 Spontaneous oscillations in cAMP are driven by certain patterns of calcium spikes in spinal neurons.**

A. Surface plot images show a spontaneous, transient increase in cAMP concentration in an immature spinal neuron loaded with the ratiometric dye, FlCRhR. Color scale represents the 520 nm/580 nm fluorescence ratio. (s) soma, (a) axon, (gc) growth cone. Scale bar, 10 μm.

B-D. Fluorescence ratio traces of $F_{520}/F_{580}$ in a spinal neuron loaded with FlCRhR show cAMP response to induced calcium influx. Arrows indicate stimulated $Ca^{2+}$ spikes. (A) single spikes, (B) three spikes, (C) five spikes. From Gorbunova and Spitzer, 2002.

Chapter 2
From: Journal of Neuroscience

# Imaging of cAMP levels and PKA activity reveals that retinal waves drive oscillations in second messenger cascades

Timothy A. Dunn[1*], Chih-Tien Wang[1*], Michael A. Colicos[1,2], Manuela Zaccolo[3], Lisa M. DiPilato[5], Jin Zhang[4,5], Roger Y. Tsien[4], Marla B. Feller[1]

[1]Neurobiology Section, Division of Biological Sciences, UCSD, La Jolla, CA, USA.

[2]current address: Department of Physiology and Biophysics, University of Calgary

[3] Dulbecco Telethon Institute, Venetian Institute of Molecular Medicine, ITALY

[4] Departments of Pharmacology and Chemistry/Biochemistry and Howard Hughes Medical Institute, UCSD, La Jolla, CA, USA

[5] current address: Departments of Pharmacology and Molecular Sciences and Neuroscience, The Johns Hopkins University School of Medicine

*These two authors contributed equally.

Correspondence should be addressed to

Marla B. Feller
Neurobiology Section 0357
UCSD, 9500 Gilman Dr.
La Jolla, CA 92093-0357
mfeller@ucsd.edu
858-822-4273

**ABSTRACT**

Recent evidence demonstrates that low frequency oscillations of intracellular calcium on time scales of seconds to minutes drive distinct aspects of neuronal development, but the mechanisms by which these calcium transients are coupled to signaling cascades are not well understood. Here we test the hypothesis that spontaneous electrical activity activates protein kinase A (PKA). We utilize live-cell indicators to observe spontaneous and evoked changes in cAMP levels and PKA activity in developing retinal neurons. Expression of cAMP and PKA indicators in neonatal rat retinal explants reveals spontaneous oscillations in PKA activity that are temporally correlated with spontaneous depolarizations associated with retinal waves. In response to short applications of forskolin, dopamine or high potassium concentration, we image an increase in cAMP levels and PKA activity, indicating this second messenger pathway can be activated quickly by neural activity. Depolarization-evoked increases in PKA activity were blocked by the removal of extracellular calcium, indicating they are mediated by a calcium-dependent mechanism. These findings demonstrate for the first time that spontaneous activity in developing circuits is correlated with activation of the cAMP/PKA pathway, and that PKA activity is turned on and off on the timescale of tens of seconds. These results show a link between neural activity and an intracellular biochemical cascade associated with plasticity, axon guidance and neural differentiation.

## INTRODUCTION

Neuronal activity is linked to long-term changes in cells, such as activity-dependent expression of genes, by activation of second messenger cascades (West et al., 2002). Though several such cascades have been identified, there is a short list of second messengers, such as calcium, cAMP, cGMP, DAG, and IP3 that mediate these effects. Therefore the activation of specific cascades is not likely to be determined by overall concentrations of second messengers but rather by subcellular spatial localization and dynamic changes in their concentrations. Oscillations have been detected in both calcium and cAMP concentrations, and there is growing evidence that these oscillations are "tuned" to drive particular cellular events (Zaccolo and Pozzan, 2003; Spitzer et al., 2004; Fields et al., 2005; Dyachok et al., 2006).

The establishment and refinement of retinal projection patterns occurs at an early stage of development, prior to the development of vision (for reviews, see Grubb and Thompson, 2004; Ruthazer and Cline, 2004; for reviews, see Torborg and Feller, 2005). During this time, retinal ganglion cells (RGCs) exhibit spontaneous bursts of action potentials that periodically propagate across the developing ganglion cell layer, an activity pattern termed retinal waves (Meister et al., 1991; Wong et al., 1993). The cAMP/PKA pathway has been implicated in the establishment and normal refinement of RGC axonal projections. Knockout mice lacking calcium-activated adenylate cyclase 1, an enzyme that produces cAMP, exhibit defects in retinotopic and eye-specific refinement (Ravary et al., 2003; Plas et al., 2004). Knockdown of the transcription factor CREB, a known

target of PKA, leads to a reduction in eye-specific segregation (Pham et al., 2001). These effects of the cAMP/PKA pathway on refinement of retinal projections may be mediated by activation of this pathway in RGCs, perhaps by regulating the response of RGC growth cones to guidance molecules (Nicol et al., 2006) or modulating release probability at RGC axon terminals (Lu et al., 2006). Although spontaneous patterned activity and the cAMP/PKA pathway are important for the establishment of retinal projections, how retinal waves affect the cAMP/PKA second messenger cascades either in RGCs or their targets remains unknown.

Here we used three genetically encoded fluorescence-based indicators to monitor the cAMP/PKA pathway in both dissociated retinal neurons and the intact retina. The indicators are: 1) a PKA based cAMP sensor (CS) (Zaccolo et al., 2002), 2) ICUE2 (indicator of cAMP using Epac), which is modified from ICUE1 (DiPilato et al., 2004) and 3) A-Kinase Activity Reporter, AKAR2.2 (Zhang et al., 2001; Zhang et al., 2005), which undergoes changes in its fluorescent properties in response to phosphorylation by PKA. To demonstrate the utility of CS, ICUE2, and AKAR2.2, we compared their responses to direct activation of adenylate cyclase, to activation of G-protein coupled receptors by dopamine, and to depolarization. We also detected spontaneous oscillations in cAMP levels and PKA activity in retinal explants. These oscillations were blocked by agents that block retinal waves, and exhibited a temporal correlation to spontaneous depolarizations associated with retinal waves. Together, these findings indicate that retinal waves induce oscillations in cAMP levels and PKA activity in RGCs.

**METHODS**

Dissociated cultures: Dissociated neurons and glia from postnatal day 1 (P1) rat retinas were plated on coverslips, with a subset of cultures placed on superior colliculus cultures from litter mates plated the day before as described previously (Colicos et al., 2004). Cells were plated on surfaces treated with 10 µg/mL poly-D-lysine (70 kD, Sigma) overnight, followed by 2 µg/mL laminin for 2 h at 37 ℃. Retinal neurons were plated at a density of 2 x $10^4$ cells /$cm^2$ in serum-free Neurobasal medium (serum free culture media, SFCM) supplemented with B27 (Gibco), 0.6% glucose, 2mM glutamine, 10mM HEPES, 1mM Na-Pyruvate, 50 µg/mL penicillin G, 50 units/mL streptomycin, 2.5µg/mL Insulin, 6 µM forskolin, 10ng/mL CNTF & 50ng/mL BDNF. Forskolin was added to the medium to ensure survival of RGCs (Meyer-Franke et al., 1995). It is not known whether forskolin enhances cell survival by elevating baseline levels of activity or by influencing periodic activation of the cAMP/PKA pathway. To avoid complications with the interpretation of cAMP imaging experiments, cultures were removed from forskolin-containing media for 10 hours prior to experiments. Control experiments indicated stable baselines of cAMP after this treatment.

Transfections: Transfection of dissociated neurons was performed by electroporation using an exponentially decaying pulse. Acutely isolated whole retinas from P0-P2 rats were mounted on filter paper precoated with 100 µg/µL poly-D-lysine and 50 µg/µL laminin. They were incubated in dissection solution (Colicos et al., 2004) containing plasmid DNA (concentration ~ 0.2 µg/µL) for 10 min and then electroporated with two square wave pulses with an electric field

strength of 6.75V/mm, then allowed to recover for 10 min in dissection solution and cultured in SFCM-A (same media as above, except using Neurobasal-A). Overnight before imaging, electroporated retinas were transferred to SFCM-A without forskolin. For recordings, explants are placed ganglion cell layer up in a temperature-controlled chamber (30˚C, Warner Systems) mounted on the stage of an upright microscope (Zeiss Axioskop) and perfused continuously with artificial cerebrospinal fluid (ACSF: 119 mM NaCl, 2.5 mM KCl, 1.3 mM $MgCl_2$, 1.0 mM $K_2HPO_4$, 2.5 mM $CaCl_2$, 26.2 mM $NaHCO_3$, 11 mM D-glucose) bubbled with 95% $O_2$/5% $CO_2$. Explant health was assayed using whole cell recording to measure resting potentials, action potentials and spontaneous depolarizations (Figure 2.3). Imaging experiments without independent evidence of retinal waves in explants were discarded from analysis.

Imaging: Live imaging of FRET indicators was performed on an upright Zeiss Axioskop 2, using a 60x LUMPLFLW water immersion objective (Olympus). Individual FRET channel detection was accomplished by using a Dual-View image splitter with appropriate yellow and cyan channel filters. Images were captured on a Photometrics CoolSnap HQ CCD camera and analyzed in MetaMorph v6.3. Background fluorescence was subtracted from both channels and CFP bleedthrough into the YFP channel was corrected ($F_{YFP} = F_{FRET} - 0.51* F_{CFP}$)(Gordon et al., 1998; van Rheenen et al., 2004).

We conducted acceptor photobleaching experiments to measure FRET efficiency. FRET efficiency is defined as $E= 1-( F_{DA} / F_D)$ where $F_{DA}$ is the intensity of the donor (in our case, CFP) in the presence of the acceptor (YFP)

and $F_D$ is the intensity of the donor in the absence of the acceptor. In our experiments, YFP was only partially photobleached, so to compute $F_D$, we used the equation $F_D = (F- F_{DA})/x + F_{DA}$, where F is the CFP intensity after partial photobleaching of YFP and $x= (F_{A\text{-}pre} – F_{A\text{-}post})/F_{A\text{-}pre}$, the fraction of the acceptor that is photobleached.

FRET ratios are calculated as $R = (F_{YFP} / F_{CFP})$. The magnitude of drug or depolarization-induced change was represented by the change in FRET ratio. Changes in FRET ratio, ΔR, were computed by subtracting the value of the FRET ratio averaged over 5 images prior to manipulation from the value of the FRET ratio averaged over 5 images around the maximum response within 40 seconds after the drug application or depolarization. We observed oscillations in baseline lasting 1-3 frames; therefore an average of 5 frames (corresponding to 10 seconds) gave an accurate measure of the baseline without decrementing the amplitude of the induced changes. Note, for the cAMP sensor or ICUE2, increases in cAMP levels lead to a decrease in FRET efficiency. For ease of comparison, ratio changes for all three indicators are represented as the absolute value of $\Delta R=(F_{YFP}/F_{CFP})_{control}- (F_{YFP}/F_{CFP})_{manipulation}$. Live $Ca^{2+}$ imaging was performed with the same equipment as for FRET imaging. Fura-2-AM loading was performed as described previously (Bansal et al., 2000).

All pharmacological agents were purchased from Sigma. External solution for dissociated neurons contained 5 mM KCl, 123 mM NaCl, 3 mM $CaCl_2$, 2 mM $MgCl_2$, 10 mM glucose and 10 mM HEPES, pH was adjusted with NaOH to 7.3. High potassium solution was similar, with 100 mM KCl substituted for an

equivalent amount of NaCl. Short applications of dopamine or high $K^+$ external solution were delivered through a glass electrophysiology electrode (approximately 2 µm tip size, located less than 20 microns from transfected neuron) using a PV830 Pneumatic PicoPump at 2-10 psi, 50 msec pulse duration at 4 Hz to RGCs in retinal explants. The duration of dopamine and potassium applications was altered by increasing the number of pulses. For experiments with zero external calcium, ACSF was modified to replace 2.5 mM $CaCl_2$ with 2 mM EGTA and 1.7 mM $MgCl_2$.

Electrophysiology: Whole-cell voltage-clamp recordings from retinal explants were made using an Axopatch 200B amplifier and pClamp6 software (Axon Instruments). The intracellular solution consisted of 98.3 mM potassium-gluconate, 1.7 mM KCl, 0.6 mM EGTA, 5 mM $MgCl_2$, 2 mM $Na_2$-ATP, 0.3 mM GTP, 40 mM HEPES, pH 7.25 with KOH. The calculated $E_{Cl}$ was -60 mV in ACSF. Whole-cell current clamp recordings were used to compare spontaneous depolarizations recorded from explants and acutely isolated retinas (Figure 2.3). The duration of spontaneous depolarization was defined as the time between membrane potential deviations from baseline that were greater than 2X the RMS (which was approximately 0.5 mV at 5 kHz sampling).

Cell-attached recordings were used to depolarize RGCs transfected with AKAR2.2. We were unable to use whole-cell current clamp recordings since dialyzing the contents of the cell in whole cell configuration led to significantly decreased sensitivity of the indicator. Gigaohm seals were obtained with a series resistance of approximately 500 MOhm. Depolarizing pulses of 150 pA,

lasting 1-3 seconds, caused local increases in membrane potential of approximately 150mV.

## RESULTS

### *Expression of FRET indicators in dissociated retinal neurons*

To monitor cAMP levels and PKA activity in living mammalian neurons, we utilized three different genetically encoded indicators dependent upon fluorescence resonance energy transfer (FRET). The first, which we will refer to as the cAMP sensor (CS), utilizes an intermolecular FRET paradigm where CFP is fused to a regulatory subunit of PKA and YFP is fused to the catalytic subunit of PKA (Zaccolo et al., 2002). An increase in cAMP concentration results in the binding of two cAMP molecules to the regulatory subunit of this fusion protein, and a consequent release of the catalytic subunit. This results in a measurable decrease in FRET efficiency. The second indicator, ICUE2, consists of a fusion of CFP, a truncated form of Epac1 including a cAMP binding site, and YFP (modified from ICUE, described in DiPilato et al., 2004). Binding of cAMP to the site on Epac1 leads to a disruption of basal FRET interactions. The third indicator, AKAR2.2 (Zhang et al., 2005), is derived from AKAR2 (Zhang et al., 2001). Both AKAR2 and AKAR2.2 consist of a fusion of CFP, a phosphothreonine-binding domain (FHA1), a PKA consensus phosphorylation target, and the YFP variant citrine (Griesbeck et al., 2001). When PKA is activated, the catalytic subunit of PKA phosphorylates the target in AKAR2.2, causing a conformational change that increases FRET efficiency. AKAR2.2

differs from AKAR2 (Zhang et al., 2005) in that it includes A206K substitutions within both the CFP and YFP moieties to eliminate their tendency to dimerize (Zacharias et al., 2002). These mutations also greatly accelerate the phosphatase-mediated decrease in FRET efficiency that follows a PKA-induced increase in FRET efficiency (Kain et al, 2006).

To determine if the indicators were forming functional FRET pairs, a partial acceptor photobleach assay was performed for CS and AKAR2.2. For both indicators, $F_{CFP}$ significantly increased after YFP was selectively photobleached using 515nm light, indicating that before stimulation, there was a baseline FRET interaction for both indicators. We measured FRET efficiencies of 0.11± .09 (n=9) and 0.18± 0.06 (average ±SD, n=10) for CS and AKAR2.2, respectively (see Methods).

To characterize the physiological responses of CS, ICUE2, and AKAR2.2 the indicators were expressed in dissociated retinal neurons. Retinas from P0-P1 rats were dissociated and electroporated with plasmids encoding one of the three indicators. The neurons were plated and cultured *in vitro* for 2-4 days using conditions which promote survival of all classes of retinal neurons (Meyer-Franke et al., 1995; Goldberg et al., 2002; Colicos et al., 2004). The indicators were strongly expressed throughout the cell (Figures 2.1A-C). For comparisons across indicators, all ratio changes are represented as the absolute value of $\Delta R=(F_{YFP}/F_{CFP})_{control}-(F_{YFP}/F_{CFP})_{manipulation}$.

We next determined the maximal response of the indicators to direct elevation of intracellular levels of cAMP. Neurons expressing either CS, ICUE2,

or AKAR2.2 exhibited large responses to bath application of both the adenylate cyclase activator forskolin (10 µM) and the phosphodiesterase inhibitor IBMX (100 µM), a manipulation that strongly stimulates the cAMP/PKA pathway (Figures 2.1D-G)($\Delta R_{CS}$ =0.099±0.048, n=10; $\Delta R_{ICUE}$=0.346±0.065, n=8; $\Delta R_{AKAR}$=0.118±0.040, n=10). The response to forskolin alone was significantly smaller than the response to the combination of forskolin and IBMX for both AKAR2.2 ($\Delta R_{AKAR}$=0.044±0.014, n=8, $p<0.01$) and CS ($\Delta R_{CS}$=0.012±0.005, n=8, $p<0.01$) demonstrating that the indicator response was correlated with the strength of activation of the cAMP/PKA pathway. We found no correlation between the starting ratio and the size of the FRET ratio change, indicating a lack of saturation of the indicator while in the basal state or with forskolin alone (data not shown).

***Evoked changes in cAMP levels and PKA activity in retinal explants***

To determine the effectiveness of indicators in monitoring activation of the cAMP/PKA pathway in the intact retina, we introduced the plasmids into neonatal rat retinal explants using electroporation (see Methods). After 20 hours, indicators were strongly expressed in RGCs, readily identified by the appearance of axons at the inner retinal surface (an example of an AKAR2.2-expressing RGC is shown in Figure 2.2A).

First, we assessed the changes in PKA activity in response to brief application of forskolin (50µM). Short applications of forskolin caused a transient increase in the AKAR2.2 FRET ratio (Figure 2.2C, ΔR= 0.037± 0.012, n=6

neurons). The amplitude of the AKAR2.2 FRET ratio change did not change in calcium-free solutions (Figure 2.2C, ΔR= 0.036± 0.019, n=6 neurons, p=0.929). Hence, forskolin induced PKA activity in a calcium-independent manner. Second, we investigated whether AKAR2.2 could detect changes in PKA activity due to activation of G-protein coupled receptors. Dopamine D1 receptor immunolabelling is present throughout the IPL in neonate rats (Koulen, 1999), and D1R, but not D2R, mRNA is present in the ganglion cell layer of late prenatal rats (Schambra et al., 1994). D1-like receptors are positively coupled to adenylate cyclase; therefore, dopamine application in neonate rats is predicted to increase PKA activity. Indeed, brief application of dopamine (150μM) caused an increase in the AKAR2.2 FRET ratio in a majority RGCs (Figure 2.2B,ΔR=0.034±0.027, n=6/8 neurons).

Third, we investigated whether the cAMP/PKA pathway in RGCs is activated by depolarization in retinal explants. RGCs express calcium-dependent adenylate cyclases (Abdel-Majid et al., 2002; Nicol et al., 2005) and therefore depolarization is likely to elevate cAMP/PKA levels (Ferguson and Storm, 2004). Short applications of external solution containing high concentrations of KCl (105mM) to neurons expressing ICUE2 or AKAR2.2 induced changes in their FRET ratios (Figure 2.2C, $\Delta R_{ICUE}$=0.011±0.003, n=6 neurons, $\Delta R_{AKAR}$=0.010±0.006, n=12 neurons), about one-third the amplitude of those seen in response to forskolin or dopamine applications (Figure 2.2C). Depolarization-induced increases in AKAR2.2 FRET ratio were blocked in the presence of calcium-free external, implying that calcium influx is necessary for

depolarization-induced activation of the cAMP/PKA pathway in RGCs. Depolarization-induced increases in the AKAR2.2 FRET ratio were significantly inhibited by the presence of H89 (25 μM), a specific PKA inhibitor (Zhang et al., 2001) (Figure 2.2D, $\Delta R_{H89}/\Delta R_{control}$ = 0.25±0.10, n=7, p<0.0001), confirming that AKAR2.2 was reporting increases in PKA activity.

***Spontaneous oscillations in cAMP concentration and PKA activity are induced by and temporally correlated with retinal waves***

We have demonstrated that depolarization transiently activates the cAMP/PKA pathway. We next investigated the kinetics of the second messenger pathway in response to spontaneous depolarizations associated with retinal waves. As described above, we introduced ICUE2 and AKAR2.2 plasmids into neonatal retinal explants using electroporation. Calcium imaging and whole-cell current-clamp recordings from individual RGCs in retinal explants revealed that RGCs exhibited correlated increases in intracellular calcium and periodic spontaneous depolarizations, consistent with the persistence of retinal waves after 48 hours in culture (Figure 2.3). However, there was a decrease in the duration of depolarization in explants compared to acutely isolated retina (explant: duration = 1.7±0.6 sec, n=8; acutely isolated retina: duration = 3.9±0.5 sec, n=8, p<0.001). These shorter depolarizations were reflected in reduced amplitude calcium transients. While greater than ninety-five percent of cells in the ganglion cell layer exhibited spontaneous calcium transients in both acutely isolated and explanted retinas, there was a stark difference in amplitude in most

cells (Figure 2.3C). Sixty percent of cells in explant retinas exhibited average fractional changes in fluorescence of less than 4%, whereas only five percent of cells in acutely isolated retinas had calcium transients that small.

Despite this decrease in depolarization and calcium influx, we detected spontaneous increases in FRET ratio in a subset of RGCs expressing either ICUE2 or AKAR2.2. ($\Delta R_{ICUE}$=0.015 $\pm$ 0.011, n = 7/31 RGCs, Figure 2.4A; $\Delta R_{AKAR}$=0.025 $\pm$ 0.015, n = 12/96 RGCs, Figure 2.4B). The magnitude of FRET ratio changes for both ICUE2 and AKAR2.2 were similar in amplitude and kinetics to those induced by acute application of potassium in RGCs (rise time measured trough to peak: ICUE2: $\tau_{spontaneous}$=13.6 ± 3.7 sec, n=7; AKAR2.2: $\tau_{spontaneous}$=20.5 ± 4.6 sec, n=12; $\tau_{evoked}$=18.2±10.3 sec, n=14, p>0.5) (Figure 2.4D). These similarities suggest that retinal waves may lead to cAMP and PKA activity transients via depolarization.

Several observations indicate that spontaneous transients in PKA activity were induced by retinal waves. First, the spontaneous AKAR2.2 FRET ratio changes occurred with a periodicity similar to that of spontaneous depolarizations associated with retinal waves (peak-to-peak interval 2.05 $\pm$ 0.94 min, n=12, p=0.173). Second, spontaneous AKAR2.2 FRET ratio changes were blocked by bath application of the nicotinic acetylcholine receptor antagonist dihydro-$\beta$-erythroidine (10-20μM, DH□E), which reliably blocks retinal waves (n = 5, Figure 2.4C). Third, in one instance where we observed two transfected RGCs in the same field of view, we observed simultaneous AKAR2.2 FRET ratio changes (data not shown).

To determine whether the spontaneous PKA transients exhibit a consistent temporal relationship with retinal waves, we conducted simultaneous AKAR2.2 imaging and whole cell voltage clamp recordings from a nearby cell to detect the compound synaptic currents associated with retinal waves (n=38 waves from 4 cells, Figure 2.5A). We computed the "wave-triggered" AKAR2.2 FRET ratio change by averaging the segment of the FRET ratio for AKAR2.2 from 5 seconds preceding to 40 seconds following the compound PSC. We found that, on average, the AKAR2.2 FRET ratio increased following a barrage of synaptic current (Figure 2.5B). For comparison, we computed the wave-triggered fura-2 response using simultaneous whole cell recording and calcium imaging. In contrast to the AKAR2.2 FRET ratio change, the calcium increase in nearby cells occurred during the compound synaptic event (Figures 2.5C and D, n= 21 waves from 5 cells). This is consistent with previous measurements that indicate increases in intracellular calcium associated with retinal waves are driven by influx through voltage–gated channels during spontaneous depolarizations (Penn et al, 1998). Combined with the observation that blockade of retinal waves also blocks AKAR2.2 FRET ratio changes, the increase in FRET ratio following a retinal wave is consistent with the hypothesis that retinal waves induce PKA activity transients.

***Depolarization-induced activation of cAMP/PKA pathway requires 3-second long depolarizations and calcium influx***

Why do we detect spontaneous PKA transients in only a subset of RGCs? In transfected RGCs that did not exhibit spontaneous oscillations in the FRET ratio, we measured substantial ratio changes in response to bath application of forskolin (10 μM, $\Delta R = 0.091 \pm 0.058$, N = 5/5 neurons), demonstrating that the absence of oscillations is not due to a lack of functional AKAR2.2. In addition, we found that non-oscillating cells had detectable FRET ratio changes in response to strong depolarization either via short applications of high potassium solutions or cell-attached recordings (Figure 2.6). Based on these observations, we hypothesized that AKAR2.2 detected oscillations only in the RGCs that exhibited the strongest depolarizations during waves.

To quantify the magnitude of depolarization necessary to induce a PKA activity transient, we varied the duration of depolarization induced by short applications of a high potassium solution (Figure 2.6A, inset). Evoked FRET ratio changes and rise times are similar to those due to spontaneous PKA oscillations. We found that longer duration depolarizations more reliably induced detectable changes in FRET ratio of AKAR2.2, (n=11 RGCs, Figure 2.6B). To verify that these changes in FRET ratio were due to direct depolarization of RGCs, we reproduced these findings using a cell-attached patch electrode (Figures 2.6C and D) (n=10 RGCs). Using both stimulation methods, we found a significant increase in detectable AKAR2.2 FRET ratio changes in response to depolarizations greater than 2 seconds (Figure 2.6E).

Based on these observations, we hypothesize that the low percentage of RGCs with spontaneous PKA activity transients in explants is due to the shorter spontaneous depolarization associated with retinal waves (Figure 2.3). Hence, we would predict that in acutely isolated retina, or more importantly *in vivo*, where recent experiments report spiking bursts lasting 3-4 seconds (Hanganu et al., 2006), a larger percentage of RGCs exhibit PKA transients.

### *Depolarization-induced PKA activity transients require $Ca^{2+}$-influx*

Depolarization-induced activation of second messenger pathways are proposed to function via calcium-dependent adenylate cyclases (Ferguson and Storm, 2004). Calcium imaging of RGCs loaded with fura-2-AM revealed that longer duration depolarizations led to larger increases in intracellular calcium concentration (Figure 2.6F). Hence, longer depolarizations increase the likelihood of PKA activity transients because they lead to a larger increase in intracellular calcium. In addition, we found that removal of calcium from ACSF abolished the depolarization-induced AKAR2.2 FRET ratio changes observed in RGCs (Figure 2.6D) (n=17 events from 4 RGCs and 4 retinas). Together, these findings indicate that PKA activity transients in RGCs are induced by depolarization in a calcium-dependent manner.

## DISCUSSION

We demonstrate that live indicators for cAMP levels and PKA activity can reliably measure activation of this second messenger pathway in neurons in the

intact circuitry of the developing retina. In addition, our findings for the first time link spontaneous neural activity in developing networks with temporal oscillations in kinase activity. This temporal coding of second messenger pathway activation may be critical for the onset and timing of downstream developmental processes that are driven by spontaneous neural activity.

***Comparison of cAMP and PKA indicators***

We found that the genetically encoded indicators ICUE2 and AKAR2.2 reliably reported both evoked (Figures 2.1,2.2 and 2.6) and spontaneous (Figures 2.4 and 2.5) changes in cAMP concentration and PKA activity in retinal neurons. These measurable changes in FRET efficiency occurred as responses to either direct (via stimulation of adenylate cyclase, Figures 2.1B and 2.2A) or indirect (via activation of a G-protein coupled receptor or depolarization, Figures 2.2B-D) activation of the cAMP/PKA pathway. One notable difference between the three indicators was the kinetics of the response to strong stimulation (Figures 2.1D-F). The CS ratio change was much slower than that of ICUE2 and AKAR2.2. One possible explanation is that cAMP may activate PKA kinase activity before completely dissociating the regulatory and catalytic subunits (Yang et al., 1995; Nikolaev et al., 2004). For this reason, the CS FRET ratio changes occur only after PKA dissociates, while AKAR2.2 ratio changes occur faster. Similarly, ICUE2 FRET ratio changes will occur as cAMP concentration increases independent of PKA dissociation. In summary, we conclude that in our system, ICUE2 and AKAR2.2 function as more sensitive reporters for monitoring brief

activation of the cAMP/PKA pathway. These findings indicate that ICUE2 and AKAR2.2 can be used to observe activity of the cAMP/PKA pathway *in vivo*, for example in developing neocortex, where strong calcium transients have been observed in newborn mice (Adelsberger et al., 2005). In addition, immobilized AKAR2.2 can be used to monitor subcellular compartments of PKA activity, such as those observed in growth cones (Terman and Kolodkin, 2004; Kain et al., 2005).

***Potential function of periodic PKA activation in developing circuits***

AKAR2.2 FRET ratio changes were induced in nearly all RGCs with sufficient depolarization (Figure 2.6). In our explants that had shorter spontaneous depolarizations than observed in acutely isolated retina (Figure 2.3), retinal waves induce transient activation of the cAMP/PKA pathway (Figures 2.4 and 2.5). This evidence suggests that most RGCs *in vivo* exhibit periodic activation of PKA.

There are several examples that demonstrate that temporal coding of second messenger pathway activation is critical for influencing development (Berridge et al., 2000; Spitzer et al., 2004). For example, in developing xenopus spinal neurons, the frequency of calcium transients is critical in establishing neurotransmitter phenotype (Gu and Spitzer, 1995; Borodinsky et al., 2004). Similarly, in the ventricular zone in neocortex (Owens et al., 2000) and retina (Pearson et al., 2002; Pearson et al., 2004), calcium transients are important for proliferation of ventricular zone cells and the subsequent fate differentiation of

postmitotic neurons. Later in development, after distinct neuronal classes are specified but before motoneurons innervate their targets, spontaneous activity in the developing spinal cord is frequency-tuned to modulate the expression of proteins critical for pathfinding of motoneurons (Hanson and Landmesser, 2004). The frequency of calcium transients in growth cones has also been implicated in mediating interactions of the growth cone with the local environment (Henley and Poo, 2004). Periodic activation of isolated RGCs and the spontaneous activity in retinal explants profoundly increase the rate of axonal outgrowth in response to BDNF (Goldberg et al., 2002). This enhancement of BDNF-induced outgrowth is blocked by adenylate cyclase inhibitors (Goldberg et al., 2002), indicating that the endogenous pattern of retinal activity regulates axon outgrowth via this second messenger cascade, possibly by increasing the surface expression of neurotrophin receptors (Meyer-Franke et al., 1998; Nagappan and Lu, 2005).

Whether periodic activation of RGCs is required for normal development of the visual system is not yet determined. Though it is well established that spontaneous retinal activity patterns are critical for the refinement of retinal projections to central targets, the precise role of correlated activity patterns is the subject of intense debate. In a knockout mouse that has uncorrelated retinal ganglion cell firing instead of retinal waves (Bansal et al., 2000; McLaughlin et al., 2003), it has recently been shown that several features of both retinocollicular projections (McLaughlin et al., 2003; Chandrasekaran et al., 2005; Mrsic-Flogel et al., 2005) and retinogeniculate projections (Rossi et al., 2001; Muir-Robinson et al., 2002; Grubb et al., 2003) were altered. In contrast, both pharmacological

manipulations of activity patterns in ferret and a different knockout mouse with altered retinal patterns develop normal refinement of retinal projections (Stellwagen and Shatz, 2002; Huberman et al., 2003; Torborg et al., 2005). By comparing the retinal firing patterns that drive or permit segregation to those that do not, we identified several candidate activity features that may be essential for this refinement process (Torborg et al., 2005).

The primary hypothesis that arose from these studies is that RGCs must fire high frequency bursts with a slow periodicity for normal eye-specific refinement. Such an activity pattern would strongly activate both calcium-dependent and cAMP-dependent second messenger cascades. However, a critical component of the argument that retinal waves are instructive for driving eye-specific segregation or retinotopic refinement is that the plasticity process that reads out this instructive signal must be able to distinguish firing from neighboring cells vs. firing from distant cells. Therefore, the elongated PKA transients we observed in RGCs are not likely to provide an instructive signal for driving map refinement but rather may function in a cell autonomous fashion. However, the plasticity mechanisms that convert this firing pattern into long-term changes in cellular morphology remain to be determined.

Another potential role for PKA oscillations may be in the generation of retinal waves. Retinal waves are generated by a network of starburst amacrine cells (Zheng et al., 2004; Zheng et al., 2006) and the frequency of retinal waves is determined by changes in cAMP levels in starburst amacrine cells (Zheng et al., 2006). Indeed, bath application of the PKA inhibitor Rp-cAMP blocks retinal

waves (Stellwagen et al., 1999). The data presented here do not address the role of PKA activity in the generation of retinal waves because we recorded PKA activity exclusively in RGCs, which “read out” the activity of the starburst network (Feller et al., 1997; Zheng et al., 2006) but are not thought to participate in the generation of retinal waves. Whether cAMP levels or PKA activity spontaneously oscillate in developing starburst amacrine cells has yet to be determined.

Models of the complex interplay between calcium and cAMP levels demonstrate that changes in either the level or kinetics of intracellular cAMP or calcium concentrations can lead to dramatic changes in the emergent behavior of the intracellular network (Gorbunova and Spitzer, 2002). The implications of these models is that neural activity patterns can activate different spatiotemporal patterns of second messenger networks which in turn may be uniquely tuned to drive specific long-term cellular changes. For example, expression of BDNF, a neurotrophic factor critical for normal arborization of retinal ganglion cell dendrites and axons as well synapse formation (Cohen-Cory and Lom, 2004), is up-regulated by increased intracellular calcium and cAMP concentration, but not by stimulation of the cAMP pathway alone (Fukuchi et al., 2005). Similarly, surface expression of TrkB may also be regulated by neuronal activity and cAMP levels (Nagappan and Lu, 2005). This suggests that the pattern of intracellular calcium and cAMP oscillations caused by periodic depolarizations may be critical for determining mature morphology in the developing visual system.

In conclusion, we report data that support the hypothesis that retinal waves induce oscillations in cAMP concentration and PKA activity of RGCs.

Visualization of second messenger cascade kinetics is an important step in elucidating the link between activity and the mechanisms by which it influences development of neural circuits.

**ACKNOWLEDGEMENTS**

Chapter 2, in full, is a reprint of the material as it appears in the Dunn TA, Wang CT, Colicos MA, Zaccolo M, DiPilato LM, Zhang J, Tsien RY, Feller MB. 2006. Imaging of cAMP levels and protein kinase A activity reveals that retinal waves drive oscillations in second-messenger cascades. Journal Of Neuroscience 26:12807-12815.

**REFERENCES**

Abdel-Majid RM, Tremblay F, Baldridge WH (2002) Localization of adenylyl cyclase proteins in the rodent retina. Brain Res Mol Brain Res 101:62-70.

Adelsberger H, Garaschuk O, Konnerth A (2005) Cortical calcium waves in resting newborn mice. Nat Neurosci 8:988-990. Epub 2005 Jul 2010.

Bansal A, Singer JH, Hwang B, Feller MB (2000) Mice lacking specific nAChR subunits exhibit dramatically altered spontaneous activity patterns and reveal a limited role for retinal waves in forming ON/OFF circuits in the inner retina. J Neurosci 20:7672-7681.

Berridge MJ, Lipp P, Bootman MD (2000) The versatility and universality of calcium signalling. Nat Rev Mol Cell Biol 1:11-21.

Borodinsky LN, Root CM, Cronin JA, Sann SB, Gu X, Spitzer NC (2004) Activity-dependent homeostatic specification of transmitter expression in embryonic neurons. Nature 429:523-530.

Chandrasekaran AR, Plas DT, Gonzalez E, Crair MC (2005) Evidence for an instructive role of retinal activity in retinotopic map refinement in the superior colliculus of the mouse. J Neurosci 25:6929-6938.

Cohen-Cory S, Lom B (2004) Neurotrophic regulation of retinal ganglion cell synaptic connectivity: from axons and dendrites to synapses. Int J Dev Biol 48:947-956.

Colicos MA, Firth SI, Bosze J, Goldstein J, Feller MB (2004) Emergence of realistic retinal networks in culture promoted by the superior colliculus. Dev Neurosci 26:406-416.

DiPilato LM, Cheng X, Zhang J (2004) Fluorescent indicators of cAMP and Epac activation reveal differential dynamics of cAMP signaling within discrete subcellular compartments. Proc Natl Acad Sci U S A 101:16513-16518. Epub 12004 Nov 16515.

Dyachok O, Isakov Y, Sagetorp J, Tengholm A (2006) Oscillations of cyclic AMP in hormone-stimulated insulin-secreting beta-cells. Nature 439:349-352.

Feller MB, Butts DA, Aaron HL, Rokhsar DS, Shatz CJ (1997) Dynamic processes shape spatiotemporal properties of retinal waves. Neuron 19:293-306.

Ferguson GD, Storm DR (2004) Why calcium-stimulated adenylyl cyclases? Physiology (Bethesda) 19:271-276.

Fields RD, Lee PR, Cohen JE (2005) Temporal integration of intracellular Ca2+ signaling networks in regulating gene expression by action potentials. Cell Calcium 37:433-442.

Fukuchi M, Tabuchi A, Tsuda M (2005) Transcriptional Regulation of Neuronal Genes and Its Effect on Neural Functions: Cumulative mRNA Expression of PACAP and BDNF Genes Controlled by Calcium and cAMP Signals in Neurons. J Pharmacol Sci 98:212-218. Epub 2005 Jul 2009.

Goldberg JL, Klassen MP, Hua Y, Barres BA (2002a) Amacrine-signaled loss of intrinsic axon growth ability by retinal ganglion cells. Science 296:1860-1864.

Goldberg JL, Espinosa JS, Xu Y, Davidson N, Kovacs GT, Barres BA (2002b) Retinal ganglion cells do not extend axons by default: promotion by neurotrophic signaling and electrical activity. Neuron 33:689-702.

Gorbunova YV, Spitzer NC (2002) Dynamic interactions of cyclic AMP transients and spontaneous Ca(2+) spikes. Nature 418:93-96.

Gordon GW, Berry G, Liang XH, Levine B, Herman B (1998) Quantitative fluorescence resonance energy transfer measurements using fluorescence microscopy. Biophys J 74:2702-2713.

Griesbeck O, Baird GS, Campbell RE, Zacharias DA, Tsien RY (2001) Reducing the environmental sensitivity of yellow fluorescent protein. Mechanism and applications. J Biol Chem 276:29188-29194. Epub 22001 May 29131.

Grubb MS, Thompson ID (2004) The influence of early experience on the development of sensory systems. Curr Opin Neurobiol 14:503-512.

Grubb MS, Rossi FM, Changeux JP, Thompson ID (2003) Abnormal functional organization in the dorsal lateral geniculate nucleus of mice lacking the beta 2 subunit of the nicotinic acetylcholine receptor. Neuron 40:1161-1172.

Gu X, Spitzer NC (1995) Distinct aspects of neuronal differentiation encoded by frequency of spontaneous Ca2+ transients. Nature 375:784-787.

Hanganu IL, Ben-Ari Y, Khazipov R (2006) Retinal waves trigger spindle bursts in the neonatal rat visual cortex. J Neurosci 26:6728-6736.

Hanson MG, Landmesser LT (2004) Normal patterns of spontaneous activity are required for correct motor axon guidance and the expression of specific guidance molecules. Neuron 43:687-701.

Henley J, Poo MM (2004) Guiding neuronal growth cones using Ca2+ signals. Trends Cell Biol 14:320-330.

Huberman AD, Wang GY, Liets LC, Collins OA, Chapman B, Chalupa LM (2003) Eye-specific retinogeniculate segregation independent of normal neuronal activity. Science 300:994-998.

Kain K, Zhang J, Goldfinger L, Tsien R, Ginsberg M (2005) Transient Adhesion-mediated PKA activation at the leading edge of migrating cells.

Koulen P (1999) Postnatal development of dopamine D1 receptor immunoreactivity in the rat retina. J Neurosci Res 56:397-404.

Lu HC, Butts DA, Kaeser PS, She WC, Janz R, Crair MC (2006) Role of efficient neurotransmitter release in barrel map development. J Neurosci 26:2692-2703.

McLaughlin T, Torborg CL, Feller MB, O'Leary DD (2003) Retinotopic map refinement requires spontaneous retinal waves during a brief critical period of development. Neuron 40:1147-1160.

Meister M, Wong RO, Baylor DA, Shatz CJ (1991) Synchronous bursts of action potentials in ganglion cells of the developing mammalian retina. Science 252:939-943.

Meyer-Franke A, Kaplan MR, Pfrieger FW, Barres BA (1995) Characterization of the signaling interactions that promote the survival and growth of developing retinal ganglion cells in culture. Neuron 15:805-819.

Meyer-Franke A, Wilkinson GA, Kruttgen A, Hu M, Munro E, Hanson MG, Jr., Reichardt LF, Barres BA (1998) Depolarization and cAMP elevation rapidly recruit TrkB to the plasma membrane of CNS neurons. Neuron 21:681-693.

Mrsic-Flogel TD, Hofer SB, Creutzfeldt C, Cloez-Tayarani I, Changeux JP, Bonhoeffer T, Hubener M (2005) Altered map of visual space in the superior colliculus of mice lacking early retinal waves. J Neurosci 25:6921-6928.

Muir-Robinson G, Hwang BJ, Feller MB (2002) Retinogeniculate axons undergo eye-specific segregation in the absence of eye-specific layers. J Neurosci 22:5259-5264.

Nagappan G, Lu B (2005) Activity-dependent modulation of the BDNF receptor TrkB: mechanisms and implications. Trends Neurosci 21:21.

Nicol X, Muzerelle A, Bachy I, Ravary A, Gaspar P (2005) Spatiotemporal localization of the calcium-stimulated adenylate cyclases, AC1 and AC8, during mouse brain development. J Comp Neurol 486:281-294.

Nicol X, Muzerelle A, Rio JP, Metin C, Gaspar P (2006) Requirement of adenylate cyclase 1 for the ephrin-A5-dependent retraction of exuberant retinal axons. J Neurosci 26:862-872.

Nikolaev VO, Bunemann M, Hein L, Hannawacker A, Lohse MJ (2004) Novel single chain cAMP sensors for receptor-induced signal propagation. J Biol Chem 279:37215-37218. Epub 32004 Jul 37211.

Owens DF, Flint AC, Dammerman RS, Kriegstein AR (2000) Calcium dynamics of neocortical ventricular zone cells. Dev Neurosci 22:25-33.

Pearson R, Catsicas M, Becker D, Mobbs P (2002) Purinergic and muscarinic modulation of the cell cycle and calcium signaling in the chick retinal ventricular zone. J Neurosci 22:7569-7579.

Pearson RA, Catsicas M, Becker DL, Bayley P, Luneborg NL, Mobbs P (2004) Ca(2+) signalling and gap junction coupling within and between pigment epithelium and neural retina in the developing chick. Eur J Neurosci 19:2435-2445.

Pham TA, Rubenstein JL, Silva AJ, Storm DR, Stryker MP (2001) The cre/creb pathway is transiently expressed in thalamic circuit development and contributes to refinement of retinogeniculate axons. Neuron 31:409-420.

Plas DT, Visel A, Gonzalez E, She WC, Crair MC (2004) Adenylate Cyclase 1 dependent refinement of retinotopic maps in the mouse. Vision Res 44:3357-3364.

Ravary A, Muzerelle A, Herve D, Pascoli V, Ba-Charvet KN, Girault JA, Welker E, Gaspar P (2003) Adenylate cyclase 1 as a key actor in the refinement of retinal projection maps. J Neurosci 23:2228-2238.

Rossi FM, Pizzorusso T, Porciatti V, Marubio LM, Maffei L, Changeux JP (2001) Requirement of the nicotinic acetylcholine receptor beta 2 subunit for the anatomical and functional development of the visual system. Proc Natl Acad Sci U S A 98:6453-6458.

Ruthazer ES, Cline HT (2004) Insights into activity-dependent map formation from the retinotectal system: a middle-of-the-brain perspective. J Neurobiol 59:134-146.

Schambra UB, Duncan GE, Breese GR, Fornaretto MG, Caron MG, Fremeau RT, Jr. (1994) Ontogeny of D1A and D2 dopamine receptor subtypes in rat brain using in situ hybridization and receptor binding. Neuroscience 62:65-85.

Spitzer NC, Root CM, Borodinsky LN (2004) Orchestrating neuronal differentiation: patterns of Ca2+ spikes specify transmitter choice. Trends Neurosci 27:415-421.

Stellwagen D, Shatz CJ (2002) An instructive role for retinal waves in the development of retinogeniculate connectivity. Neuron 33:357-367.

Stellwagen D, Shatz CJ, Feller MB (1999) Dynamics of retinal waves are controlled by cyclic AMP. Neuron 24:673-685.

Terman JR, Kolodkin AL (2004) Nervy links protein kinase a to plexin-mediated semaphorin repulsion. Science 303:1204-1207.

Torborg CL, Feller MB (2005) Spontaneous patterned retinal activity and the refinement of retinal projections. Prog Neurobiol 76:213-235. Epub 2005 Nov 2008.

Torborg CL, Hansen KA, Feller MB (2005) High frequency, synchronized bursting drives eye-specific segregation of retinogeniculate projections. Nat Neurosci 8:72-78. Epub 2004 Dec 2019.

van Rheenen J, Langeslag M, Jalink K (2004) Correcting confocal acquisition to optimize imaging of fluorescence resonance energy transfer by sensitized emission. Biophys J 86:2517-2529.

West AE, Griffith EC, Greenberg ME (2002) Regulation of transcription factors by neuronal activity. Nat Rev Neurosci 3:921-931.

Wong RO, Meister M, Shatz CJ (1993) Transient period of correlated bursting activity during development of the mammalian retina. Neuron 11:923-938.

Yang S, Fletcher WH, Johnson DA (1995) Regulation of cAMP-dependent protein kinase: enzyme activation without dissociation. Biochemistry 34:6267-6271.

Zaccolo M, Pozzan T (2003) CAMP and Ca2+ interplay: a matter of oscillation patterns. Trends Neurosci 26:53-55.

Zaccolo M, Magalhaes P, Pozzan T (2002) Compartmentalisation of cAMP and Ca(2+) signals. Curr Opin Cell Biol 14:160-166.

Zacharias DA, Violin JD, Newton AC, Tsien RY (2002) Partitioning of lipid-modified monomeric GFPs into membrane microdomains of live cells. Science 296:913-916.

Zhang J, Ma Y, Taylor SS, Tsien RY (2001) Genetically encoded reporters of protein kinase A activity reveal impact of substrate tethering. Proc Natl Acad Sci U S A 98:14997-15002.

Zhang J, Hupfeld CJ, Taylor SS, Olefsky JM, Tsien RY (2005) Insulin disrupts beta-adrenergic signalling to protein kinase A in adipocytes. Nature 437:569-573.

Zheng J, Lee S, Zhou ZJ (2006) A transient network of intrinsically bursting starburst cells underlies the generation of retinal waves. Nat Neurosci 9:363-371. Epub 2006 Feb 2005.

Zheng JJ, Lee S, Zhou ZJ (2004) A developmental switch in the excitability and function of the starburst network in the Mammalian retina. Neuron 44:851-864.

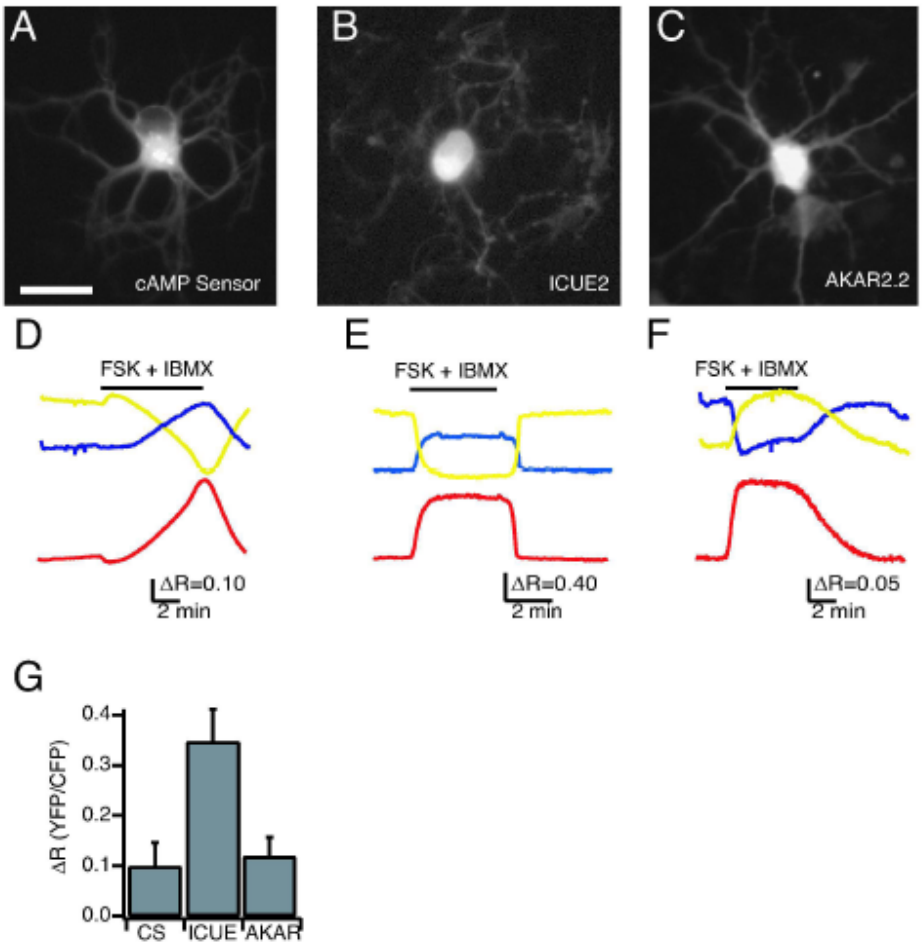


**Figure 2.1 Expression of functional indicators in dissociated retinal neurons**

A-C. Fluorescence images of cultured retinal neurons expressing the cAMP sensor (A), ICUE2 (B), AKAR2.2 (C). Retinal neurons were dissociated at P0 and imaged after 2 days in culture. Scale bar is 20µm.

D-F. Time course of $F_{CFP}$ (blue), $F_{YFP}$ (yellow), (imaged simultaneously) and the FRET ratio (red) of $F_{YFP}/F_{CFP}$ for the cAMP sensor (CS) (D), ICUE2 (E), AKAR2.2 (F) during application of both the adenylate cyclase activator forskolin (10µM) and phosphodiesterase inhibitor IBMX (100µM). Bar represents time of drug applications. All ratios are corrected for CFP bleedthrough into YFP channel and differential bleaching of the two fluorophores. Ratio traces for CS and ICUE2 are inverted to show increases in cAMP concentration as upward deflections.

G. Summary of maximal FRET ratio (ΔR) changes in response to both forskolin and IBMX. ΔR was computed by subtracting the value of the FRET ratio averaged over 5 images prior to manipulation from the value of the FRET ratio averaged over 5 images around the maximum response.

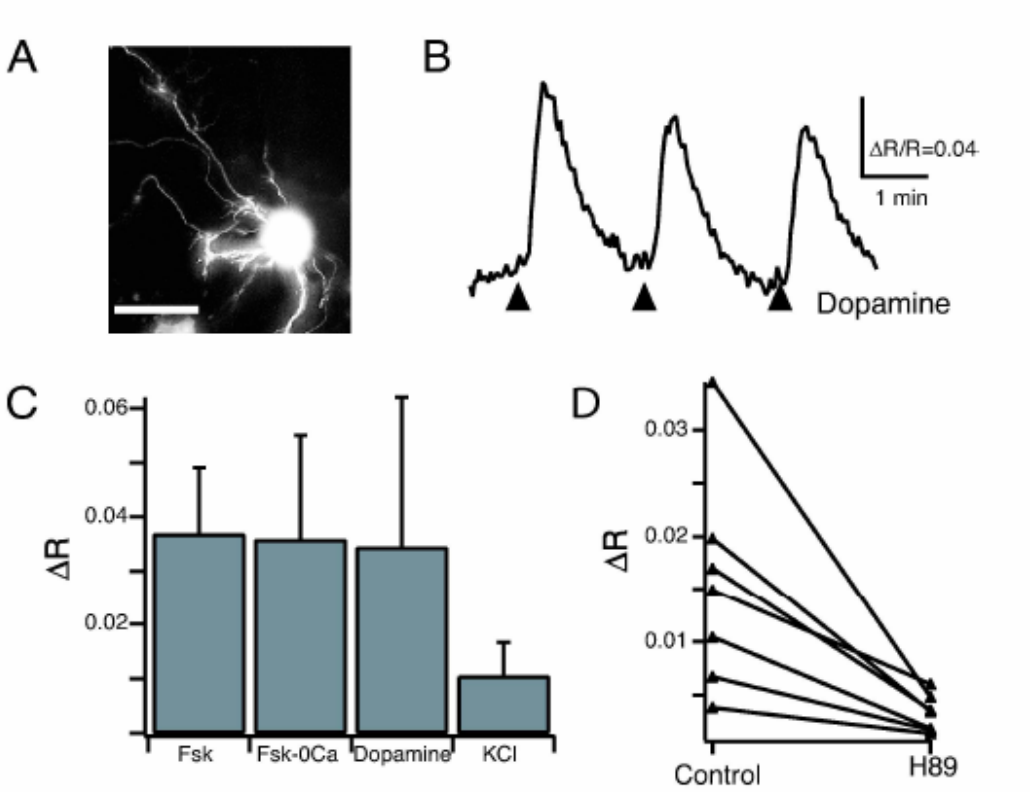


**Figure 2.2 AKAR2.2 responds to elevations in PKA activity induced by forskolin, dopamine and depolarization.**

A. Fluorescence image of RGC in a retinal explant transfected with AKAR2.2. Scale bar = 20 µm.

B. Time course of the AKAR2.2 FRET ratio change in response to short applications of dopamine (150 µM) of varying duration (3 arrows correspond to 2, 4, and 8 50 msec puffs, respectively, delivered at 4 Hz).

C. Summary of the AKAR2.2 FRET ratio change in response to acute application of forskolin (FSK, 50µM, 2x50 msec puffs at 4Hz), forskolin in the absence of extracellular calcium (FSK-0Ca, 2x50 msec puffs at 4Hz), dopamine (150 µM, 8x50 msec puffs at 4Hz) and high-$K^+$ solution (105 mM KCl, 8 50xmsec puffs at 4Hz).

D. The amplitude of depolarization-induced AKAR ratio changes in the absence and presence of H89, a specific PKA antagonist (25 µM, after 15-25 minute incubations, $p<0.0001$).

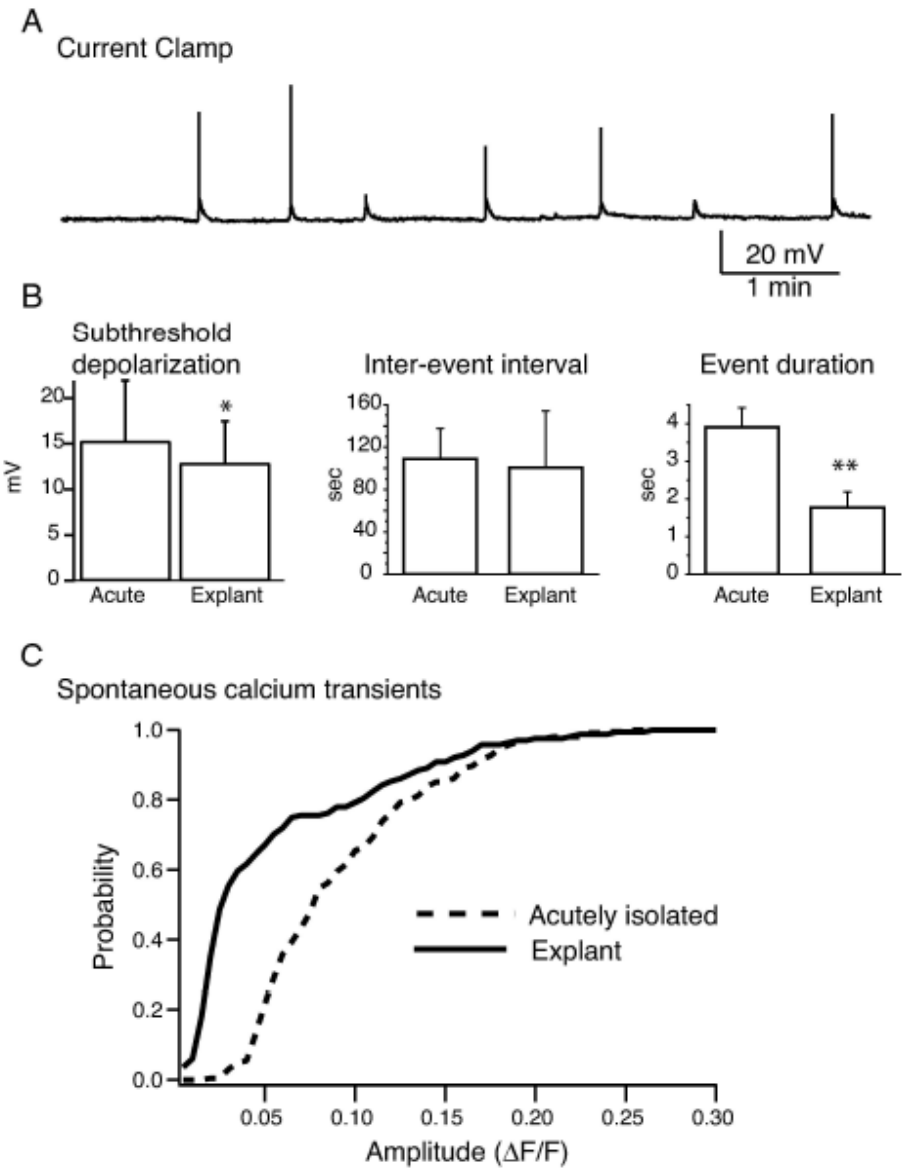


**Figure 2.3 Spontaneous depolarizations in retinal explants are shorter in duration and lead to smaller increases in intracellular calcium than in acutely isolated retinas.**

A. Current clamp recording from a RGC in a retinal explant.

B. Summary data comparing the amplitude, inter-event interval and duration of spontaneous depolarizations in retinal explants and acutely isolated retinas. Retinal explants were isolated from P0-P1 rats and kept 24-48 hours in culture (n=8 RGCs). Acutely isolated retinas are from P2 or P7 rats (n=8 RGCs from 8 retinas). (** indicates significance $p<0.001$, * indicates significant $p< 0.05$).

C. Cumulative probability plot of the fractional change of fura-2-AM fluorescence individual cells imaged at 60x magnification. Mean amplitude of spontaneous calcium transients was calculated for RGCs from acutely isolated retinas (n=203 cells) or explants cultured for 24 hours (n=164 cells).

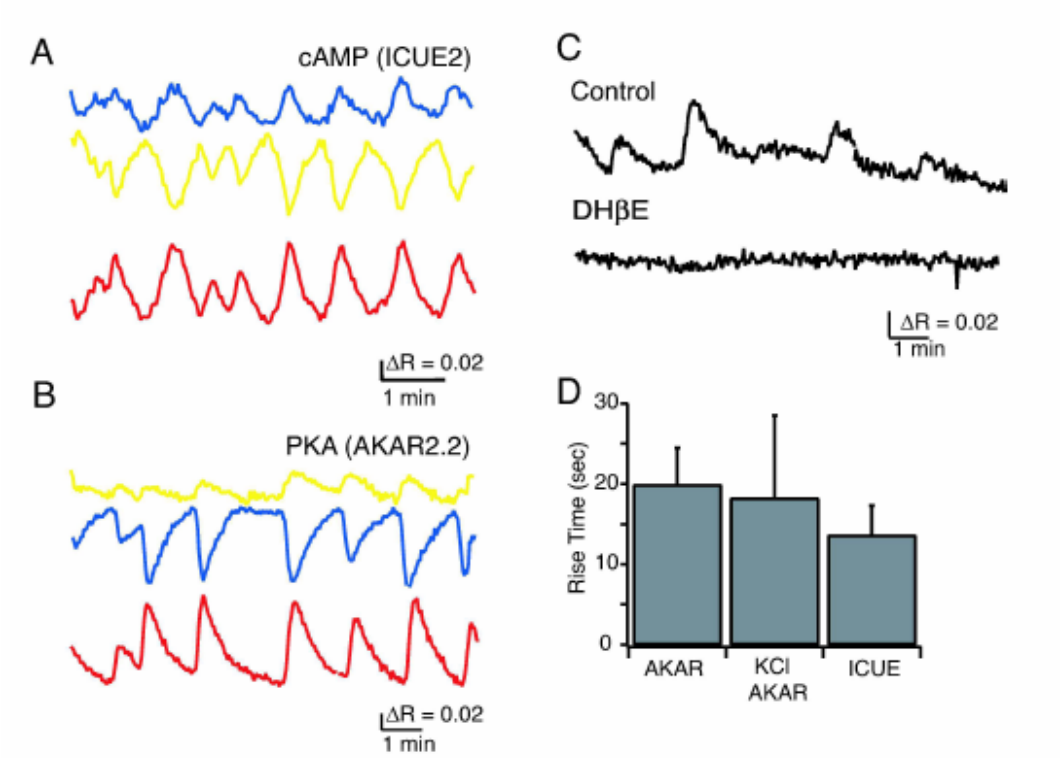


**Figure 2.4 Spontaneous cAMP level and PKA activity changes induced by retinal waves**

A. Time course of $F_{CFP}$ (blue), $F_{YFP}$ (yellow) recorded simultaneously and averaged over the cell body of a RGC expressing ICUE2. The ICUE2 FRET ratio is computed as $F_{YFP}/F_{CFP}$, inverted to show cAMP increases as upward deflections, corrected for CFP bleedthrough into YFP channel, and corrected for differential bleaching of CFP and YFP.

B. Time course of $F_{CFP}$ (blue), $F_{YFP}$ (yellow) recorded simultaneously and averaged over the cell body of a RGC expressing AKAR2.2. The ratio is computed as $F_{YFP}/F_{CFP}$, corrected for CFP bleedthrough into YFP channel and corrected for differential bleaching.

C. Blockade of retinal waves with the nAChR antagonist dihydro-β-erythroidine (DHβE, 10-20 μM) blocked spontaneous PKA oscillations.

E. Comparison of risetime of FRET ratio response to K-evoked and spontaneous events for ICUE2 and AKAR2.2.

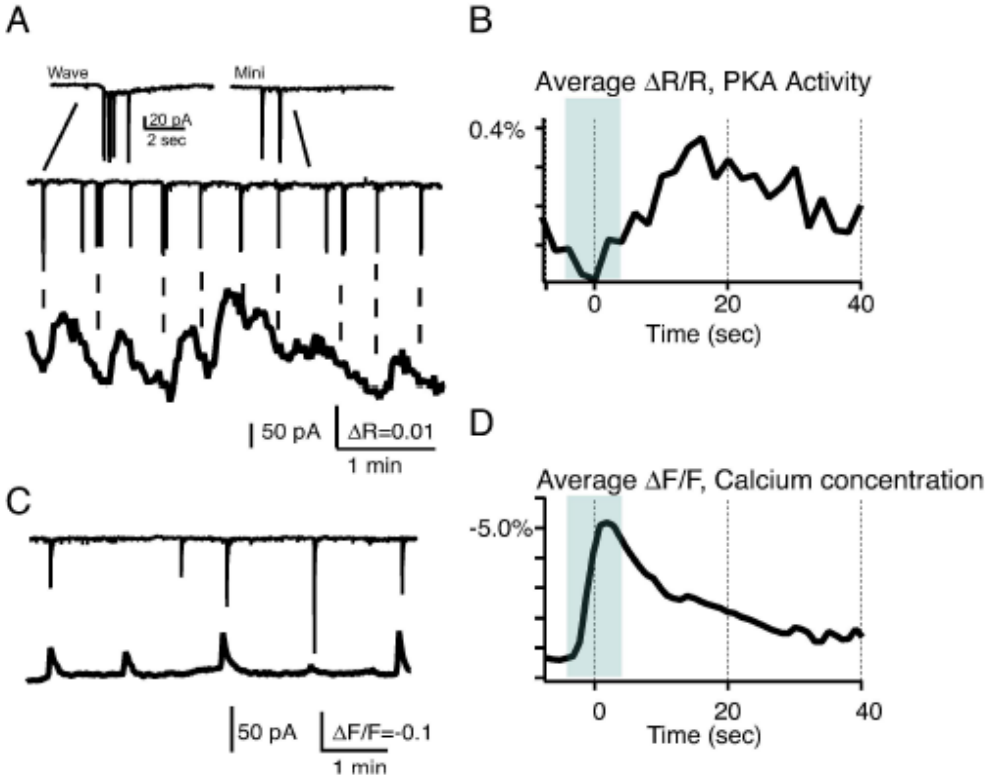


**Figure 2.5 Spontaneous PKA transients are temporally correlated with retinal waves**

A. Simultaneous voltage clamp (top) and AKAR2.2 FRET imaging (bottom) from nearby retinal ganglion cells. Inset: Two events, a compound EPSC corresponding to a retinal wave (left) and single synaptic events (right). Wave-related events are distinguished by a slow inward current.

B. The wave-triggered average indicates a barrage of synaptic currents associated with retinal waves is followed by an increase in PKA activity and preceded by a decrease in PKA activity from the previous transient. Gray bar indicates average length of compound PSCs.

C. Simultaneous voltage clamp recording (top) and fractional change in fluorescence of calcium indicator, fura-2, loaded via its AM ester (bottom), in nearby cells.

D. The wave-triggered average for $Ca^{2+}$ transients indicate that barrages of synaptic currents are simultaneous with calcium increases. Gray bar indicates average length of compound PSCs.

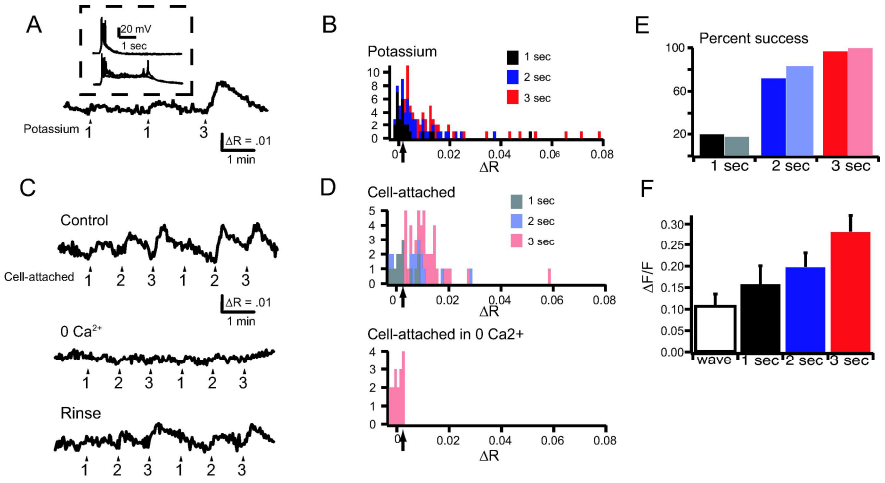


**Figure 2.6: Three-second depolarizations reliably evoked PKA activity transients in a calcium-dependent manner.**

A. Time course of AKAR2.2 FRET ratio ($F_{YFP}/F_{CFP}$) in response to 1 or 3 second applications of solutions containing 105 mM $K^+$. The arrows show the starting time for an application of high-K+ solution. The numbers underlying the arrows indicate the duration of the potassium application. Inset: current clamp response of a RGC in response to 1 second (top) or 3 second (bottom) application of high-$K^+$ solution.

B. Histogram distribution of the change in FRET ratio (ΔR) in response to application of high-$K^+$ solution of varying duration (black for 1 sec; blue for 2 sec; red for 3 sec-duration). Arrow refers to threshold over which we could reliably distinguish responses from the noise.

C. Time course of AKAR2.2 FRET ratio in response to depolarization of RGC neurons induced via a cell-attached pipette in the presence and absence of 0-$Ca^{2+}$ ACSF. The arrows indicate the starting time for a given depolarization pulse. The numbers underlying the arrows indicate the duration of the depolarization pulses.

D. Histogram distribution of the change in FRET ratio (ΔR) to depolarization of RGC neurons induced via a cell-attached pipette of varying duration. BOTTOM - histogram distribution of responses to 3 second depolarizations in the absence of extracellular calcium. Arrows refer to threshold over which we could reliably distinguish response from the noise.

E. The percentage of detectable depolarization induced changes in FRET ratio computed from histogram distributions in parts B and D. For both potassium and electrophysiologically induced depolarizations, longer durations more reliably induced changes in FRET ratios.

F. Comparison of the fractional change of fluorescence of fura-2-AM induced by increases in intracellular calcium during retinal waves and calcium increases induced by applications of high-$K^+$ solution of varying duration. All categories are significantly different from each other (paired student t-test, $p<.0001$).

Chapter 3

# The mechanisms underlying depolarization-induced PKA transients in retinal ganglion cells

Timothy A. Dunn[1], Marla B. Feller[2]

[1]Neurobiology Section, Division of Biological Sciences, UCSD, La Jolla, CA, USA.

[2] Department of Molecular and Cell Biology and the Helen Wills Neuroscience Institute, University of California, Berkeley, CA, USA.

Correspondence should be addressed to

Marla B. Feller, Associate Professor
University of California, Berkeley
Department of Molecular and Cell Biology &
Helen Wills Neuroscience Institute
142 Life Sciences Addition - 3200
Berkeley, CA 94720-3200
mfeller@berkeley.edu
Tel (510) 643-1726
Fax (510) 643-6791

**ABSTRACT**

Before vision is possible, developing retinal ganglion cells (RGCs) exhibit spontaneous depolarizations, known as retinal waves. Though spontaneous activity in the retina has been implicated in several developmental processes including axonal outgrowth, refinement, and cell survival, the biochemical cascades underlying these processes are not understood. Recently, we demonstrated that the cAMP/PKA pathway is activated by spontaneous depolarizations in RGCs (Dunn and Wang, et al., 2006). Here, we use dual imaging of intracellular calcium concentration and genetically-encoded indicators of PKA activity to assay the role of different classes of calcium-dependent adenylate cyclases (ACs) in activation of this cascade. We found that in roughly half of RGCs, depolarization-induced PKA transients persist in the presence of the 2',5'-dideoxyadenosine, which inhibits all transmembrane adenylate cyclases. We further demonstrate that depolarization-induced transients persist in *barrelless* mice lacking AC1, the predominant calcium-dependent adenylate cyclase in RGCs and in double knockout mice lacking both AC1 and AC8. These results indicate that there is a calcium-dependent adenylate cyclase distinct from AC1 and AC8 in RGCs that mediates depolarization activation of the cAMP/PKA cascade.

## INTRODUCTION

The role of spontaneous activity in circuit development has been studied extensively in the retina. Prior to the onset of vision, retinas exhibit highly patterned, spontaneous activity, termed retinal waves. In rodents, this activity occurs through the first two postnatal weeks of life, during which there is tremendous development within the retina as well as refinement of retinal projections to primary targets in the brain (for review, see (Torborg and Feller, 2005). Retinal waves propagate across the ganglion cell layer, thereby correlating the firing between neighboring RGCs. It has been proposed that this property of waves is instructive for the establishment of retinotopic maps both in the superior colliculus and visual cortex.

Do retinal waves drive activity-dependent cell-autonomous processes? At the level of individual retinal ganglion cells, retinal waves appear as periodic bursts of depolarizations, lasting roughly 2-4 seconds, occurring once per minute (Feller et al., 1996; Stellwagen et al., 1999). There is growing evidence that these periodic depolarizations may drive cell-autonomous events critical for circuit development and that the cAMP/PKA cascade is an important link between periodic depolarizations and downstream effectors. First, periodic activation of RGCs enhances axonal outgrowth in response to neurotrophins (Meyer-Franke et al., 1995). This activity-induced potentiation of outgrowth is blocked by adenylate cyclase inhibitors (Goldberg et al., 2002). Second, periodic increases in cAMP in RGC growth cones are critical for their repulsive response

to guidance molecules (Ming et al., 2001; Nicol et al., 2006; Nicol et al., 2007). Third, retinal activity is critical for mediating RGC survival in a manner that relies upon cAMP (Meyer-Franke et al., 1995; Goldberg et al., 2002).

Through use of genetically encoded cAMP level and PKA activity indicators (for review, see (Dunn and Feller, 2008), we have recently demonstrated that depolarizations of RGCs reliably activate a cAMP/PKA second messenger cascade in a calcium-dependent manner (Dunn et al., 2006). Here we explore the biochemical basis of these depolarization-induced increases in PKA activity in RGCs. Cyclic AMP levels in neurons are controlled by adenylyl cyclases (ACs), which convert ATP to cAMP, and by phosphodiesterases (PDEs), which enzymatically cleave cAMP. Several adenylate cyclases have been reported to be present in the rodent GCL, including calcium regulated AC1, AC3, AC5, and AC8 (Nicol et al., 2006). Adenylyl cyclases 1 and 8 increase cAMP production in response to calmodulin activation. Adenylyl cyclase 3 has been reported to be stimulated by calcium *in vitro* (Choi et al., 1992), though recent results suggest that *in vivo*, it acts to decrease production of cAMP in response to calcium influx in vivo (Wayman et al., 1995; Wong et al., 2001), and therefore is not a good candidate to mediate the increases in PKA activity following depolarization. Adenylyl cyclase 5 is also inhibited in response to elevated calcium (Beazely and Watts, 2006), and is therefore unlikely to be important for the phenomenon we are investigating. Recent reports suggest that a soluble adenylyl cyclase (sAC) is also present in some neurons (Stessin et al., 2006; Wu et al., 2006), although it's presence in retinal neurons has not yet been

demonstrated. Only one class of PDE is directly activated by calcium/calmodulin, PDE1. It has been reported to be present in RGCs (Santone et al., 2006).

To determine the relative role of different classes of ACs and PDEs that underlies the calcium-dependent activation of PKA in RGCs, we combined calcium imaging and FRET-based imaging of the genetically encoded A-kinase activity reporter, AKAR3 (Zhang et al., 2001; DiPilato et al., 2004; Landa et al., 2005; Zhang et al., 2005; Allen and Zhang, 2006; Harbeck et al., 2006; Willoughby and Cooper, 2006). We first addressed the activity of the adenylyl cyclases that likely underlie the increase in PKA activity using a combination of pharmacology and genetically modified mice. We found that inhibition of transmembrane ACs blocked depolarization induced PKA transients in approximately half of RGCs. These experiments were supported by genetic models, which found that calcium-dependent PKA transients were still present in *barrelless* (*brl*) mice lacking functional AC1 and double knockout mice lacking both AC1 and AC8. Finally, we found that PDEs do not play a role in generating PKA transients in wild type or AC1/AC8 dKO mice, but they may have a role in modulating the cAMP pathway response to calcium influx.

## METHODS

### *Retinal Explants*

These methods are described in full in Dunn and Wang, et al., 2006. Briefly, P0-P3 mouse retinal explants from wild-type, *barrelless*, or AC1/AC8

double knockout mice were transfected using electroporation with AKAR2.2 or AKAR3, genetically encoded indicators of PKA activity (plasmids for both indicators from J. Zhang (Zhang et al., 2001; DiPilato et al., 2004; Kain et al., 2005; Zhang et al., 2005; Allen and Zhang, 2006; Saucerman et al., 2006). Mice lacking functional AC1 through a spontaneous mutation, known as *barrelless* mice (Plas et al., 2004; Chandrasekaran et al., 2005; Lu et al., 2006), were a generous gift from M. Crair. Genotyping was performed as described (Lu et al., 2003). AC1/AC8 double knockout mice (Wong et al., 1999; Maas et al., 2005) were a generous gift from D. Storm. Genotyping was performed as described (Wong et al., 1999).

Retinal explants were isolated and mounted on filter paper with the RGCs facing up. Then, 0.2 mg/mL plasmid was electroporated (30 V, 4mm, 2 pulses at 1 second interval, BTX ECM 830 electroporator). Retinal explants were then cultured in serum free culture medium (Neurobasal-A medium supplemented with B27 (Gibco), 0.6% glucose, 2mM glutamine, 10mM HEPES, 1mM Na-Pyruvate, 50 mg/mL penicillin G, 50 units/mL streptomycin, 2.5mg/mL Insulin, 6 µM forskolin, 10ng/mL CNTF & 50ng/mL BDNF) for 12-48 hours. Explants were removed to forskolin-free media overnight prior to imaging. Immediately prior to imaging, the explants were placed in serum free culture media containing 10 µM fura-2-AM, 1% DMSO, and 0.02% pluronic acid for 30-60 min.

***Dual Imaging of FRET-based indicators and calcium***

FRET imaging was performed on an upright Zeiss Axioskop 2, using a 60x LUMPLFLW water immersion objective (Olympus), and perfused continuously with warmed (30-34$^{o}$ C) artificial cerebrospinal fluid (ACSF: 119 mM NaCl, 2.5 mM KCl, 1.3 mM MgCl2, 1.0 mM K2HPO4, 2.5 mM CaCl2, 26.2 mM NaHCO3, 11 mM D-glucose) bubbled with 95% O2/5% CO2. The filter configuration was similar to previous studies of simultaneous calcium and FRET imaging (Violin et al., 2003; Harbeck et al., 2006). For FRET imaging, CFP was excited by a narrow bandwidth 436/10nm filter to minimize direct excitation of fura-2. Two emission wavelengths were collected simultaneously by using a Dual-View image splitter (Optical Insights) with appropriate yellow (535nm/30) and cyan emission filters (480nm/40). Calcium imaging was performed using fura-2-AM, with excitation at 380nm and a 455DCLP dichroic mirror (Chroma). The peak emission for fura-2 occurs at 510nm, but the emission band is broad enough that both our yellow and cyan filters passed fura-2 fluorescence. Therefore, fluorescence intensity collected by both emission filters was combined to comprise the total fura-2 emission. Images were captured with a CCD camera (CoolSnap HQ, Photometrics) and subsequently analyzed (MetaMorph v6.3, Universal Imaging). Images of CFP and YFP emission were acquired at a rate of 0.5 Hz, with exposure times ranging from 100ms to 1 sec, determined by the baseline expression of indicators. Images of fura-2 emission were acquired consecutively following each FRET image. Regions of interest were drawn

around the entire soma of a RGC expressing AKAR, and the average intensity of CFP, YFP and fura-2 was recorded for each time point.

To analyze fura-2 fluorescence intensity, background fluorescence was subtracted form both channels. Excitation at 380nm for calcium imaging led to excitation of CFP at 9% efficiency of the preferred 436nm excitation. Therefore, all fura-2 fluorescence traces were corrected for these bleedthrough factors using the following algorithm:

$$F_{fura} = \left[\frac{\left(F_{fura,c_{raw}} - .09 \bullet F_{CFP_{raw}}\right)}{\left(1-\left(.09 \bullet .082\right)\right)}\right] + \left[\frac{\left(F_{fura,y_{raw}} - .09 \bullet F_{FRET_{raw}}\right)}{\left(1-\left(.09 \bullet .098\right)\right)}\right]$$

where $F_{fura,c\ raw}$ and $F_{fura,y\ raw}$ denote the observed intensities in the two emission filters when exciting with 380nm light. $F_{CFPraw}$ and $F_{FRETraw}$ denote the observed intensities in the two emission filters when exciting with 436nm light. Amplitudes of calcium events were calculated as ΔF/F by using a five-frame average fura-2 intensity as the baseline, and the single frame with the minimum fura-2 intensity. In order to maximize the frame capture rate, fura-2 was not excited at 340nm, therefore fura-2 emission was not analyzed ratiometrically.

We estimated the resting intracellular calcium concentration using ratiometric fura-2 measurements and the following equation:

$$[Ca^{2+}]_i = K_D \bullet B(R - R\min)/(R\max - R)$$

where $R_{min}$, $R_{max}$ and B, were determined *in vitro* (Grynkiewicz et al., 1985). We recorded the following values: $R_{min}$ = 0.119, $R_{max}$ = 7.27, and B = 15.2. We assumed a $K_D$ for fura-2 in cells of 224 nM (Grynkiewicz et al., 1985). Retinal ganglion cells electroporated without plasmid, cultured for 24 hours and

incubated with fura-2-AM had a resting calcium concentration of 226 ± 21 nM (n=12). The increases in intracellular calcium concentration induced by short applications of potassium (see Figure 3.1) were calculated using the following equation:

$$[Ca^{2+}]_i = \frac{[Ca^{2+}]_{rest} + K_D \frac{(\Delta F / F)}{(\Delta F / F)_{\max}}}{1 - \frac{(\Delta F / F)}{(\Delta F / F)_{\max}}}$$

where $[Ca2+]_{rest}$ is the resting calcium concentration and ΔF/F max is based on F380 measurements.

To measure FRET ratios, background fluorescence was subtracted from both channels and bleedthrough of CFP and fura-2 were corrected. Fura-2 bleedthrough upon CFP excitation was 8.2% in the CFP channel and 9.8% in the YFP channel. Intensity of the FRET fluorophores was corrected as follows:

$$F_{CFP} = F_{CFP_{raw}} - .082 \bullet F_{fura,c}$$

$$F_{YFP} = F_{FRET_{raw}} - .45 \bullet F_{CFP} - .098 \bullet F_{fura,y}$$

where $F_{CFPraw}$ and $F_{FRETraw}$ denote the observed intensities in the two emission filters when exciting with 430nm light. $F_{fura,c}$ and $F_{fura,y}$ denote the intensity due to fura-2 in the CFP and YFP emission filters, respectively. FRET ratios were calculated as $R = (F_{YFP} / F_{CFP})$. Both AKAR2.2 and AKAR3 report increases in PKA activity as increases in FRET ratio. Changes in FRET ratio, ΔR, due to drug or depolarization were computed by subtracting the average value of the FRET ratio over 5 frames prior to the stimulus from the average value of the FRET ratio

over 5 frames at the maximum response within 60 seconds following the stimulus.

An important concern when imaging a three-fluorophore system is to correctly adjust the raw data for bleedthrough and unintentional excitation of the other fluorophores. However, we found that taking the ratio of YFP/CFP was remarkably effective at eliminating the contribution of fura-2 fluorescence, leading to minimal changes (<10%) in FRET ratio amplitude after correcting for bleedthrough. Also, because the timing of the images of calcium levels and PKA activity was not simultaneous, we were unable to completely eliminate the bleedthrough of fura-2 during rapid fluorescence changes, particularly during the first frame of a calcium event.

All pharmacological agents were purchased from Sigma. Puffing solution contained 5 mM KCl, 123 mM NaCl, 3 mM $CaCl_2$, 2 mM $MgCl_2$, 10 mM glucose and 10 mM HEPES, pH was adjusted with NaOH to 7.3. For dopamine application, freshly prepared dopamine (50μM) was added to puffing solution. High potassium puffing solution was similar, with 100 mM KCl substituted for an equivalent amount of NaCl, leading to a final concentration of 105mM KCl. One to three second applications of dopamine or high potassium solution were delivered through a glass electrophysiology electrode (approximately 2 μm tip size, located within 20 microns from transfected neuron) using a PV830 Pneumatic PicoPump at 6-8 psi, 50 msec pulse duration at 4 Hz. The duration of dopamine or potassium application was altered by increasing the number of

pulses. For experiments with zero external calcium, ACSF was modified to replace 2.5 mM $CaCl_2$ with 2 mM EGTA and 1.7 mM $MgCl_2$.

## RESULTS

### *Combined calcium and PKA activity imaging reveals calcium transients precede transient increases in PKA activity*

In previous studies, we demonstrated that depolarization-induced calcium transients transiently elevate PKA activity in RGCs with these elevations lasting approximately one minute (Dunn et al., 2006). In order to more fully elucidate the relationship between calcium levels and PKA activity in RGCs, we combined calcium imaging and FRET ratio imaging techniques (Harbeck et al., 2006). Plasmids containing the genetically encoded A-kinase activity reporter, AKAR3, under the CMV promoter, were transfected into retinal explants and cultured for 12 hours. In order to image intracellular calcium concentrations in the same cell, we used the calcium indicator fura-2, which has a spectrally separate excitation wavelength (380nm) from either CFP (430nm) or YFP (505nm). We loaded fura-2 via an AM ester immediately prior to imaging of explants transfected with AKAR3 (Figure 3.1A-C). This method loaded all neurons in the ganglion cell layer and therefore allowed us to simultaneously monitor the presence of retinal waves. RGCs, which were identified by the presence of fluorescence in an axon at the surface of the retina, exhibitinh both fura-2 and AKAR3 fluorescence were selected for subsequent experiments.

With the dual imaging technique we recorded both spontaneous and evoked changes in calcium levels and PKA activity within the same cell (Figure 3.1D). Increases in PKA activity increased the FRET efficiency, resulting in an increase in YFP fluorescence and a decrease in CFP fluorescence. All changes in PKA activity are reported as the value of $\Delta R = (F_{YFP}/F_{CFP})_{manipulation} - (F_{YFP}/F_{CFP})_{control}$. Increases in intracellular calcium led to decreases in fura-2 fluorescence, which are reported as fractional change in fluorescence, $\Delta F/F$.

Spontaneous PKA transients were always preceded by spontaneous calcium transients associated with retinal waves. However, smaller calcium transients were not followed by PKA transients (see example in Figure 3.1D). These observations are consistent with previous observations that depolarizations lasting more than 3 seconds were required for reliably inducing PKA transients in RGCs (Dunn et al., 2006).

To directly determine whether a threshold level of calcium is necessary to activate a PKA transient, we plotted the amplitude of FRET ratio changes from AKAR3 against the fractional change in fura-2 fluorescence (Figure 3.1E) or the increase in intracellular calcium concentration (Figure 3.2). We found that $\Delta F/F >$ 25% was necessary for inducing a reliable change in the AKAR 3 FRET ratio. This decrease in fura-2 fluorescence corresponds to an increase of intracellular calcium of 164 ± 7.5 nM. We cannot determine from these experiments whether this threshold is due to our detection efficiency of AKA3 FRET ratio changes or whether it represents a biochemical threshold. Though there is a positive correlation between amount of calcium influx and the amplitude of the FRET ratio

change (r = -.589), this correlation is weak and there is wide range of ΔR for a given ΔF/F. This variation of ΔR is likely due to different levels of expression of calcium-stimulated ACs in different cells (Figure 3.1E). For subsequent pharmacology experiments, we depolarized RGCs for greater than 2 seconds to assure that this stimulation induced detectable AKAR3 FRET ratio changes.

### *Blockade of transmembrane Adenylyl Cyclases Eliminates PKA transients in many RGCs*

Our goal was to determine how depolarization activates the cAMP/PKA cascade. We first explored the role of transmembrane ACs. Though most ACs in the nervous system belong to the families of transmembrane ACs, a recent report indicated that neurons may also have soluble ACs (Stessin et al., 2006; Wu et al., 2006). Soluble ACs are activated by bicarbonate and calcium, not G proteins. Soluble ACs have been studied in the context of sperm maturation and function, but have recently been reported to have a neurodevelopmental role in the outgrowth of axons.

To differentiate between the activity of calcium-dependent transmembrane ACs and soluble ACs, we utilized 2',5'-dideoxyadenosine (ddA), a drug that specifically blocks transmembrane AC activity. Since application of ddA required an extensive incubation period, the effects of ddA on dopamine and KCl responses were tested on separate population of cells than the control experiment.

To test that ddA blocked the function of all transmembrane ACs, we first assayed its effects on activation of dopamine receptors on RGCs. Rodent RGCs have D1-like dopamine receptors which elevate cAMP upon activation (Schambra et al., 1994; Koulen, 1999). Brief application of dopamine (50uM, 2 sec) led to increases in AKAR3 FRET ratio in all tested RGCs (Figure 3.3A $\Delta R = 0.070 \pm 0.045$, n= 5/5 cells). Dopamine responses were reliably blocked after incubation in the presence of ddA (Figure 3.3A, n= 7 cells).

For each cell that failed to respond to dopamine in the presence of ddA, we subsequently tested the FRET ratio response to brief application of KCl (105mM, 2 sec). As described previously (Dunn et al., 2006), direct depolarization of RGCs via this method led to a change in the AKAR3 FRET ratio ($\Delta R = 0.063 \pm 0.039$, n= 5 cells, Figure 3.3B). We found that six of eleven RGCs exhibited no change in FRET ratio in response to depolarization, indicating that transmembrane ACs are responsible for the increase in PKA activity in those cells. However, in the other five RGCs, depolarization induced FRET ratio changes were still present ($\Delta R = 0.023 \pm 0.023$, n= 5 cells). To test whether the remaining depolarization induced FRET ratio change was mediated by soluble AC, we repeated the experiment in the presence of ddA and the soluble AC antagonist 2-OHE and found that depolarization failed to increase FRET ratio ($\Delta R = -0.0004 \pm 0.0016$, n= 8 cells). This surprising finding offers the first evidence for the presence of a soluble AC activity in developing RGCs.

To confirm that AKAR 3 FRET ratio changes induced by depolarization were due to increases in PKA activity, we incubated explants in the PKA inhibitor

H89. Under these conditions, none of the RGCs showed a FRET ratio increase in response to depolarization (Figure 3.3E, n= 5 RGCs).

### *Mice lacking Adenylate Cyclase 1 (barrelless) and Adenylyl Cyclase 1/8 double Knockouts retain calcium-dependent PKA transients*

It has been reported that multiple calcium regulated adenylyl cyclases are expressed in the mammalian retina. Adenylyl cyclase 1 was reported to be the predominant AC in retinal ganglion cells in developing mice (Nicol et al., 2005; Nicol et al., 2006). To address the role of AC1 in calcium-dependent PKA activity increases, we utilized a mutant mouse lacking functional AC1, known as *brl*. Retinal ganglion cells from these mice expressing either AKAR2.2 or AKAR3 were depolarized using brief application of high concentration KCl (Figure 3.4A, B). RGCs from *brl* mice were found to retain depolarization-induced PKA transients, and furthermore, these transients were dependent on the influx of calcium. The amplitude of PKA activity transients generated by depolarization was not significantly different from control or heterozygote littermate controls (Figure 3.4B, $brl_{+/-}$ $\Delta R = 0.0076 \pm 0.0051$, n=13 neurons; $brl_{-/-}$: $\Delta R=0.010 \pm 0.0072$, n=16 neurons, wild-type: $\Delta R = 0.012 \pm 0.0071$, n=12 neurons).

A second calcium-dependent adenylate cyclase expressed in RGCs is AC8, though at this stage of developments it is expressed at much lower levels than AC1 (Abdel-Majid et al., 2002; Nicol et al., 2005; Nicol et al., 2006). To test for a role for AC8 in mediating calcium-dependent PKA transients we repeated these experiments in double knockout mice, lacking both AC1 and AC8. We

found that brief application of potassium generated transient activation of PKA in a majority of dKO cells expressing AKAR3 (Figure 3.5A, 28 of 35 cells, n= 29 mice). By comparing AKAR3 FRET ratio changes in dKOs with AC1 lacking mice and wild-types, we found that wild-type and *brl* mice were statistically indistinguishable, but AC1/AC8 dKO ratio changes were significantly diminished (Figure 3.5B, median ± standard deviation: wild-type $\Delta R=0.021\pm0.021$, n=19 neurons; AC1/AC8 $\Delta R=0.011\pm0.034$, n=35 neurons, p = 0.0012; *brl* $\Delta R=0.018\pm0.043$, n=7 neurons, p = 0.9999; two tailed Mann-Whitney test).

To confirm the unexpected result that neither of the major transmembrane calcium-dependent ACs were required for depolarization induced PKA transients, we performed a series of control experiments. First, we confirmed that AKAR3 FRET ratio changes were blocked by the PKA antagonist, H89 (50μM, Figure 3.5C, 0.5 ± 8.9 percent of control, n= 5 cells from 5 mice). Second, AKAR3 FRET ratio changes were absent in zero-calcium solutions (Figure 3.5D, 2.4 ± 12 percent of control, n= 6 cells from 5 mice), confirming that the remaining PKA transients were dependent on calcium. Third, AKAR3 FRET ratio changes persisted in the presence of the D1-like dopamine receptor antagonist, SCH 23390 (Figure 3.5E, 138 ± 111 percent of control, n= 8 cells from 7 mice), which reliably blocked all dopamine-induced increases in the AKAR3 FRET ratio (Figure 3.5E). Hence potassium-induced activation of dopamine receptors was not due to local release of dopamine. Together, these findings indicate that the combined loss of AC1 and AC8 significantly reduced the amplitude of PKA transients, but did not eliminate them.

***Phosphodiesterases are not responsible for the generation of PKA transients***

Thus far, we have determined that calcium-dependent PKA transients persist in mice lacking the primary calcium-dependent ACs found in the retina and, in a subset of RGCs, they persist in the presence of antagonists of all transmembrane ACs. A second possible biochemical basis of calcium-dependent increases in PKA activity could be calcium dependent inhibition of phosphodiesterases. While there are no reports of direct calcium/calmodulin inhibition of PDEs, activation of CaM kinases or calcineurin may modulate PDE activity.

To test whether phosphodiesterases played a role in generating PKA transients in RGCS, we bath applied the non-specific PDE inhibitor IBMX (100 µM) to retinal explants expressing AKAR3 in RGCs. IBMX significantly increased the baseline AKAR3 FRET ratio, indicating that PDEs are constitutively active in RGCs (Figure 3.6A,C $\Delta R = 0.10 \pm 0.052$, n= 9 cells in 9 mice). Because application of IBMX increases the frequency of retinal waves (data not shown), these experiments were repeated in the absence of external calcium to control for wave-induced increases in baseline PKA activity. We found the same results – blockade of PDE activity significantly increased the baseline AKAR3 FRET ratio ($\Delta R = 0.14 \pm 0.076$, n= 8 cells in 7 mice), indicating that ongoing activity of PDEs sets resting levels of PKA activity.

Next, we measured the response of retinal ganglion cells expressing AKAR3 to depolarization in the presence IBMX. Despite this large increase in the baseline FRET ratio, brief depolarization of RGCs led to AKAR3 FRET ratio changes (Figure 3.6C, $\Delta R = 0.34 \pm 0.021$, n= 9 cells in 9 mice). Hence, PDEs are unnecessary for the generation of depolarization induced PKA transients We also tested whether inhibition of PDEs might underlie the increase in PKA activity following depolarization in RGCs lacking both AC1/AC8. We found that bath application of IBMX led to FRET ratio increases in most AC1/AC8 dKO RGCs ($\Delta R = 0.13 \pm 0.085$, n= 9 cells in 9 mice) and that depolarization induced FRET ratio changes in most RGCs (n=10/14, Figure 3.6D,E). However, if the baseline FRET ratio was too high after application of IBMX, FRET ratio changes were not observed, suggesting that the indicator had saturated. If PKA activity is too high for the indicator, i.e. if all of the indicator is phosphorylated, then it will not be able to report further increases in PKA activity.

Surprisingly, in the presence of IBMX, some RGCs (n=4/14, Figure 3.6E) exhibited decreases in FRET ratio directly following depolarization. Because phosphodiesterase activity is blocked in these experiments, the most likely explanation is that phosphatase activity is increased in response to depolarization.

We hypothesized that calcium-dependent PDE1, which has been reported to be present in the GCL (Santone et al., 2006), might play a role in the regulation, if not the generation, of depolarization induced PKA transients. To test whether the calcium-dependent PDE1 mediated PKA activity transients, we

repeated these experiments in the presence of 8MM-IBMX, a specific inhibitor of calcium-activated PDE1. In contrast to IBMX, 8MM-IBMX did not lead to an increase in the baseline AKAR3 FRET ratio (Figure 3.6A,B). However, AKAR3 FRET ratio changes were increased in magnitude compared to control depolarization (Figure 3.6F, $\Delta R_{8MM}/\Delta R_{con} = 1.55 \pm 0.226$, n=6 neurons, $p = 0.002$. This increase in PKA activity transients was not due to an increase in calcium transient amplitude ($\Delta F/F_{8MM} / \Delta F/F_{con} = 0.79 \pm 0.35$, n=6 neurons, $p = 0.21$) and therefore is likely to be due to changes in PDE1 activity. These results imply that although PDEs are not responsible for generating PKA transients in response to depolarization, PDE1 is involved in regulating the amplitude of the PKA transients.

**DISCUSSION**

Here we have shown that depolarization-induced increases of PKA activity are mediated by a variety of adenylyl cyclases. First, we used dual imaging of the genetically encoded reporter of PKA activity and AM-loaded the calcium dye fura-2, to determine that a threshold calcium increase was necessary to induce a PKA transient. Second, we found that in a subset of RGCs, depolarization-induced PKA transients persisted despite of blockade of all transmembrane ACs, providing the first evidence that soluble AC is present in developing RGCs. Third, depolarization-induced PKA transients were decreased in amplitude but, surprisingly, persisted in knockout mice lacking the calcium dependent adenylate cyclase AC1 and in double knockout mice lacking both AC1 and AC8. Last, we

found that PDEs play a critical role in setting the basal levels of PKA activity and modulate the amplitude of PKA transients. Hence, a variety of calcium-dependent ACs are important for translating depolarization into activation of PKA biochemical cascade.

***Combined imaging of calcium and cAMP is a powerful technique for probing the intracellular signaling pathways of neurons***

Dual imaging of FRET-based cAMP reporters and the spectrally separate calcium indicator fura-2 has recently been used to monitor the intracellular activity of cultured, excitable cells (Landa et al., 2005; Harbeck et al., 2006; Willoughby and Cooper, 2006). In this study, we utilize this technique to determine the relationship between calcium transients and PKA activity in RGCs. Dual imaging offers several advantages over previous techniques used correlate PKA with neuronal activity. In the CNS, whole cell recording is often used to monitor activity of single neurons. However, this technique requires the disruption of the membrane of the neuron, which in turn dialyzes the contents of the cell with the solution in the electrode. In previous experiments, we found that whole cell recordings from RGCs dialyzed out important components of the cAMP pathway, making it impossible to record FRET ratio changes even in response to strong stimuli like forskolin. A second technique we previously used (Dunn and Wang, et al. 2006) utilized the electrophysiological activity of a nearby neuron as a proxy for the activity of the neuron of interest – the one expressing

the FRET reporter. While this technique is generally successful, being able to record calcium levels within the cell of interest is an obvious improvement.

By using dual imaging of AKAR3 and fura-2, we were able to determine several aspects regarding the relationship between calcium transients and PKA activity on a cell-by-cell basis. First, calcium transients reliably preceded all PKA activity transients. This is consistent with the hypothesis that calcium/calmodulin stimulated ACs are being activated to increase cAMP levels. Second, a threshold increase in intracellular calcium concentration of about 165nM was necessary for inducing a detectable PKA transient. It is unclear whether this threshold is a feature of the biochemical pathway, or if it is due to the sensitivity of AKAR3. Third, despite a correlation between the amplitude of FRET ratio changes and calcium transients, there is a large variability in FRET ratio changes fro a given calcium transient amplitude. It is unclear whether this variability is due to the indicator, or whether it reflects biological differences in cells, such as varied expression of calcium-stimulated ACs. One caveat is that AKAR3 reports the relative level of kinase and phosphatase activities on PKA target substrates, so if phosphatase activity is slowly varying over time, it may be responsible for some of the variance of FRET ratios we see in response to calcium influx.

### *Multiple calcium-stimulated adenylyl cyclases are responsible for calcium dependent PKA activity in RGCs*

Our findings indicate that there is no single AC that underlies calcium-dependent PKA transients in developing RGCs. Using pharmacological

blockade of a certain class of ACs, we found that roughly half of RGCs rely entirely on transmembrane ACs to produce calcium dependent PKA transients. This finding is consistent with our observations that mice lacking both AC1 and AC8, the dominant calcium-dependent ACs in RGCs, continue to have calcium-dependent increases in PKA activity. We observed that *brl* mice, which lack AC1, do not have significantly altered PKA transients, and that double knockouts of AC1/AC8 have smaller transients. We cannot tell whether this difference implies that AC8 is more likely to play an important role in calcium-dependent PKA activation or whether there was compensation by overexpression of AC8 in the *brl* mouse. These findings indicate that RGCs exhibit a ddA-insensitive AC activity, possibly soluble AC, though further study will be needed to confirm the expression and role of soluble AC in the neonate rodent retina.

One limitation of this finding is that we are averaging data from the entire soma, where it is most likely that different pathways for calcium dependent cAMP production will coexist. Perhaps in environments such as spines, axon terminals or growth cones a single AC subtype will be responsible for localized cAMP production.

Why do more RGCs in the AC1/AC8 dKO respond to depolarization than those with pharmacologically blocked transmembrane ACs? We first confirmed that the FRET ratio changes were due to PKA activity and calcium influx (Figure 3.5). We next tested the hypothesis that the localized depolarization caused by potassium puffs might cause the release of a neuromodulator, such as dopamine, which we have previously shown can increase PKA activity in neonate

rodent RGCs. However, blockade of D1-like receptors, while blocking dopamine induced FRET ratio changes, failed to block depolarization induced FRET ratio changes. We have not ruled out the possibility that release of other neuromodulators may play a role. These results all suggest, that in fact, AC1/AC8 dKOs have calcium-dependent PKA transients. One hypothesis as to why so few RGCs (7 of 35) fail to respond to depolarization is that RGCs exhibiting calcium induced PKA transients undergo a selective bias. During the early postnatal period, about half of RGCs undergo apoptosis (Mosinger Ogilvie et al., 1998). It has also been reported that increased cAMP improves the survival of RGCs (Meyer-Franke et al., 1995; Goldberg et al., 2002). Therefore, RGCs expressing a putative soluble AC activity would be more likely to survive and account for a greater percentage of RGCs.

***The role of phosphodiesterases in transient activation of PKA in RGCs***

Our results provide several insights into the activity of PDEs in early postnatal RGCs. First, via blockade of PDEs, a constitutive AC activity is uncovered – also indicating that PDEs are constitutively active to maintain a basal level of cAMP in the cell. Second, we rule out the possibility that PDEs are involved in the generation of transient PKA activity, in either wild-type or AC1/AC8 dKO mice. Finally, we report that blockade of calcium stimulated PDE1 leads to increased amplitude of FRET ratio changes in response to depolarization. This suggests that PDE1 plays a role in decreasing cAMP levels after calcium influx in RGCs.

One potentially interesting finding was that, even in the presence of IBMX, FRET ratio changes were transient. AKAR3 is designed to report relative PKA activity, and the temporary nature of FRET changes in the presence of a PDE inhibitor suggests that phosphatases are also involved in the FRET ratio changes we record. Indeed, in the presence of IBMX in four of fourteen RGCs from the AC1/AC8 dKO, we found that depolarization induced a decrease in FRET ratio. This is most likely due to phosphatase activity since PDEs are blocked.

**ACKNOWLEDGEMENTS**

Chapter 3, in part, is a draft of work to be submitted for publication

## REFERENCES

Abdel-Majid RM, Tremblay F, Baldridge WH. 2002. Localization of adenylyl cyclase proteins in the rodent retina. Brain Res Mol Brain Res 101:62-70.

Allen MD, Zhang J. 2006. Subcellular dynamics of protein kinase A activity visualized by FRET-based reporters. Biochemical And Biophysical Research Communications 348:716-721.

Beazely MA, Watts VJ. 2006. Regulatory properties of adenylate cyclases type 5 and 6: A progress report. Eur J Pharmacol 535:1-12. Epub 2006 Mar 2009.

Chandrasekaran AR, Plas DT, Gonzalez E, Crair MC. 2005. Evidence for an instructive role of retinal activity in retinotopic map refinement in the superior colliculus of the mouse. J Neurosci 25:6929-6938.

Choi EJ, Xia Z, Storm DR. 1992. Stimulation of the type III olfactory adenylyl cyclase by calcium and calmodulin. Biochemistry 31:6492-6498.

DiPilato LM, Cheng X, Zhang J. 2004. Fluorescent indicators of cAMP and Epac activation reveal differential dynamics of cAMP signaling within discrete subcellular compartments. Proc Natl Acad Sci U S A 101:16513-16518. Epub 12004 Nov 16515.

Dunn TA, Feller MB. 2008. Imaging second messenger dynamics in developing neural circuits. Dev Neurobiol 68:835-844.

Dunn TA, Wang CT, Colicos MA, Zaccolo M, DiPilato LM, Zhang J, Tsien RY, Feller MB. 2006. Imaging of cAMP levels and protein kinase a activity reveals that retinal waves drive oscillations in second-messenger cascades. Journal Of Neuroscience 26:12807-12815.

Feller MB, Wellis DP, Stellwagen D, Werblin FS, Shatz CJ. 1996. Requirement for cholinergic synaptic transmission in the propagation of spontaneous retinal waves. Science 272:1182-1187.

Goldberg JL, Espinosa JS, Xu Y, Davidson N, Kovacs GT, Barres BA. 2002. Retinal ganglion cells do not extend axons by default: promotion by neurotrophic signaling and electrical activity. Neuron. 33:689-702.

Harbeck MC, Chepurny O, Nikolaev VO, Lohse MJ, Holz GG, Roe MW. 2006. Simultaneous optical measurements of cytosolic Ca2+ and cAMP in single cells. Sci STKE 2006:pl6.

Kain K, Zhang J, Goldfinger L, Tsien R, Ginsberg M. 2005. Transient Adhesion-mediated PKA activation at the leading edge of migrating cells.

Koulen P. 1999. Postnatal development of dopamine D1 receptor immunoreactivity in the rat retina. J Neurosci Res. 56:397-404.

Landa LR, Jr., Harbeck M, Kaihara K, Chepurny O, Kitiphongspattana K, Graf O, Nikolaev VO, Lohse MJ, Holz GG, Roe MW. 2005. Interplay of Ca2+ and cAMP signaling in the insulin-secreting MIN6 beta-cell line. J Biol Chem 280:31294-31302. Epub 32005 Jun 31229.

Lu HC, Butts DA, Kaeser PS, She WC, Janz R, Crair MC. 2006. Role of efficient neurotransmitter release in barrel map development. J Neurosci. 26:2692-2703.

Lu HC, She WC, Plas DT, Neumann PE, Janz R, Crair MC. 2003. Adenylyl cyclase I regulates AMPA receptor trafficking during mouse cortical 'barrel' map development. Nat Neurosci 6:939-947.

Maas JW, Jr., Vogt SK, Chan GC, Pineda VV, Storm DR, Muglia LJ. 2005. Calcium-stimulated adenylyl cyclases are critical modulators of neuronal ethanol sensitivity. J Neurosci 25:4118-4126.

Meyer-Franke A, Kaplan MR, Pfrieger FW, Barres BA. 1995. Characterization of the signaling interactions that promote the survival and growth of developing retinal ganglion cells in culture. Neuron 15:805-819.

Ming G, Henley J, Tessier-Lavigne M, Song H, Poo M. 2001. Electrical activity modulates growth cone guidance by diffusible factors. Neuron 29:441-452.

Mosinger Ogilvie J, Deckwerth TL, Knudson CM, Korsmeyer SJ. 1998. Suppression of developmental retinal cell death but not of photoreceptor degeneration in Bax-deficient mice. Invest Ophthalmol Vis Sci 39:1713-1720.

Nicol X, Bennis M, Ishikawa Y, Chan GC, Reperant J, Storm DR, Gaspar P. 2006. Role of the calcium modulated cyclases in the development of the retinal projections. Eur J Neurosci 24:3401-3414.

Nicol X, Muzerelle A, Bachy I, Ravary A, Gaspar P. 2005. Spatiotemporal localization of the calcium-stimulated adenylate cyclases, AC1 and AC8, during mouse brain development. J Comp Neurol. 486:281-294.

Nicol X, Muzerelle A, Rio JP, Metin C, Gaspar P. 2006. Requirement of adenylate cyclase 1 for the ephrin-A5-dependent retraction of exuberant retinal axons. J Neurosci. 26:862-872.

Nicol X, Voyatzis S, Muzerelle A, Narboux-Neme N, Sudhof TC, Miles R, Gaspar P. 2007. cAMP oscillations and retinal activity are permissive for ephrin signaling during the establishment of the retinotopic map. Nat Neurosci 10:340-347.

Plas DT, Visel A, Gonzalez E, She WC, Crair MC. 2004. Adenylate Cyclase 1 dependent refinement of retinotopic maps in the mouse. Vision Res 44:3357-3364.

Santone R, Giorgi M, Maccarone R, Basso M, Deplano S, Bisti S. 2006. Gene expression and protein localization of calmodulin-dependent phosphodiesterase in adult rat retina. J Neurosci Res 84:1020-1026.

Saucerman JJ, Zhang J, Martin JC, Peng LX, Stenbit AE, Tsien RY, McCulloch AD. 2006. Systems analysis of PKA-mediated phosphorylation gradients in live cardiac myocytes. Proc Natl Acad Sci U S A 103:12923-12928.

Schambra UB, Duncan GE, Breese GR, Fornaretto MG, Caron MG, Fremeau RT, Jr. 1994. Ontogeny of D1A and D2 dopamine receptor subtypes in rat brain using in situ hybridization and receptor binding. Neuroscience. 62:65-85.

Stellwagen D, Shatz CJ, Feller MB. 1999. Dynamics of retinal waves are controlled by cyclic AMP. Neuron 24:673-685.

Stessin AM, Zippin JH, Kamenetsky M, Hess KC, Buck J, Levin LR. 2006. Soluble adenylyl cyclase mediates nerve growth factor-induced activation of Rap1. J Biol Chem 281:17253-17258. Epub 12006 Apr 17220.

Torborg CL, Feller MB. 2005. Spontaneous patterned retinal activity and the refinement of retinal projections. Progress In Neurobiology 76:213-235.

Violin JD, Zhang J, Tsien RY, Newton AC. 2003. A genetically encoded fluorescent reporter reveals oscillatory phosphorylation by protein kinase C. J Cell Biol 161:899-909. Epub 2003 Jun 2002.

Wayman GA, Impey S, Storm DR. 1995. Ca2+ inhibition of type III adenylyl cyclase in vivo. J Biol Chem 270:21480-21486.

Willoughby D, Cooper DM. 2006. Ca2+ stimulation of adenylyl cyclase generates dynamic oscillations in cyclic AMP. J Cell Sci 119:828-836.

Wong ST, Athos J, Figueroa XA, Pineda VV, Schaefer ML, Chavkin CC, Muglia LJ, Storm DR. 1999. Calcium-stimulated adenylyl cyclase activity is critical for hippocampus-dependent long-term memory and late phase LTP. Neuron 23:787-798.

Wong ST, Baker LP, Trinh K, Hetman M, Suzuki LA, Storm DR, Bornfeldt KE. 2001. Adenylyl cyclase 3 mediates prostaglandin E(2)-induced growth inhibition in arterial smooth muscle cells. J Biol Chem 276:34206-34212. Epub 32001 Jun 34229.

Wu KY, Zippin JH, Huron DR, Kamenetsky M, Hengst U, Buck J, Levin LR, Jaffrey SR. 2006. Soluble adenylyl cyclase is required for netrin-1 signaling in nerve growth cones. Nat Neurosci 9:1257-1264. Epub 2006 Sep 1210.

Zhang J, Hupfeld CJ, Taylor SS, Olefsky JM, Tsien RY. 2005. Insulin disrupts beta-adrenergic signalling to protein kinase A in adipocytes. Nature 437:569-573.

Zhang J, Ma Y, Taylor SS, Tsien RY. 2001. Genetically encoded reporters of protein kinase A activity reveal impact of substrate tethering. Proc Natl Acad Sci U S A 98:14997-15002.

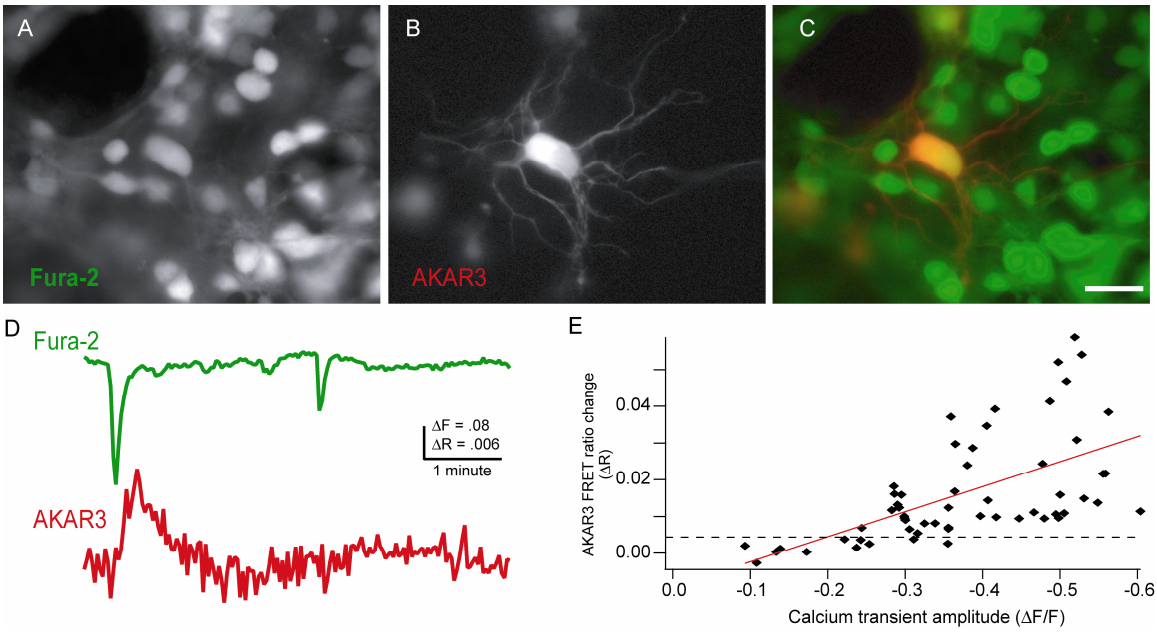


**Figure 3.1 Simultaneous FRET and calcium imaging reveal depolarization-induced PKA activity transients are temporally correlated with calcium transients** A-C) Fluorescence images of a retinal ganglion cell layer loaded with (A) calcium indicator, fura-2, (B) the PKA activity indicator AKAR3, and (C) merged. Scale bar = 20 μm. D) Simultaneous calcium and FRET imaging show that spontaneous calcium transient precedes PKA transient, however smaller calcium transients lead to no change in PKA activity. E) Comparison of AKAR3 FRET ratio changes to amplitude of calcium transients evoked by potassium induced depolarization of RGCs. A ΔF/F of –20% represents a calcium influx of 164 nM while a –60% change represents a calcium influx of 807 nM. Red line: Linear fit of data (r=-.589)

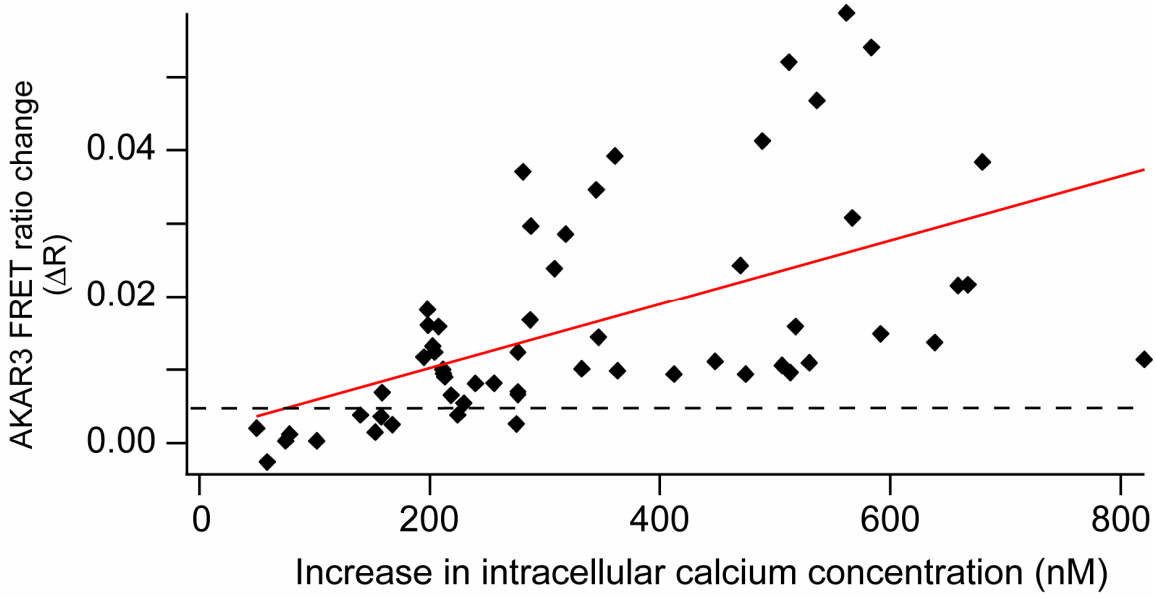


**Figure 3.2 Simultaneous FRET and calcium imaging reveal relationship between depolarization-induced PKA activity transients and amplitude of calcium concentration change.** A) Comparison of AKAR3 FRET ratio changes to amplitude of intracellular calcium concentration change evoked by potassium induced depolarization of RGCs. Red line: Linear fit of data (r= .551)

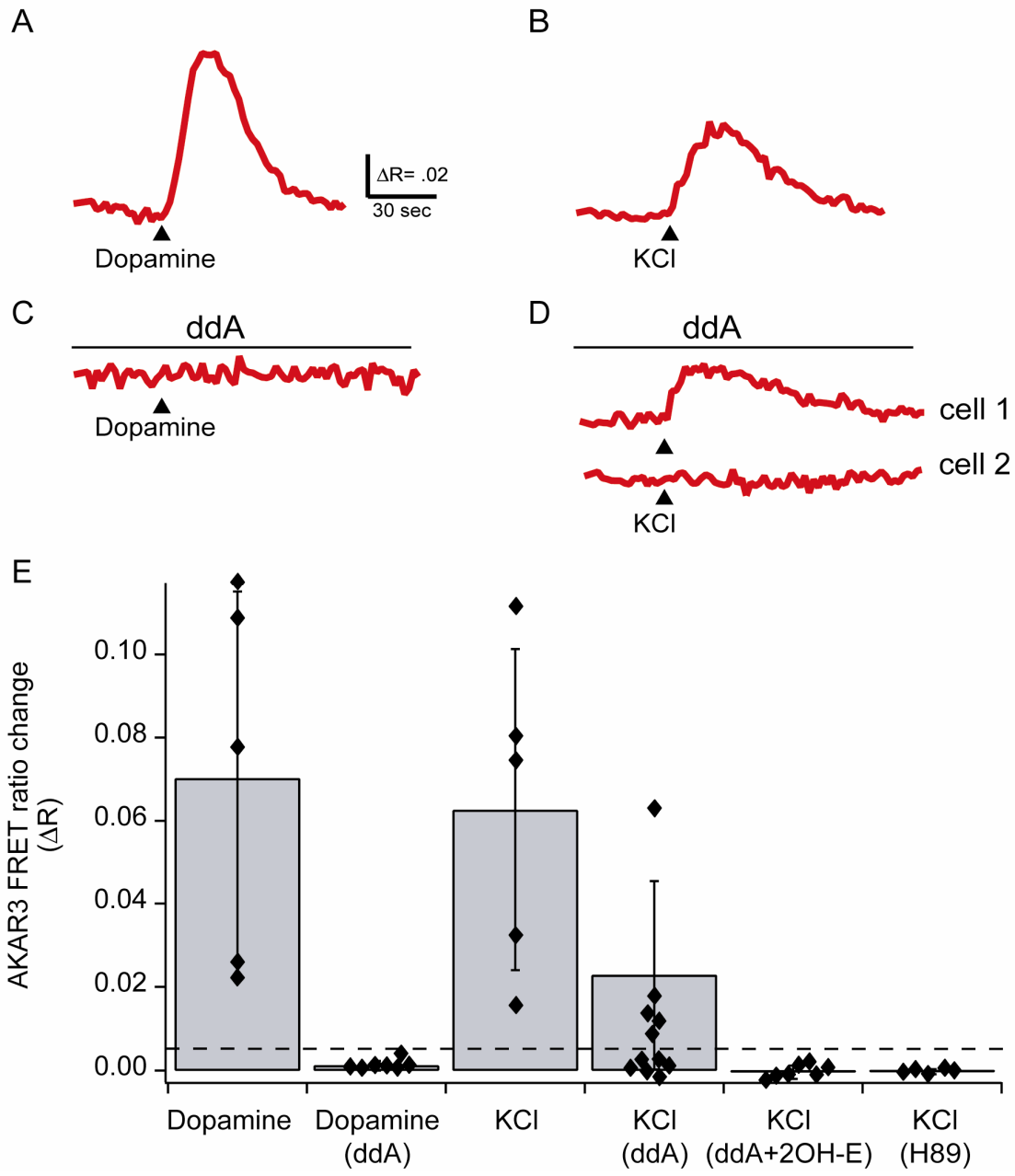


**Figure 3.3 Inhibition of transmembrane ACs eliminates depolarization-induced increases in PKA activity in a subset of RGCs.** A) Timecourse of AKAR3 FRET ratio in response to stimulation by 2 sec application of dopamine (50µM) in presence and absence of ddA, (50 µM) B) Timecourse of AKAR FRET ratio in response to stimulation by 2 sec application of KCl (105mM) in absence (TOP) and presence (BOTTOM) of ddA (50µM). Upper: Representative timecouse of KCl-induced FRET ratio change in the presence of ddA (5/11 RGCs) Lower: Example of RGC with no FRET ratio change in response to KCl depolarization (6/11 RGCs) E) Summary of FRET ratio responses in RGCs expressing AKAR3. The amplitude of depolarization-induced AKAR3 FRET ratio changes in the presence of the specific PKA inhibitor H89 (50µM).

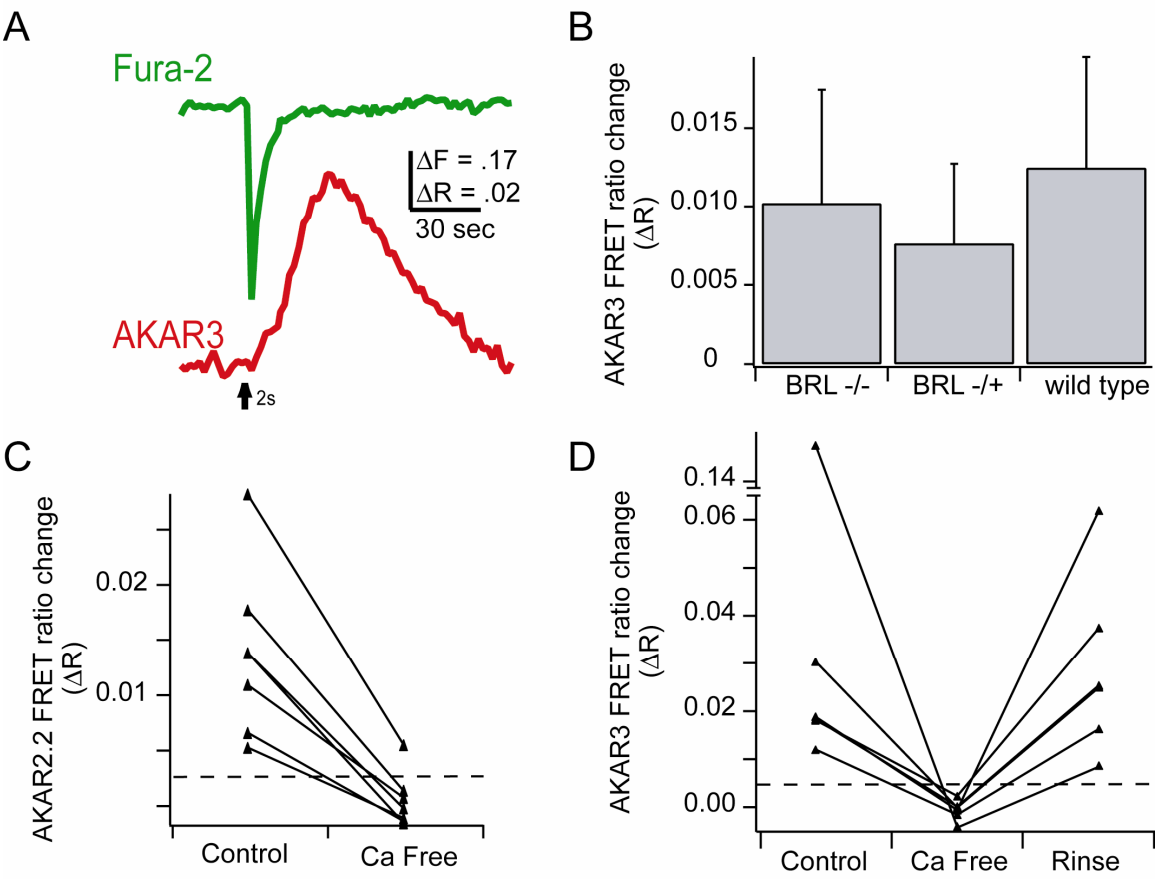


**Figure 3.4 Mice lacking Adenylyl cyclase 1 activity exhibit calcium dependent increases in PKA activity.** A) Simultaneous calcium and AKAR3 FRET imaging from a RGC in response to brief depolarization by KCl in *brl* mice, which lack the calcium-dependent adenylate cyclase AC1. B) Summary of AKAR2.2 FRET ratio change amplitudes in response to brief depolarization from *brl* mice, wild-types or heterozygotes. C) Summary of AKAR2.2 FRET ratio changes in response to depolarization in the presence or absence of extracellular calcium. D) Summary of AKAR3 FRET ratio changes in *brl* mice in response to depolarization in the presence or absence of extracellular calcium.

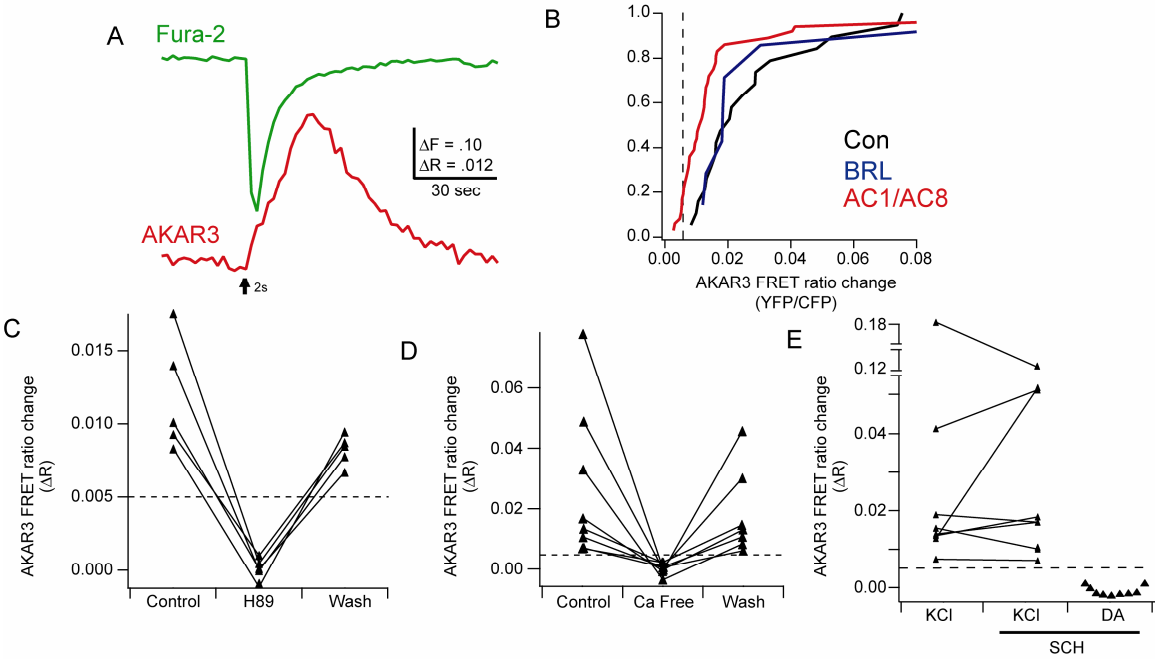


**Figure 3.5 Depolarization-induced increases in PKA activity persist in Adenylyl Cyclase 1/8 Knockouts.** A) Timecourse of fura-2 fluorescence and FRET ratio change in response to KCl puff in AC1/AC8 DKOs. B) Summary of AKAR3 FRET ratio changes in wild type, AC1 lacking, and AC1/AC8 DKOs. C) Summary of depolarization induced PKA transients in presence or absence of H89, external calcium (D) and the D1-like dopamine receptor antagonist, SCH 23390 (E).

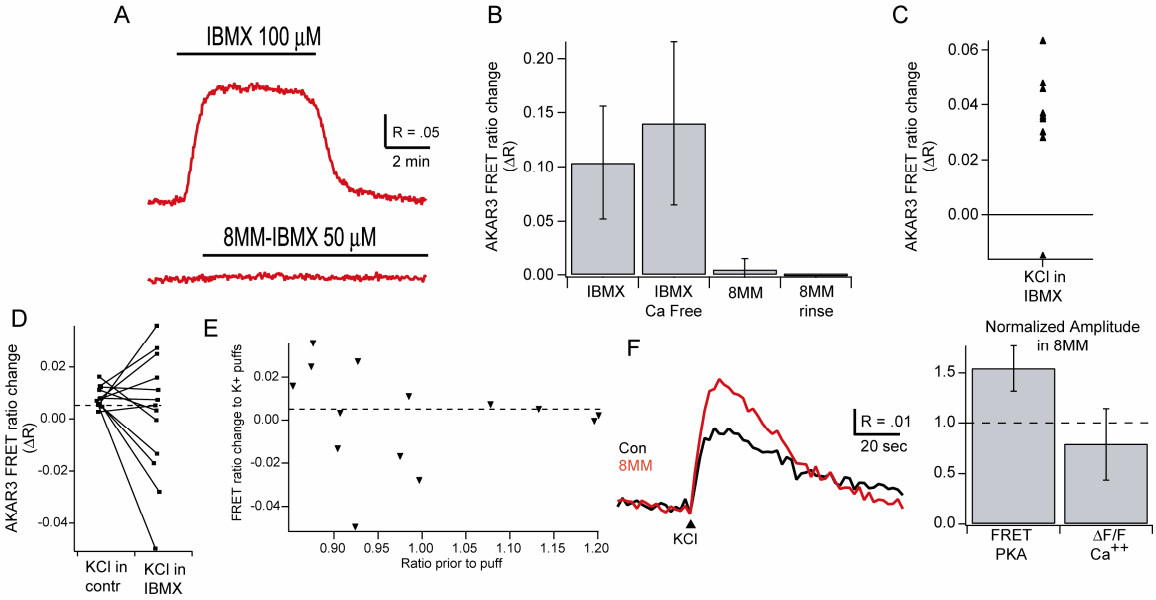


**Figure 3.6 PDEs are not necessary for the generation of depolarization induced PKA transients.** AKAR3 FRET ratio traces during bath application of 100µM IBMX (black bar) (upper) or 50µM 8MM-IBMX (lower). B) Summary of FRET ratio changes in response to IBMX or 8MM-IBMX. C) FRET response of a RGC in response to depolarization in the presence of IBMX. D) Summary of depolarization induced PKA transients in AC1/AC8 dKOs in the presence or absence of IBMX, a general antagonist of phosphodiesterases. E) FRET ratio change due to depolarization in the presence of IBMX as a function of ratio prior to depolarization. F) Left: Ratio traces of a RGC response to KCl in the presence (red) or absence (black) of 8MM-IBMX. Right: Summary of FRET ratio changes and fluorescence changes in response to KCl puffs, while in the presence of 8MM-IBMX. Amplitudes are normalized to changes observed in control conditions for each RGC.

## Chapter 4
## Concluding Remarks

### Relationship between AKAR FRET ratio and PKA activity

In this thesis, we have used different indicators for cAMP and PKA activity. Before establishing a model of cAMP/PKA signaling in RGCs based on these indicators, it is critical to take into account how these indicators function. For example FRET ratio changes of AKARs do not directly reflect PKA activity, but rather reports changes in relative levels of phosphorylation of PKA target substrates. This is in contrast to other FRET-based kinase reporters that are based on conformational changes in the kinases themselves. For example, CaMuia, a reporter of CaMKII activation, changes FRET efficiency when CaMKII undergoes a conformational change when it is activated (Takao et al., 2005). In contrast to CaMuia where FRET ratios are not influenced by the activity of phosphatases on its targets, the phosphorylation state of AKAR is controlled by both PKA and serine-threonine phosphatases. AKARs therefore report the net effect of kinase and phosphatase activity of PKA targets.

How accurately does AKAR3 indicate the phosphorylation state of endogenous targets of PKA? During the development of the AKAR indicators, the phosphobinding domain of the indicator was switched from a peptide based on 14-3-3 to a peptide based on FHA1(Zhang et al., 2001; Zhang et al., 2005). The reason underlying this change was an improvement in the off-kinetics of the indicator. The 14-3-3 domain bound the phospho-serine too tightly and the indicator would not return to baseline levels of FRET after stimulation. Switching the serine to a threonine and replacing the 14-3-3 domain with the

phosphobinding region of FHA1 allowed the indicator to return to baseline levels after stimulation. The proposed explanation for this change was increased access to the phosphate group by phosphatases (Zhang et al., 2005). However, it is unclear which phospho-binding proteins the endogenous targets of PKA will partner with. 14-3-3 is a ubiquitous protein and has been reported to associate with a wide variety of phosphorylated targets (Fu et al., 2000). If endogenous 14-3-3 protects against dephosphorylation of its binding partners, the transient, repeated activation of PKA found in developing RGCs may lead to protein targets that are continuously phosphorylated. Different proteins might also have different phospho-binding partners, leading to different durations of phosphorylation amongst different proteins. Therefore, we hypothesize that AKAR3 FRET ratio changes are likely to be a good measure of phosphorylation of targets that interact with FHA1 phospho-binding domains, but might fail to represent the dynamics of targets that interact with 14-3-3. To determine whether the dephosphorylation kinetics of AKAR3 match those of PKA targets of interest, one could measure the variation of duration of phosphorylation by performing a timecourse of phospho-blots for several candidate proteins known to interact with different phospho-binding proteins.

**Model of activity-induced activation of the cAMP/PKA pathway in RGCs**

Based on the result of experiments described in chapters 2 and 3, we propose the following model of the activity-induced activation of the cAMP/PKA signaling pathway in retinal ganglion cells (Figure 4.1). Calcium influx via

depolarization also leads to transient PKA activation, implying that calcium-dependent adenylate cyclases are present in the soma of RGCs. Further, bath application of the phosphodiesterase inhibitor IBMX increased baseline PKA activity. This implies that both adenylate cyclases and phosphodiesterases are constitutively active. Blockade of PDE1 activity led to an increase in FRET ratio amplitude, indicating that calcium influx is activating PDE1 and allowing it to play a modulatory role. Blockade of all PDEs, using IBMX, did not eliminate the off kinetics of the FRET ratio change. This suggests that PDEs alone are not responsible for the transient nature of depolarization induced PKA activation. Instead, phosphatase activity must also play a role in determining the duration of the increase in PKA activity. We do not have clear evidence implicating particular phosphatases. We observed FRET ratio decreases in some RGCs in response to depolarization in the presence of IBMX; calcineurin, a calcium/calmodulin activated phosphatase is a candidate to mediate these decreases in FRET ratio.

We also have evidence that PKA activity in RGCs is elevated by brief application of dopamine. This finding is consistent with the hypothesis that RGCs express a D-1 like dopamine receptor during development, since this class of G-protein coupled receptors stimulate transmembrane adenylate cyclases. In contrast, we found that the neuromodulator adenosine, which also activated GPCRs did not increase PKA activity in RGCs (data not shown). We did not test extensively for the existence of other classes of GPCRs.

Our recordings were limited to observation in the soma of RGCs. Limited expression did not allow for us to reliably detect changes in subcellular compartments, which may have a different complement of cAMP effectors. In addition, retinal ganglion cells are comprised of many different subclasses, and not all of them will necessarily follow all of these rules. Recently, promoters for particular classes of RGCs have been discovered (Kim et al., 2008; Yonehara et al., 2008) that will allow for expression of genetically encoded indicators in specific classes to determine differences in the signaling pathways.

**Tools for elucidating the mechanisms underlying retinal waves**

One of the original goals of this project was to investigate the role of the cAMP/PKA pathway in determining the properties of retinal waves. This work was predicated in large part on prior studies that found that the frequency of retinal waves could be increased through application of forskolin, and diminished in the presence of the PKA inhibitor Rp-cAMPS (Stellwagen et al., 1999; Stellwagen and Shatz, 2002). Retinal waves are initiated by a subclass of amacrine cells termed starburst amacrine cells (Zheng et al., 2006). Starburst amacrine cells function as pacemakers with a time-varying membrane potential – they spontaneously fire a burst of calcium spikes, which are followed by a slow after-hyperpolarization. The after-hyperpolarization is sufficient to explain the minute-long intervals between retinal waves. Zheng et al., went on to show that this after hyperpolarization is significantly shortened by elevated cAMP.

To address the question of how cAMP levels alter retinal wave frequency, we have started to develop techniques to selectively express FRET indicators in starburst amacrine cells. In coordination with Kevin Ford, a fellow graduate student in the Feller lab who is now working on this question, we were able to express AKAR3 in starburst amacrine cells using the mGlur2 promoter (Watanabe et al., 1998; Yoshida et al., 2001). In preliminary experiments, we found there were spontaneous decreases in PKA in the starburst amacrine cell that were not present in a nearby ganglion cell (Figure 4.2). (Note - these decreases were observed only under conditions where baseline levels of cAMP were elevated by bath application of forskolin). This is consistent with the hypothesis that PDE1, the family of calcium activated PDEs, decreases cAMP in response to depolarization of starburst amacrine cells. It has also been recently reported that PDE1 immunostaining colocalizes with choline acetyltransferase staining, indicating that PDE1 is present in starburst amacrine cells (Santone et al., 2006). The current hypothesis for this process is that upon depolarization of a starburst amacrine cell, calcium flows into the cell, activating PDE1, which breaks down cAMP, leading to a disinhibition of the hyperpolarizing conductance. As calcium is sequestered and removed from the cell, PDE1 activity diminishes, cAMP levels increase, and the conductance slowly turns off. Consistent with this model, the specific PDE1 inhibitor, 8MM-IBMX, does not change baseline FRET ratios in retinal ganglion cells, but does increase the frequency of retinal waves. Kevin Ford is currently investigating these intriguing results.

There is also a possible role for transient activation of the cAMP/PKA pathway in RGCs to play a role in retinal waves. Cyclic AMP/PKA transients in retinal ganglion cells may alter the excitability of the cell through phosphorylation of ion channels. PKA is known to phosphorylate voltage gated sodium and calcium channels (Cantrell et al., 1999; Cantrell et al., 2002; Hall et al., 2007; Vela et al., 2007). A second possibility is that this biochemical pathway modulated gap junction coupling, via phosphorylation of connexins (Kothmann et al., 2007). Connexin36 is the most common connexin in the rodent retina, and it disrupts the pattern of spontaneous activity (Hansen et al., 2005; Torborg et al., 2005). Upon phosphorylation of connexin36 by PKA, the junctional conductance is diminished (Urschel et al., 2006), possibly altering the rate of propagation of retinal waves.

**Role for cAMP/PKA transients in driving activity-dependent developmental processes**

Further study of will be needed to specify a function for the periodic, transient activation of the cAMP/PKA pathway. Our goal was to design a manipulation that would allow us to preserve spontaneous depolarizations and even calcium influx and then specifically block the transient activation of PKA. However, it has been previously reported that manipulations that increase cAMP concentration increase wave frequency, and manipulations that block PKA activity block retinal waves (Stellwagen et al., 1999). Therefore, treatment with

pharmacological agents affecting the cAMP/PKA pathway will confound the experiment.

For this reason, we instead sought to determine the mechanism underlying the depolarization induced PKA transients. We could then use this information to identify mutant mice lacking the necessary components of the cAMP/PKA pathway. Both barrelless mice, which lack the calcium-dependent adenylate cyclase AC1, and AC1/AC8 dKO mice exhibited spontaneous, periodic calcium transients. However, both strains of mice also exhibited depolarization-induced, calcium dependent PKA transients in the somas of RGCs.

Interestingly, both strains of mice have disrupted refinement of retinal projections to the superior colliculus (Plas et al., 2004; Chandrasekaran et al., 2005; Nicol et al., 2006; Nicol et al., 2007) and the dLGN (Ravary et al., 2003). The observation that brl mice have normal retinal waves, and normal PKA transients, implies that AC1 is exerting its effect on refinement of retinal projections downstream of waves and PKA transients. Two possibilities have been proposed. First, AC1 has been implicated in mediating growth cone responses to guidance molecules (Nicol et al., 2006; Nicol et al., 2007). Second AC1 has been implicated in synaptic plasticity (Lu et al., 2003; Chandrasekaran et al., 2005). To test these models, it is critical to improve the expression levels of these indicators to allow for imaging in subcellular compartments. Preliminary experiments (performed by M. Colicos, and reanalyzed later by me) demonstrated that we could detect FRET ratio changes in some RGC growth cones (Figure 4.3), though these findings led to inconsistent results.

Though transient activation of PKA in the soma of RGCs is not critical for refinement of retinal projections, it may mediate cell autonomous processes. The cAMP/PKA pathway can exert its biochemical influence either through activation of transcription factors or by phosphorylation of existing proteins. It has been reported that repeated calcium influx with a period of about one minute is most effective for activating certain transcription factors (Dolmetsch et al., 1998; Li et al., 1998). Similar results for repeated activation of the cAMP/PKA pathway have not been reported. Periodic PKA transients are not likely to increase the activation of its most familiar target, the transcription factor CREB, because a single PKA event seems to be enough to cause phosphorylation (Fields et al., 1997). Periodic PKA transients may allow CREB to remain phosphorylated for a longer duration, however. A second possibility is that transient PKA activation might lead to phosphorylation of local targets but have no effect on transcription. In order for PKA to phosphorylate CREB, the catalytic subunit needs to translocate to the nucleus of the cell. Recent reports suggest that brief activation of PKA does not allow the catalytic subunit to fully dissociate and translocate to the nucleus (Dyachok et al., 2006). We currently do not have evidence for which (or both) of these pathways is important. One could test for PKA translocation to the nucleus by using an AKAR tagged with a nuclear localization signal (Allen and Zhang, 2006).

Periodic activation of PKA may play a critical role in neuronal survival. During the period in which periodic spontaneous PKA transients occur, half of retinal ganglion cells undergo apoptosis (Mosinger Ogilvie et al., 1998). RGC

survival *in vitro* is promoted by the addition of forskolin (Meyer-Franke et al., 1995). Furthermore, the presence of periodic neuronal activity is sufficient to promote survival of RGCs (Meyer-Franke et al., 1995; Goldberg et al., 2002). This suggests that spontaneous activity in RGCs increases cAMP levels, consistent with our imaging findings. We hypothesize that wave-activated PKA transients act as a "heartbeat" for developing RGCs, conferring a survival signal if PKA transients are frequent enough. In our experiments, we found that the RGCs exhibiting larger calcium transients were more likely to exhibit PKA transients, thereby providing a mechanism to select for RGCs that are well connected to the surrounding network.

## REFERENCES

Abdel-Majid RM, Tremblay F, Baldridge WH. 2002. Localization of adenylyl cyclase proteins in the rodent retina. Brain Res Mol Brain Res 101:62-70.

Allen MD, Zhang J. 2006. Subcellular dynamics of protein kinase A activity visualized by FRET-based reporters. Biochemical And Biophysical Research Communications 348:716-721.

Cantrell AR, Scheuer T, Catterall WA. 1999. Voltage-dependent neuromodulation of Na+ channels by D1-like dopamine receptors in rat hippocampal neurons. J Neurosci 19:5301-5310.

Cantrell AR, Tibbs VC, Yu FH, Murphy BJ, Sharp EM, Qu Y, Catterall WA, Scheuer T. 2002. Molecular mechanism of convergent regulation of brain Na(+) channels by protein kinase C and protein kinase A anchored to AKAP-15. Mol Cell Neurosci 21:63-80.

Chandrasekaran AR, Plas DT, Gonzalez E, Crair MC. 2005. Evidence for an instructive role of retinal activity in retinotopic map refinement in the superior colliculus of the mouse. J Neurosci 25:6929-6938.

Dolmetsch RE, Xu K, Lewis RS. 1998. Calcium oscillations increase the efficiency and specificity of gene expression [see comments]. Nature 392:933-936.

Dunn TA, Feller MB. 2008. Imaging second messenger dynamics in developing neural circuits. Dev Neurobiol 68:835-844.

Dunn TA, Wang CT, Colicos MA, Zaccolo M, DiPilato LM, Zhang J, Tsien RY, Feller MB. 2006. Imaging of cAMP levels and protein kinase a activity reveals that retinal waves drive oscillations in second-messenger cascades. Journal Of Neuroscience 26:12807-12815.

Dyachok O, Isakov Y, Sagetorp J, Tengholm A. 2006. Oscillations of cyclic AMP in hormone-stimulated insulin-secreting beta-cells. Nature. 439:349-352.

Fields RD, Eshete F, Stevens B, Itoh K. 1997. Action potential-dependent regulation of gene expression: temporal specificity in ca2+, cAMP-responsive element binding proteins, and mitogen-activated protein kinase signaling. J Neurosci 17:7252-7266.

Fu H, Subramanian RR, Masters SC. 2000. 14-3-3 proteins: structure, function, and regulation. Annu Rev Pharmacol Toxicol 40:617-647.

Goldberg JL, Espinosa JS, Xu Y, Davidson N, Kovacs GT, Barres BA. 2002. Retinal ganglion cells do not extend axons by default: promotion by neurotrophic signaling and electrical activity. Neuron. 33:689-702.

Hall DD, Davare MA, Shi M, Allen ML, Weisenhaus M, McKnight GS, Hell JW. 2007. Critical role of cAMP-dependent protein kinase anchoring to the L-type calcium channel Cav1.2 via A-kinase anchor protein 150 in neurons. Biochemistry 46:1635-1646. Epub 2007 Jan 1620.

Hansen KA, Torborg CL, Elstrott J, Feller MB. 2005. Expression and function of the neuronal gap junction protein connexin 36 in developing mammalian retina. Journal Of Comparative Neurology 493:309-320.

Kim IJ, Zhang Y, Yamagata M, Meister M, Sanes JR. 2008. Molecular identification of a retinal cell type that responds to upward motion. Nature 452:478-482.

Kothmann WW, Li X, Burr GS, O'Brien J. 2007. Connexin 35/36 is phosphorylated at regulatory sites in the retina. Vis Neurosci 24:363-375. Epub 2007 Jul 2020.

Li W, Llopis J, Whitney M, Zlokarnik G, Tsien RY. 1998. Cell-permeant caged InsP3 ester shows that Ca2+ spike frequency can optimize gene expression. Nature 392:936-941.

Lu HC, She WC, Plas DT, Neumann PE, Janz R, Crair MC. 2003. Adenylyl cyclase I regulates AMPA receptor trafficking during mouse cortical 'barrel' map development. Nat Neurosci 6:939-947.

Meyer-Franke A, Kaplan MR, Pfrieger FW, Barres BA. 1995. Characterization of the signaling interactions that promote the survival and growth of developing retinal ganglion cells in culture. Neuron 15:805-819.

Mosinger Ogilvie J, Deckwerth TL, Knudson CM, Korsmeyer SJ. 1998. Suppression of developmental retinal cell death but not of photoreceptor degeneration in Bax-deficient mice. Invest Ophthalmol Vis Sci 39:1713-1720.

Nicol X, Bennis M, Ishikawa Y, Chan GC, Reperant J, Storm DR, Gaspar P. 2006. Role of the calcium modulated cyclases in the development of the retinal projections. Eur J Neurosci 24:3401-3414.

Nicol X, Muzerelle A, Bachy I, Ravary A, Gaspar P. 2005. Spatiotemporal localization of the calcium-stimulated adenylate cyclases, AC1 and AC8, during mouse brain development. J Comp Neurol. 486:281-294.

Nicol X, Muzerelle A, Rio JP, Metin C, Gaspar P. 2006. Requirement of adenylate cyclase 1 for the ephrin-A5-dependent retraction of exuberant retinal axons. J Neurosci. 26:862-872.

Nicol X, Voyatzis S, Muzerelle A, Narboux-Neme N, Sudhof TC, Miles R, Gaspar P. 2007. cAMP oscillations and retinal activity are permissive for ephrin signaling during the establishment of the retinotopic map. Nat Neurosci 10:340-347. eniculate axons. Neuron 31:409-420.

Plas DT, Visel A, Gonzalez E, She WC, Crair MC. 2004. Adenylate Cyclase 1 dependent refinement of retinotopic maps in the mouse. Vision Res 44:3357-3364.

Ravary A, Muzerelle A, Herve D, Pascoli V, Ba-Charvet KN, Girault JA, Welker E, Gaspar P. 2003. Adenylate cyclase 1 as a key actor in the refinement of retinal projection maps. J Neurosci 23:2228-2238.

Santone R, Giorgi M, Maccarone R, Basso M, Deplano S, Bisti S. 2006. Gene expression and protein localization of calmodulin-dependent phosphodiesterase in adult rat retina. J Neurosci Res 84:1020-1026.

Stellwagen D, Shatz CJ. 2002. An instructive role for retinal waves in the development of retinogeniculate connectivity. Neuron 33:357-367.

Stellwagen D, Shatz CJ, Feller MB. 1999. Dynamics of retinal waves are controlled by cyclic AMP. Neuron 24:673-685.

Takao K, Okamoto K, Nakagawa T, Neve RL, Nagai T, Miyawaki A, Hashikawa T, Kobayashi S, Hayashi Y. 2005. Visualization of synaptic Ca2+ /calmodulin-dependent protein kinase II activity in living neurons. J Neurosci 25:3107-3112.

Torborg CL, Hansen KA, Feller MB. 2005. High frequency, synchronized bursting drives eye-specific segregation of retinogeniculate projections. Nat Neurosci 8:72-78. Epub 2004 Dec 2019.

Torborg CL, Hansen KA, Feller MB. 2005. High frequency, synchronized bursting drives eye-specific segregation of retinogeniculate projections. Nature Neuroscience 8:72-78.

Urschel S, Hoher T, Schubert T, Alev C, Sohl G, Worsdorfer P, Asahara T, Dermietzel R, Weiler R, Willecke K. 2006. Protein kinase A-mediated phosphorylation of connexin36 in mouse retina results in decreased gap junctional communication between AII amacrine cells. J Biol Chem 281:33163-33171. Epub 32006 Sep 33166.

Vela J, Perez-Millan MI, Becu-Villalobos D, Diaz-Torga G. 2007. Different kinases regulate activation of voltage-dependent calcium channels by depolarization in GH3 cells. Am J Physiol Cell Physiol 293:C951-959. Epub 2007 May 2016.

Watanabe D, Inokawa H, Hashimoto K, Suzuki N, Kano M, Shigemoto R, Hirano T, Toyama K, Kaneko S, Yokoi M, Moriyoshi K, Suzuki M, Kobayashi K, Nagatsu T, Kreitman RJ, Pastan I, Nakanishi S. 1998. Ablation of cerebellar Golgi cells disrupts synaptic integration involving GABA inhibition and NMDA receptor activation in motor coordination. Cell 95:17-27.

Yonehara K, Shintani T, Suzuki R, Sakuta H, Takeuchi Y, Nakamura-Yonehara K, Noda M. 2008. Expression of SPIG1 reveals development of a retinal ganglion cell subtype projecting to the medial terminal nucleus in the mouse. PLoS ONE 3:e1533.

Yoshida K, Watanabe D, Ishikane H, Tachibana M, Pastan I, Nakanishi S. 2001. A key role of starburst amacrine cells in originating retinal directional selectivity and optokinetic eye movement. Neuron 30:771-780.

Zhang J, Hupfeld CJ, Taylor SS, Olefsky JM, Tsien RY. 2005. Insulin disrupts beta-adrenergic signalling to protein kinase A in adipocytes. Nature 437:569-573.

Zhang J, Ma Y, Taylor SS, Tsien RY. 2001. Genetically encoded reporters of protein kinase A activity reveal impact of substrate tethering. Proc Natl Acad Sci U S A 98:14997-15002.

Zheng J, Lee S, Zhou ZJ. 2006. A transient network of intrinsically bursting starburst cells underlies the generation of retinal waves. Nat Neurosci. 9:363-371. Epub 2006 Feb 2005.

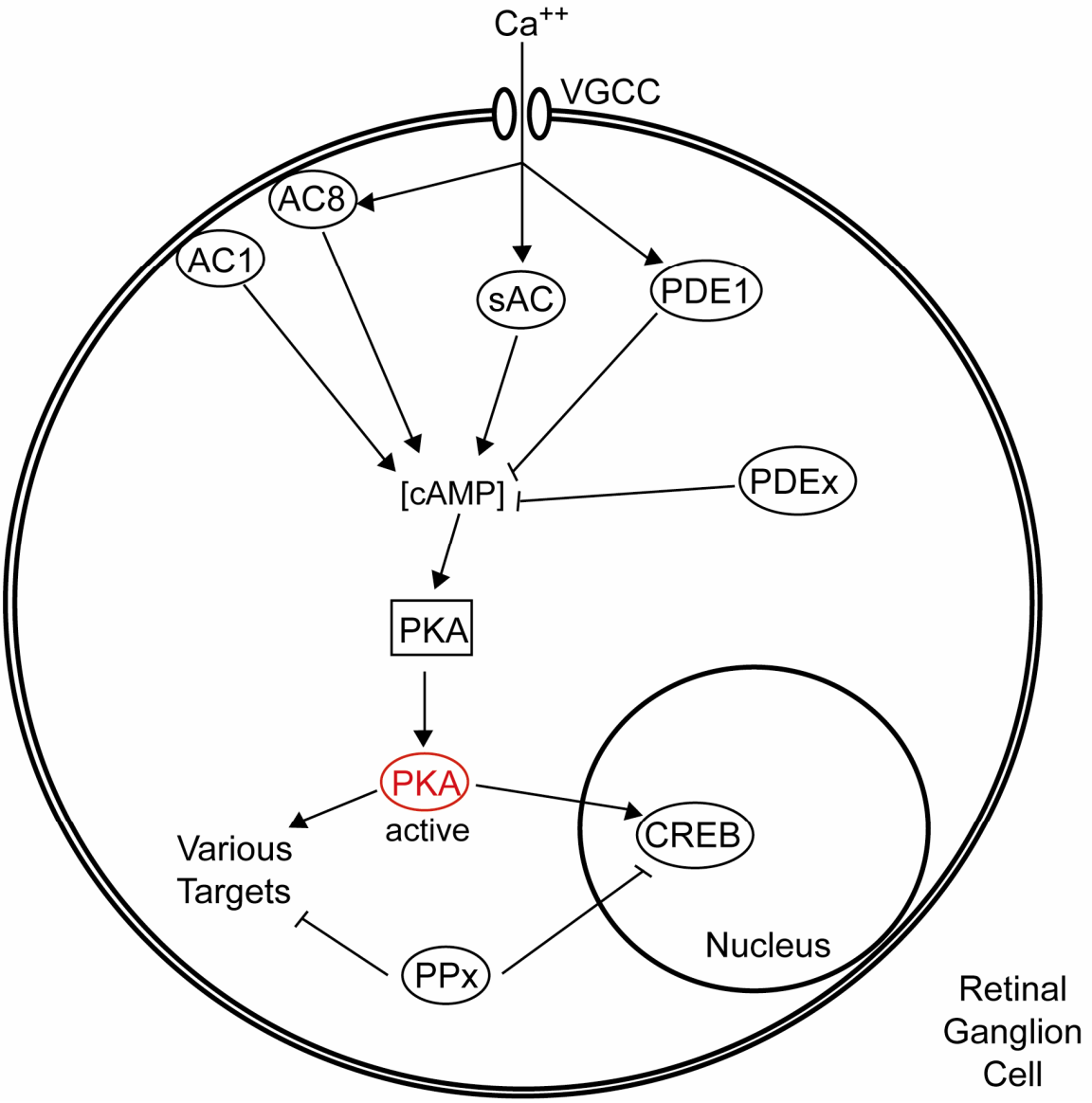


**Figure 4.1 Model of the activity-induced activation of the cAMP/PKA signaling pathway in retinal ganglion cells**. Abbreviations: VGCC: Voltage-gated calcium channel, PPx: Unidentified protein phosphatase, PDEx: Unidentified phosphodiesterase.

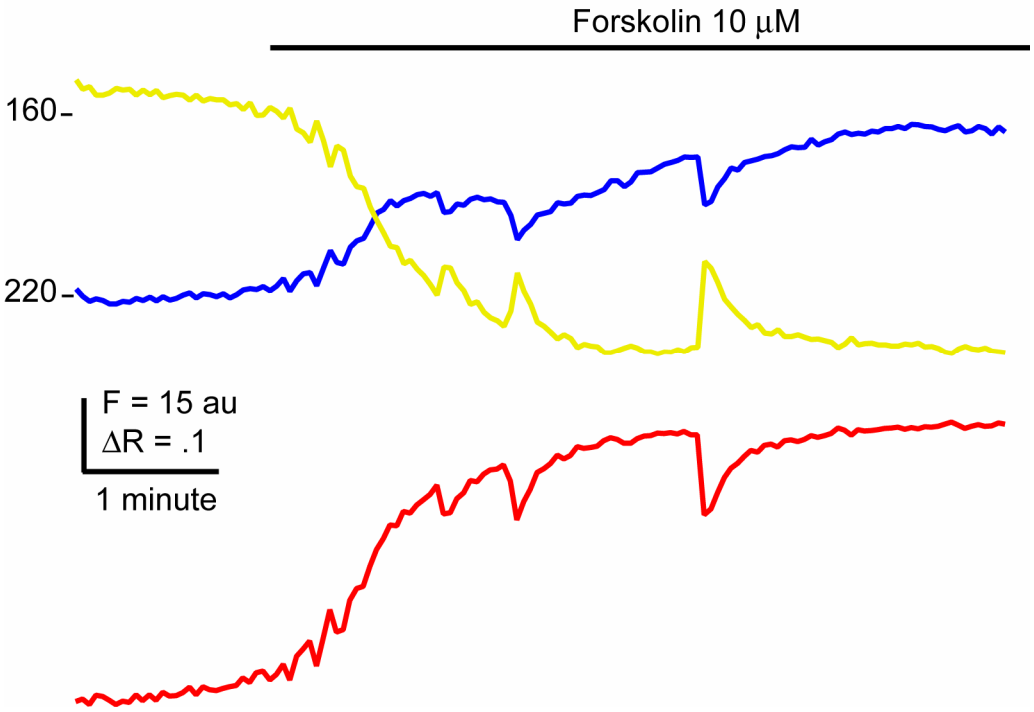


**Figure 4.2 Starburst amacrine cells exhibit spontaneous decreases in cAMP.** Top: Time course of $F_{CFP}$ (blue), $F_{YFP}$ (yellow) and (bottom) the FRET ratio (red) of $F_{YFP}/F_{CFP}$ for a starburst amacrine cell expressing ICUE2. After application of the adenylate cyclase activator forskolin (10µM), spontaneous decreases in cAMP occur.

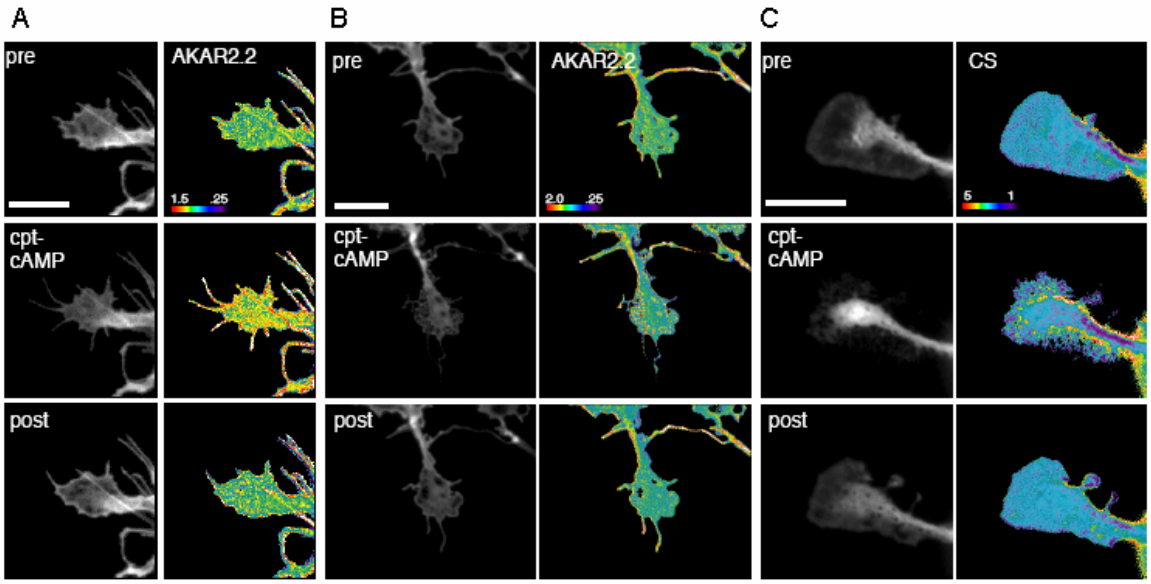


**Figure 4.3 FRET ratio changes are detectable in the growth cones of some RGCs**. A) LEFT: Fluorescence images of a growth cone transfected with AKAR2.2 before, during and after application of 50μM CPT-cAMP. RIGHT: Pseudo-color images represent FRET ratio images for the corresponding time points. Red represents high levels of PKA activity. Scale bar = 10μm. B) A second RGC growth cone expressing AKAR2.2 with no detectable change in FRET ratio. C) A RGC growth cone expressing the cAMP sensor. FRET ratio decreases, corresponding to cAMP increases occur at sites of lamellipodial retraction.